Genome-wide mRNA expression profiling and expression patterns of iron-related genes in mouse kidney during primary and secondary iron overload

Master's thesis
Institute of Medical Technology
University of Tampere
Henna Luukkonen
May 2009

PRO GRADU –TUTKIELMA

Paikka:	TAMPEREEN YLIOPISTO Lääketieteellinen tiedekunta Lääketieteellisen teknologian instituutti
Tekijä:	LUUKKONEN, HENNA MARIA
Otsikko:	Koko genomin laajuinen mRNA:n ilmentymisprofiili ja rautaan liittyvien geenien ilmentyminen munuaisessa liiallisten rautakertymien aikana.
Sivumäärä:	76 s. + liitteet 11 s.
Ohjaajat:	Professori Seppo Parkkila, MSc Alejandra Rodriguez Martinez
Tarkastajat:	Professori Vesa Hytönen, Professori Seppo Parkkila
Aika:	Toukokuu 2009

TIIVISTELMÄ

Tutkimuksen tausta ja tavoitteet: Hemokromatoosi on sairaus, joka johtuu liiallisesta raudan kertymisestä elimiin, kuten maksaan. Raudan kertyminen johtuu siitä, että raudan imeytymistä ja vapautumista ei pystytä estämään kunnolla, koska hepsidiinin ilmentämisen stimulaatio on estynyt. Mutaatiot hepsidiinin ilmentymistä säätelevissä geeneissä, *Hfe*:ssa, *HJV*:ssa ja *TfR2*:ssa, aiheuttavat liian vähäisen hepsidiinin määrän verrattuna elimistön rautapitoisuuteen. Tässä tutkimuksessa tutkittiin näiden hepsidiinin ilmentymistä säätelevien geenien ilmentymistä liiallisten rautakertymien aikana munuaisessa, minkä lisäksi koko genomin kattavan mRNA profiilin avulla tutkittiin rautakertymien vaikutuksia kaikkien geenien ilmentämiseen munuaisessa.

Metodit: cDNA mikrosirututkimuksessa määritettiin mRNA-profiili munuaisessa, kun rautaa on kertynyt liiallisesti elimistöön. Samassa tutkimuksessa määritettiin myös reittejä, joihin liitettyjä geenejä on normaalia enemmän yli- tai ali-ilmentyneitten geenien joukossa. Mikrosirututkimuksen perusteella valittiin joitakin geenejä, joiden ilmentymisen muutokset varmistettiin Q-RT-PCR:n avulla, myös muutokset rautaan liittyvien geenien ilmentymisessä tutkittiin Q-RT-PCR:n avulla.

Tulokset: Mikrosirututkimus paljasti monia geenejä, joita joko yli- tai ali-ilmennettiin liiallisten rautakertymien aikana, jotka oli aiheutettu joko ruokavalion kautta tai poistamalla hiirten genomista *Hfe*-geeni. Mikrosirututkimus ei kuitenkaan paljastanut juurikaan geenejä, jotka voitaisiin liittää suoraan rautakertymiin tai hemokromatoosiin. Suurin osa geeneistä, joiden muuttunut ilmentyminen varmennettiin Q-RT-PCR:n avulla, olivat myös tämän tutkimuksen perusteella yli- tai ali-ilmentyneitä. Mikrosirutuloksista löydettiin myös muutamia reittejä, jotka olivat yli-edustettuina tuloksissa. Muutokset rautaan liittyvien geenien ilmentymisessä olivat samansuuntaisia kuin niiden on aikaisemmin todettu olevan esimerkiksi maksassa. Hepsidiinin ilmentäminen munuaisessa on ollut kiistanalaista, mutta tämän tutkimuksen perusteella kumpaakaan hepsidiinin geeneistä ei ilmennetä munuaisessa. Myöskään *HJV*:n mRNA:ta ei löydetty munuaisesta.

Johtopäätökset: Mikrosirututkimuksessa löytyi paljon geenejä, joiden ilmentyminen oli muuttunut vasteena ylimääräiselle raudalle. Koska myös tiettyjen rautaan liittyvien geenien ilmentyminen muuttui, voidaan todeta, että munuaisella on tärkeä rooli rauta-aineenvaihdunnassa ja sen säätelyssä, vaikka se ei pystykään syntetisoimaan hepsidiiniä.

MASTER'S THESIS

Place:	UNIVERSITY OF TAMPERE Faculty of Medicine Institute of Medical Technology
Author:	LUUKKONEN, HENNA MARIA
Title:	Genome-wide mRNA expression profiling and expression patterns of iron-related genes in mouse kidney during iron overload
Pages:	76 pp. + appendices 11 pp.
Supervisors:	Professor Seppo Parkkila, MSc Alejandra Rodriguez Martinez
Reviewers:	Professor Vesa Hytönen, Professor Seppo Parkkila
Date:	May 2009

ABSTRACT

Background and aims: Hemochromatosis is a disease characterized by excess iron deposition in parenchymal organs. Failure to control iron absorption and release from cells is often caused by inability to properly induce hepcidin expression. This defect is in turn caused by mutations in hepcidin or its regulators *Hfe*, *HJV*, and *TfR2*. In this study, expression profiles of these regulatory proteins in kidney was explored and, using genome-wide mRNA expression profiling the overall effects of iron overload in kidney was determined.

Methods: cDNA microarray technology was used to determine the genes with altered patterns in two mouse models: dietary iron overloaded and *Hfe*$^{-/-}$. Additionally, microarray data were analyzed in order to identify molecular pathways over-represented among the regulated genes. Altered expression of genes selected from the microarray data, as well as the expression patterns of certain iron-related genes, were confirmed and explored using Q-RT-PCR.

Results: The microarray analysis revealed many genes that were either up- or down-regulated during iron overload. However, only few genes could be directly linked to iron overload or hemochromatosis. The regulation of most of the genes which expression profile was double-checked using Q-RT-PCR was confirmed. Microarray data revealed few pathways that were over-represented throughout the data. The iron-related genes, of which expression turned to be altered in kidney, had the same kind of expression pattern as for example in the liver. The expression of *hepcidin*-genes in kidney is controversial, but the present data indicates that neither *hepcidin1* nor *hepcidin2* are expressed in this organ. The results also revealed the absence of HJV mRNA in the kidney.

Conclusions: According to the present data the expression of many genes is altered in response to iron overload, including several iron-related genes. Therefore, it can be concluded that kidney has an important role in iron homeostasis, even though it can not synthesize hepcidin.

CONTENTS

ABBREVIATIONS

Acaa	Acetyl-CoA acyltransferase
Acot	Acyl-CoA thioesterase
Acox	Acyl-CoA oxidase
Angptl	Angiopoietin-like
apo-transferrin	Iron-free transferrin
ATP	Adenosine triphosphate
BMP	Bone morphogenetic protein
cDNA	Complementary DNA
CoA	Coenzyme A
Cyp	Cytochrome P450
Dcytb	Duodenal cytochrome b
DMT1	Divalent Metal Transporter 1
DNA	Deoxyribonucleic acid
E	Embryonic day
EPO	Erythropoietin
FD	Ferroportin disease
Fe^{3+}	Ferric iron
Fe^{2+}	Ferrous iron
Fpn	Ferroportin
GPI	Glycosylphosphatidyl inositol
Gpx	Glutathione peroxidase
HAMP	Hepcidin antimicrobial peptide
HCP1	Heme carrier protein 1
20-HETE	20-hydroxyeicosatetraenoic acid
HFE	Hemochromatosis protein
HH	Hereditary hemochromatosis
HIF	Hypoxia-inducible factor
HJV	Hemojuvelin
HLA	Human leukocyte antigen
Hmox1	Heme oxygenase 1
holo-transferrin	Diferric transferrin
Hsp	Heat shock protein
IMP	Integrin-mobilferrin pathway
IRE	Iron regulatory element
IRP	Iron regulatory protein
JH	Juvenile hemochromatosis
KEGG	Kyoto Encyclopedia of Genes and Genomes
LEAP-1	Liver expressed antimicrobial peptide 1
LNA	Locked nucleic acid
LPL	Lipoprotein lipase
MHC	Major histocompatibility complex
mRNA	Messenger RNA
OD	Optical density
NTBI	Non-transferrin-bound iron
PCR	Polymerase chain reaction
PNA	Peptide nucleic acid
PPAR	Peroxisome proliferator-activated receptor

RES	Reticulo-endothelial system
RGM	Repulsive guidance molecule
RNA	Ribonucleic acid
ROI	Reactive oxygen intermediate
RT	Reverse transcriptase
SD	Standard deviation
serpin	Serine protease inhibitor
TfR1	Transferrin receptor 1
TfR2	Transferrin receptor 2
Tfrc	Transferrin receptor 1
Ttr	Transthyretin
USF2	Upstream stimulatory factor 2
UTR	Untranslated region
VHL	von Hippel-Landau

1 INTRODUCTION

Iron is an indispensable trace element for all living organisms. It has a crucial role in many biochemical activities, including oxygen sensing and transport, electron transfer, and catalysis (Papanikolaou & Pantopoulos 2005). The biochemical functions of iron are based on its chemical properties. Generally, three types of reactions account for the biochemical activity of iron, namely, oxidation-reduction reactions, hydrolysis and polynuclear complex formation (Papanikolaou & Pantopoulos 2005, Aisen et al. 2001). Iron can for example form a variety of coordination complexes with organic ligands (Papanikolaou & Pantopoulos 2005). Even though iron is essential for normal growth and differentiation, its excess has deleterious consequences; free iron promotes the formation of reactive oxygen radicals which can damage proteins, lipids and nucleic acids (Ganz & Nemeth 2006). Because mammals have no active mechanism to excrete iron, its absorption must be tightly regulated (Papanikolaou & Pantopoulos 2005). Recent findings of proteins involved in regulation of iron homeostasis have offered new insights for understanding iron homeostasis in detail. Especially the discovery of hepcidin has provided large amount of new information (Feder et al 1996, Krause et al. 2000, Park et al. 2001, Papanikolaou et al. 2004).

Hereditary hemochromatosis (HH) is a common inherited metabolic disorder found in whites; its prevalence is ten times higher than that of cystic fibrosis. It is caused by excess iron absorption from duodenum which leads to iron overload in vital organs. The first case of HH was described in 1856 by Trousseau, although the term hemochromatosis was used for the first time in 1889 by von Recklinghausen. Both of these early cases of HH were defined with massive organ damage and dark tissue staining (Franchini & Veneri 2005, Pietrangelo 2006). In 1935 Sheldon suggested that hemochromatosis was an inherited disease (Pietrangelo 2006). However, evidence for this had to wait until 1976 when Simon and colleagues described the autosomal recessive inheritance of the disease and identified the linkage of the causing gene to human leukocyte antigen-A (HLA-A) locus, in the short arm of chromosome 6 (Franchini & Veneri 2005). Two decades later, *Hfe* (originally named HLA-H), the gene whose mutation causes most of the HH cases, was finally identified (Feder et al. 1996). Nevertheless, it was soon realized that HH is both a clinically and genetically heterogeneous group of diseases. Besides mutations in *Hfe*, also later defined rarer mutations in *HJV*, *hepcidin*, *TfR2* and *Fpn* are known to cause different types of HH (Papanikolaou et al. 2004, Roetto et al. 2003, Camaschella et al. 2000, Montosi et al. 2001, Njajou et al. 2001). In most HH cases patient's urinary hepcidin levels are very low (Pietrangelo 2006). Based on these

observations, it is suggested that pathogenesis of HH is due to impaired hepcidin expression when body iron levels are high. Consequently the control of iron export through Fpn is lost, leading to increased release of iron from macrophages and increased intestinal absorption of iron (Pietrangelo 2006, Donovan et al. 2005).

2 REVIEW OF THE LITERATURE

2.1 Iron Homeostasis

2.1.1 Properties of Iron

In aqueous solutions iron has two principal oxidation states; the ferric (Fe^{3+}) and the ferrous (Fe^{2+}) state. Usually, reducing agents can convert ferric iron to ferrous and, while, under aerobic conditions and in solution ferrous iron is readily oxidized to its ferric form. In solutions with physiological pH ferric iron is virtually insoluble and therefore iron-dependent life had to evolve specialized molecules to maintain iron in soluble and simultaneously bioavailable forms (Aisen et al. 2001, Papanikolaou & Pantopoulos 2005). In most biological complexes of iron redox chemistry is facile and two-way; redox reactions are reversible when the reduction potential of complexed iron falls within the range accessible to biological oxidants: from +820 mV to -320 mV. Outside this range redox reactions might be irreversible. Iron must be in its ferrous state in order to participate in such processes as transmembrane transport, storage as ferritin and heme synthesis (Fleming et al. 1997, Gunshin et al. 1997, Fleming et al. 2008, Bauminger et al. 1993, Dailey et al. 1994). However, at physiological oxygen level the stable state of iron in most of its biological complexes is ferric form, thus reduction reactions have a critical role in iron metabolism (Aisen et al. 2001).

The redox capabilities of iron turn it into a potential biohazard since, under aerobic conditions oxidation of iron can catalyze the generation of noxious radicals (Papanikolaou & Pantopoulos 2005). Electron transfer from ferrous iron to dioxygen causes superoxide formation, which in turn generates hydroxyl radicals (Aisen et al. 2001). The reactions leading to hydroxyl radical formation are called Fenton and Haber-Weiss reactions (Papanikolaou & Pantopoulos 2005). Superoxides and hydroxyl radicals are known as reactive oxygen intermediates or ROIs. Certainly, ROIs are also produced under normal circumstances, as byproducts of aerobic respiration or enzymatic reactions (Halliwell & Gutteridge 1990). Notably, redox active iron can catalyze the formation of other harmful reactive species as well. These organic reactive species include for example peroxyl ($ROO^{\cdot}$), alkoxyl ($RO^{\cdot}$), thiyl (RS) and thiyl-peroxyl ($RSOO^{\cdot}$). In addition to iron's role as a catalyst, ferrous iron can contribute to the formation of free radicals as a reactant by interacting directly with oxygen via ferryl (Fe^{2+}-O) or perferryl (Fe^{2+}-O_2) intermediates. Also iron bound to heme may catalyze formation of free radicals (Papanikolaou & Pantopoulos 2005). Toxicity of free radicals is

based on their ability to promote oxidation of proteins, initiate chain-propagating lipid peroxidation and modify nucleic acids (Aisen et al. 2001). Nevertheless, in physiological conditions iron is bound to transferrin and it is unable to engage in Fenton or Haber-Weiss reactions (Ponka et al 1998).

Two other important processes in which iron is involved are its hydrolysis and the formation of polynuclear complexes. In strongly acidic solutions, both ferric and ferrous iron forms exist as the hexaaquo complex, in which they bind six molecules of water. As far as oxygen tension remains low, autooxidation is prevented and aquated ferrous iron can be detected throughout the pH range found in biological systems. However, when pH raises the complex undergoes a stepwise series of hydrolytic deprotonations yielding H_3O^+ and $[Fe(H_2O)_3(OH^-)_3]$, being this uncharged species an extremely insoluble one. The concentration of aquated ferric iron at neutral pH is only about 10^{-17} M, while the total concentration of ferric iron on solutions is about 10^{-9} M. Iron polymers in biological systems may range from two iron atoms to three-dimensional arrays of more than 4000 iron atoms. Iron complexes usually form by dehydration and iron atoms are linked by oxo- or hydroxobridges (Aisen et al. 2001).

2.1.2 Iron Distribution

Iron is an essential component in many proteins and enzymes with vital role in energy metabolism, cell proliferation and DNA repair (Ganz & Nemeth 2006). In these proteins iron is bound to iron-sulfur clusters, such as 2Fe-2S, 3Fe-4S and 4Fe-4S. Clusters have different roles in different proteins, ranging from electron transfer, transcriptional regulation and structural stabilization to catalysis. Protein-associated iron can also be found from iron-oxo clusters and mononuclear iron centers. Free iron has a central function also in a recently discovered mechanism for oxygen sensing, via hypoxia-inducible factors (HIFs). The vast majority of protein-associated iron is bound to heme, a prosthetic group composed of protoporphyrin IX and a ferrous iron ion. The most abundant heme-containing proteins are hemoglobin and myoglobin, which serve as oxygen carriers in erythroid tissue and in muscle respectively. Other hemoproteins are for example oxygenases, peroxidases, nitric oxide synthases and guanylate cyclases (Papanikolaou & Pantopoulos 2005).

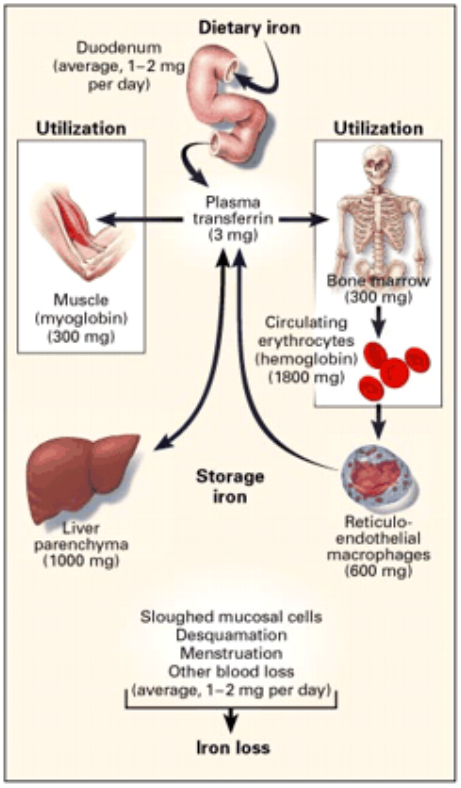

Figure 1. Distribution of iron in the human body. Amounts presented are approximate, variation between individuals occur. Figure adopted from Andrews 1999.

The human body contains approximately 3-4 g of iron, 35-45 mg of iron per kilogram of body weight in adult men (Ganz & Nemeth 2006, Andrews 1999). More than two thirds of body iron is incorporated into hemoglobin in developing erythroid precursors and mature red cells (Figure 1) (Andrews 1999). Normal erythrocytes live around 120 days, and under average circumstances 20 ml of erythrocytes (packed volume) containing a total of 20 mg of iron are destroyed each day (Ganz & Nemeth 2006). In order to maintain homeostasis, this same amount of iron has to be incorporated to the erythron every day via the transferrin cycle. 20 mg of iron corresponds to the incorporation of 2×10^{20} atoms of this metal because each erythrocyte contains billion atoms of iron. Some 300 mg of iron is bound to myoglobin, the other heme-containing protein, and in this way stored to muscles (Andrews 1999).

About 25% of total body iron, 0.5-1.0 g, is stored in reticuloendothelial macrophages and hepatocytes as a reserve which can be easily mobilized for erythropoiesis (Figure 1) (Ganz & Nemeth 2006). Most iron is stored in the form of ferritin which is a heteropolymer of 24 subunits of two types, H and L. In mature ferritin, subunits are arranged to form a nearly spherical structure which encloses a cavity which can accommodate up to 4500 oxygen- and hydroxyl-bridged iron atoms. Most mature ferritin molecules are found in the cytoplasm of cells, but a small fraction can

be detected also in the nucleus. Iron is released by lysosomal or proteosomal degradation of ferritin, when it is needed. Iron is also stored as hemosiderin, a degradation product of ferritin, which appears to result from incomplete lysosomal processing (Aisen et al. 2001). In the liver iron accumulates mostly in the periportal regions with a decreasing gradient toward the centrilobular areas (Muckenthaler et al. 2008). Iron overload disorders develop when iron uptake exceeds iron utilization and loss and, because liver is the main storage organ of iron, it is often affected. Liver damage occurs when liver iron concentration is increased to more than 10 times normal, which contributes to serum ferritin levels over 1000 ng/ml (Ganz & Nemeth 2006).

To maintain iron homeostasis 20 mg iron is needed daily for production of hemoglobin for new erythrocytes. Most of this iron is derived from recycling of damaged and senescent erythrocytes by macrophages of reticuloendothlelial system (RES). Only 1-2 mg of iron is absorbed daily from the diet (Figure 1) (Ganz & Nemeth 2006). Humans have no active mechanism to excrete iron, but some iron losses still occur (Papanikolaou & Pantopoulos 2005). Iron is released from the body by sloughing of mucosal cells (duodenal enterocytes), desquamation of skin cells, blood loss (menstrual and other) and urinary excretion (Muckenthaler et al. 2008). The mechanism behind iron loss due to sloughing of mucosal cells is that some iron is always stored to intestinal cells as ferritin. Because the duodenal enterocytes turnover rapidly, intracellular ferritin iron is quickly lost into the intestinal lumen as the ageing cells are sloughed off at villus tip (Sharp & Srai 2007). About 1-2 mg of iron is lost every day by these mechanisms (Papanikolaou & Pantopoulos 2005).

2.1.3 Iron Absorption & Transport

Iron is absorbed in the duodenum in two forms, heme and non-heme. Heme is found in meat and meat products and non-heme iron is present for example in cereals, vegetables, pulses, beans and fruits. Non-heme iron has a number of forms, ranging from iron oxides and salts to more complex organic chelates (Sharp & Srai 2007). In western countries heme iron accounts for 5%-10% of dietary iron, but it can contribute up to 50% of iron entering the body, because it is absorbed more efficiently than non-heme iron (Sharp & Srai 2007, Anderson et al. 2005). The absorption efficiency, i.e. bioavailability, of both heme and non-heme iron is influenced by a number of variables, such as the amount of iron in foods, the forms of iron present and other dietary components (Sharp & Srai 2007). Non-heme iron is more responsive than heme iron to differences in body iron status. It can be absorbed nearly as well as heme iron by individuals with very low iron stores. Other dietary components can enhance or inhibit non-heme iron biovailability: meat, poultry

and fish, ascorbic acid, alcohol and retinol and carotenes are potent enhancers of non-heme iron absorption while phytic acid, polyphenols, soy protein, egg, calcium, phosphate salts and antacids are potent inhibitors of non-heme iron absorption (Hunt 2003).

The majority of dietary non-heme iron is in the ferric form, and it must be converted to ferrous state prior to absorption. Numerous dietary components can reduce ferric iron to ferrous form. For example, ascorbic acid and some amino acids such as cysteine and histidine can function as reductants (Sharp & Srai 2007). Additionally, ferric reductase enzymatic activity has also been detected in the brush-border surface of duodenal enterocytes. The plasma membrane b-type cytochrome (Dcytb) (also known as Cybrd1) contributes to this activity (Sharp & Srai 2007, McKie et al. 2001). Dcytb is capable of reducing ferric iron complexes, and its mRNA and protein levels are upregulated by several stimulators of iron absorption (McKie et al. 2001). However, as more recently evidenced, inactivation of *Cybrd1* gene in mice has no effect on body's ability to accumulate tissue iron stores. Therefore, there may be some complementary enzymatic mechanisms to reduce ferric iron in the brush border (Gunshin et al. 2005). Once reduced, ferrous iron becomes a substrate for the divalent metal transporter (DMT1) (also known as DCT1 and Nramp2). DMT1 transports iron across the apical membrane of duodenal enterocytes via a proton-coupled mechanism (1 Fe:1 H^+), and iron appears to be its preferred substrate (Figure 2) (Tandy et al. 2000, Gunshin et al. 1997, Aisen et al. 2001). The low pH and the acidic microclimate at the duodenum brush border stabilize iron in its ferrous form, and provide protons for DMT1-mediated transport (Sharp & Srai 2007).

Intestinal absorption of heme is more efficient than that of non-heme iron. Prior to absorption, heme must be released from proteins, like hemoglobin and myoglobin, by proteolytic activity in the lumen of the stomach and the small intestine. After the release heme is stabilized by various compounds, including hemoglobin degradation products (Anderson et al. 2005). ATP-binding cassette protein (ABCG2), the feline leukaemia virus C receptor protein (FLVCR), and the heme carrier protein (HCP1) are the candidate proteins for binding free heme in the enterocytes (Sharp & Srai 2007, Shayeghi et al. 2005). HCP1 is highly expressed in the duodenum, and its expression is regulated in response to changes in iron stores. Thus far, evidence tells that ABCG2 and FLVCR are heme exporters, while HCP1 may mediate energy-dependent transmembrane uptake of heme (Figure 2) (Shayeghi et al. 2005). However, more recent data shows that, independently of HCP1's heme transporting activities, it may also function as a proton-coupled folate transporter (Qiu et al. 2006). After transport across the apical membrane, heme is detected in caveolae between the

microvilli, in membrane-bound tubules in the apical cytoplasm, and finally in secondary lysosomes. In the lysosomes iron is released from the protoporphyrin, probably by heme oxygenase 1 (Hmox1) and released iron joins the same pathway as non-heme iron (Anderson et al. 2005).

In addition to what has been discussed above, other ways to absorb non-heme iron from the diet have been suggested. Integrin-mobilferrin pathway (IMP) transports ferric iron to intestinal enterocytes. The proteins associated with IMP, mobilferrin and β3-integrin, bind ferric iron, and enter the enterocyte through the apical membrane. Once in the cytosol, falvin monooxygenase and β2-microglubulin join the existing protein-iron complex forming paraferrin, a larger conglomerate with ferrireductase activity. It is suggested that DMT1 is also a component of paraferrin and, thus DMT1 may permit the delivery of ferrous iron to intracellular organelles (Conrad et al. 2002, Sharp & Srai 2007). The major iron storage protein ferritin may also be an important nutritional source of iron. Evidence shows that both plant and animal ferritin sources are absorbed in humans but with a mechanism not yet defined. One possibility is that ferritin is absorbed intact via ferritin receptors and then degraded in the lysosomes to liberate its iron load (Sharp & Srai 2007).

To enter circulation iron needs to be transported across the basolateral membrane of the intestinal epithelia. The ability to export iron is also needed in reticuloendothelial macrophages, and the iron delivery to the brain, testis and placenta requires transport into and across endothelial cells (Aisen et al. 2001). It is poorly understood how iron is transported from the apical membrane of enterocytes to the basolateral membrane, but it is likely that the transport involves vesicular trafficking (Sharp & Srai 2007). When ferrous iron reaches the basolateral membrane, it is transported across it by ferroportin (Fpn) (also known as IREG1), the only known iron exporter (Figure 2). Ferroportin is a transmembrane protein, which exports ferrous iron in unidirectional efflux and is expressed in many different tissue types; including the liver, spleen and kidney (Donovan et al. 2000, McKie et al. 2000). Ferroportin appears to be essential for iron excretion in the enterocytes, reticuloendothelial macrophages and hepatocytes, whereas the lack of ferroportin causes iron retention in these cell types (Donovan et al. 2005). After iron is released from enterocytes (or other cell types) it has to be oxidized to ferric state before it can bind to transferrin. Oxidation is mediated by hephaestin, an intestinal membrane bound copper-dependent ceruloplasmin homologue. Hephaestin and ceruplasmin are also essential for iron export because copper-deficient animals fail to mobilize iron (Sharp & Srai 2007, Aisen et al. 2001).

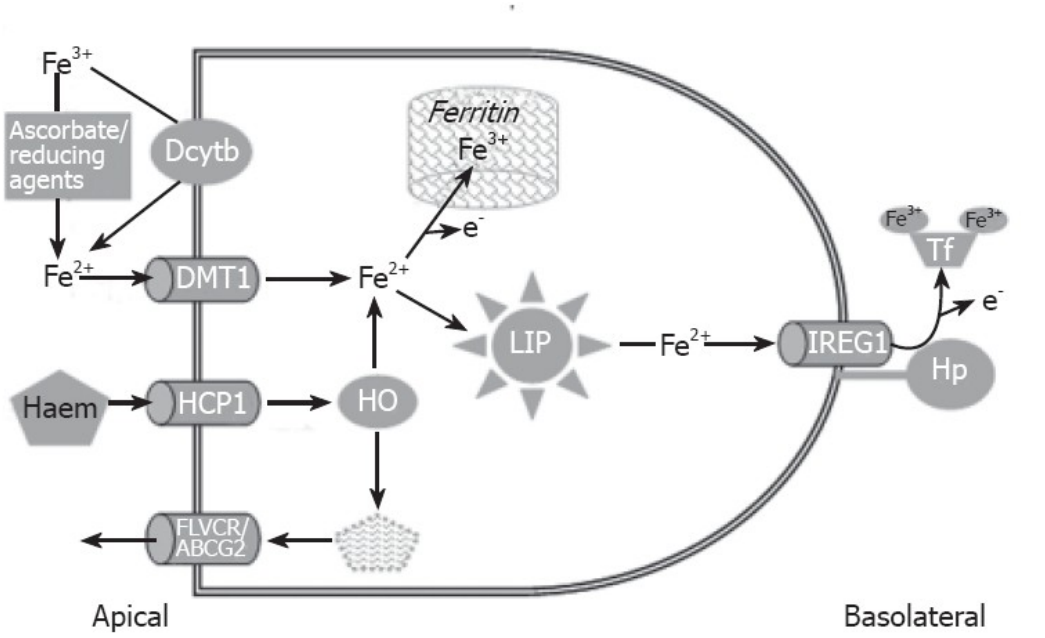

Figure 2. The pathways through which iron is absorbed from the duodenum and exported to the circulation. DMT1 mediated pathway imports non-heme iron to the enterocytes, HCP1 mediated pathway imports heme iron to the enterocytes, and Fpn mediated pathway exports iron from various cell types. Figure adopted from Sharp & Srai 2007.

Once exported, iron is rapidly bound to transferrin, which is a high affinity iron-binding protein capable of binding two ferric iron ions (Andrews & Schmidt 2007). Transferrin molecules contain two structurally similar but functionally distinct iron-binding sites. After binding iron the transferrin domains undergo a conformational rotation to enclose the iron-binding sites (Aisen et al. 2001). Under normal circumstances transferrin carries nearly all serum iron but only 30% of its iron-binding sites are occupied. The free binding sites serve as buffering capacity sites for iron which become occupied during iron overload (Andrews & Schmidt 2007, Aisen et al. 2001). Iron is assimilated into most cells via transferrin cycle, in which transferrin receptor 1 (TfR1) takes up mainly holo-transferrin (diferric transferrin). Especially erythroid precursors seem to be dependent on the transferrin cycle (Figure 3); other cells apparently have other mechanisms to assimilate iron (Levy et al. 1999a, Andrews & Schmidt 2007). During binding of transferrin to TfR1, the latter dimerisizes and each TfR1-dimer can bind two holo-transferrin molecules. After binding the complex is taken up by endocytosis. Ferric iron is released from the complex when the endosome is acidified and ferric iron is then reduced to the ferrous state by STEAP3. Reduced iron is then released from the endosome via DMT1. Meanwhile the transferrin-TfR1 complex is recycled back to the cell surface and transferrin molecules are released (Andrews & Schimdt 2007, Andrews 1999,

Ohgami et al. 2005). Conformational changes in TfR1, needed for the release of ferric iron and transferrin from TfR1, are mediated by changes in pH, because interaction between transferrin and TfR1 strongly depends on it. The initial binding of transferrin takes place in slightly basic pH, the iron atoms are released in acidic pH and resulting apo-transferrin is released again in slightly basic pH due to decreased affinity of TfR1 to apo-transferrin (Yersin et al. 2008). Although most iron in plasma is bound to transferrin, some remains as non-transferrin-bound (NTBI) free iron, especially when serum iron levels exceed transferrin binding capacity. At least hepatocytes can take up NTBI; the involved transporters that mobilize it may include for example L-type calcium channels and molecules that can transport other metal ions (Andrews & Schmidt 2007).

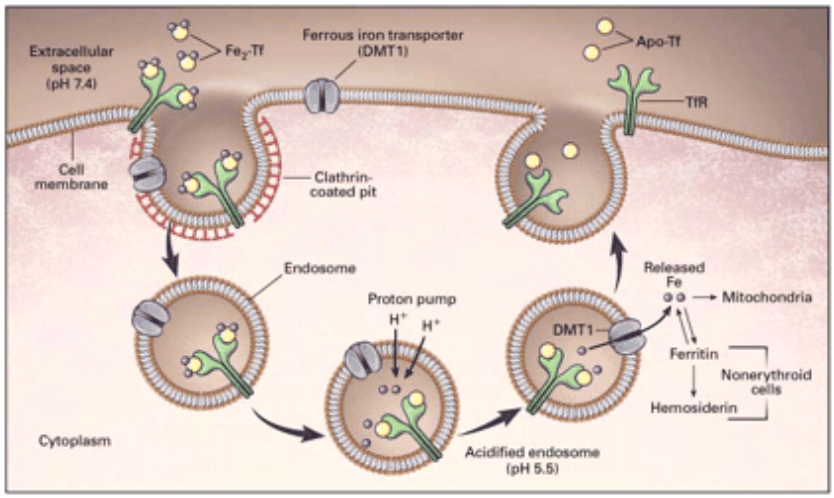

Figure 3. The transferrin cycle. Figure adopted from Andrews 1999.

2.1.4 Iron Recycling

Body iron needs are mainly provided by the recycling of iron via RES, which consists of specialized macrophages present mainly in the spleen, the liver (also known as Kupffer cells) and bone marrow (Muckenthaler et al. 2008). Efficiency of RES is high; the pool of transferrin-bound iron undergoes over 10 times daily recycling (Papanikolaou & Pantopoulos 2005). Macrophages of the RES phagocyte and lyse old and damaged erythrocytes. After lysing the erythrocytes, heme is catabolized by Hmox1 to liberate inorganic iron (Muckenthaler et. al 2008, Poss et al. 1997). Besides phagocytosis, macrophages of the RES also have other mechanisms to acquire iron. Free hemoglobin circulating in the bloodstream is quickly bound to haptoglobin and the complex can be endocytosed via hemoglobin scavenger receptor CD163. CD163 is expressed in macrophages of the RES and it is supposed to be involved in iron recycling (Kristiansen et al. 2001, Muckenthaler et al.

2008). Macrophages also express LDL receptor-related protein/CD91, which can mediate endocytosis of the hemopexin-heme complexes. Hemopexin binds to free heme-groups in circulation and its endocytosis may also be an important mechanism in iron recycling (Hvidberg et al. 2005). Besides these mechanisms macrophages can also take up transferrin-bound iron via the transferrin cycle. The intracellular trafficking of heme-derived iron involves DMT1, but the mechanisms behind it have not been defined yet. Iron can be used in metabolic processes, stored as ferritin or released as in the form of free iron, hemoglobin, heme or ferritin. Iron release is regulated by the needs of the bone marrow (Muckenthaler et al. 2008). Even though recycled iron accounts for most of the daily iron supply, the rate of intestinal iron absorption is important in the long term, because 1-2 mg of iron is lost every day (Ganz & Nemeth 2006).

2.1.5 Regulation of Iron Homeostasis

Because mammals have no active mechanism to excrete iron, iron homeostasis must be tightly regulated at the level of iron absorption. It is suggested that three different factors contribute the maintenance of iron homeostasis; the dietary regulator, the stores regulator and the erythropoietic regulator. The dietary regulator controls iron absorption based on how much is accumulated in duodenal enterocytes, the phenomenon is also known as mucosal block (Papanikolaou & Pantopoulos 2005). When iron levels in the enterocyte are high, expression of DMT1 and Dcytb is decreased and thus iron absorption is decreased (Frazer et al. 2003). The stores regulator controls iron uptake in response to body iron stores, by sensing plasma transferrin saturation. The erythropoietic regulator has a dominant function in the control of iron homeostasis and it modulates iron absorption in response to erythropoiesis (Papanikolaou & Pantopoulos 2005).

Locally, the expression of genes involved in iron uptake, export and utilization is regulated by the IRE/IRP (iron regulatory element/iron regulatory protein) system. The IRE/IRP system mediates posttranscriptional regulation of certain iron-related genes and it has been shown to be essential for mammals (Muckentahler et al. 2008). Genes that are regulated by IRE/IRP systems contain an IRE element in their mRNA. The IRE element can be found either in the 3' untranslated region (UTR) or in the 5' UTR and it consists of about 30 nucleotides which fold and form a loop with the 5'-CAGUGN-3' consensus sequence (Papanikolaou & Pantopulos 2005). The IRPs, IRP1 and IRP2, bind to the IRE elements of the target mRNA when iron levels are low. Binding to 3'-UTR IRE stabilizes the mRNA molecule and enhances its translation whereas binding to 5'-UTR IRE blocks the initiation of translation and the translation is decreased. Both IRP1 and IRP2 are degraded in the

presence of excess iron. IRP1 cannot incorporate the iron-sulfur cluster which acts as its iron sensor, and IRP2 is ubiquinated and degraded via proteasomal degradation (Andrews & Schmidt 2007, Muckenthaler et al. 2008). IRP1 has also an aconitase activity, and it has been suggested that it is mostly in the form of an aconitase and is not needed to regulate iron metabolism in iron deficient animals. Therefore, IRP2 is the main posttranscriptional regulator of iron metabolism in most tissues. IRP2 can compensate the loss of IRP1 by an unknown mechanism in IRP1 deficient animals. There are only two tissues, the kidney and brown fat, where the compensation is incomplete. In these tissues the expression of IRP1 is high, and it is possible that IRP1 is needed for the basal IRE-binding capacity of these tissues (Meyron-Holtz et al. 2004). IRE elements can be found in the 3'-UTR of TfR1, which has five IREs in tandem, and in one of DMT1 splice variants, so the transcripts of both genes are stabilized when iron is deplete (Papanikolaou & Pantopoulos 2005, Shapr & Srai 2007). The mucosal block phenomenon can be explained by degradation of IRPs when iron levels rise in the enterocyte, because the IRE-containing isoform of DMT1 is widely expressed in the intestinal mucosa (Frazer et al. 2003). Genes containing IREs at their 5'-UTR include both *H-* and *L-ferritins*, *Fpn* and *the heme biosynthetic enzyme aminolevulinate synthase (ALAS)* (Andrews & Schmidt 2007). Recently, an IRE was found in the 5'-UTR of HIF-2α mRNA. HIF-2α is a regulatory protein which is stabilized in hypoxic conditions and it then regulates the expression of hypoxia-sensitive genes, especially *EPO*. Therefore, HIF-2α might have a specific role in EPO regulation, because both hypoxia and iron conditions can modulate its stability. It is possible that HIF-2α can adjust the rate of erythrocyte production to iron availability (Sanchez et al. 2007, Muckenthaler et al. 2008).

The regulation of systemic iron homeostasis is mainly mediated by hepcidin (also known as HAMP or LEAP-1), which is a cationic, cysteine-rich peptide hormone. This antimicrobial 25 amino acids containing peptide is mainly expressed in the liver (Nemeth & Ganz 2006, Park et al. 2001, Krause et al. 2000). Expression of hepcidin in the liver is restricted to hepatocytes; Kupffer cells only have an inhibitory effect on hepcidin expression, which they can mediate for example through cell-cell interactions (Theurl et al. 2008). Expression of hepcidin is regulated by different factors. It is upregulated during iron overload and inflammation and downregulated during anemia and hypoxia (Pigeon et al. 2001, Nicolas et al. 2002b). The iron-related function of hepcidin is to inhibit intestinal iron uptake, release of iron from macrophages, placental transport of iron and export of iron from hepatocytes. Therefore, hepcidin is a negative regulator of iron export. The mechanism behind this effect involves binding to Fpn and inducing its internalization. This decreases the

release of iron from cells (Nemeth et al. 2004). Binding of hepcidin to Fpn causes phosphorylation of Fpn, which is critical for its internalization. Once in the cytosol Fpn is ubiquitinated and transported to lysosomes for degradation. These data indicate that hepcidin regulates iron release by affecting the concentration of Fpn in the plasma membrane (DeDomenico et al. 2007). Interestingly, a recent study has suggested that in intestinal cells, mainly enterocytes, hepcidin diminishes apical iron uptake by decreasing transcription of DMT1 rather than by triggering degradation of Fpn from the basolateral membrane (Mena et al. 2008).

Several iron-related proteins are regulators of hepcidin expression, namely hemochromatosis protein (HFE), transferrin receptor 2 (TfR2) and hemojuvelin (HJV) (Figure 4) (Nemeth & Ganz 2006). HFE is a MHC class I-like molecule, which was initially characterized as the most frequently mutated protein in patients with hemochromatosis (HH) (Feder et al. 1996). HFE is always bound non-covalently to β_2-microglobulin, and the complex associates with TfR1 lowering its affinity for transferrin binding (Feder et al. 1996, Parkkila et al. 1997, Feder et al. 1998, Graham et al. 2007). However, affinity of TfR1 for HFE is much lower than its affinity for transferrin and because they compete for the same binding site, at normal transferrin concentrations almost no HFE is bound to TfR1 (Graham et al. 2007). TfR1 and HFE remain associated as they pass through acidic vesicles inside the cell, while TfR1-transferrin complex is normally recycled back to the cell membrane, the TfR1-HFE complex is targeted to lysosome for degradation, thus HFE may lower the number of TfR1 molecules at the cell membrane (Davies et al. 2003). HFE is shown to act primarily in the hepatocytes, in which it induces expression of hepcidin. In HFE deficient mice and HH patients, hepcidin mRNA expression is significantly lowered, likely due to dysfunction of HFE-mediated regulation of hepcidin expression. HFE is thus needed for appropriate hepcidin expression in response to changes in body iron stores. The pathogenesis of HH seems to be due to inability to effectively upregulate hepcidin expression as liver iron stores increase (Vujic Spasic et al. 2008, Bridle et al. 2003). It has been suggested that in normal conditions HFE is sequestered by TfR1 and when transferrin saturation augments, it probably displaces HFE from TfR1. Released HFE then acts to increase expression of hepcidin, thus the rate of hepcidin production rises only when saturation of transferrin is high (Schmidt et al. 2008).

TfR2 is a homolog of TfR1, but its binding affinity for holo-transferrin is pH-dependent and 25-30 times lower than that of TfR1 (Graham et al. 2007). It is highly expressed in hepatocytes and its expression increases when transferrin saturation increases; transferrin stabilizes TfR2 by increasing its half-life (Andrews & Schmidt 2007, Graham et al. 2007). Like TfR1, also TfR2 associates with

HFE. Recent data indicate that HFE and TfR2 associate throughout the endocytic cycle and, in the ER, this association accelerates the maturation of HFE (Goswami & Andrews 2006, Waheed et al. 2008). It has been suggested that TfR2 competes with TfR1 for binding to HFE, and when TfR2 levels rise, the association of TfR1 and HFE lowers (Goswami & Andrews 2006). The domain of HFE that binds to TfR2 is different from the domain binding to TfR1 and as a result the interaction between TfR2 and HFE is not competed by holo-transferrin. To the contrary, not only holo-transferrin but also HFE seems to increase the amount of TfR2 in hepatocytes (Chen et al. 2007). Besides its function as an inducer of number of TfR2 molecules, HFE also increases the affinity of holo-transferrin for TfR2, thus HFE can act as positive allosteric ligand for the interaction of holo-transferrin and TfR2. This property of HFE may lead to increased uptake of transferrin bound iron to hepatocytes (Waheed et al. 2008). Based on these observations, it has been suggested that TfR2 and HFE form an iron sensing complex which senses the saturation transferrin and then induces signalling cascade that leads to altered expression of hepcidin (Figure 4) (Goswami & Andrews 2006, Chen et al. 2007, Schmidt et al. 2008, Waheed et al. 2008).

HJV is a glycosylphosphatidyl inositol (GPI)-linked protein that belongs to the family of repulsive guidance molecules (RGMs). It is expressed mainly in the periportal hepatocytes of the liver, in skeletal muscle and in the heart (Papanikolaou et al. 2004, Niederkofler et al. 2005, Nemeth & Ganz 2006). HJV is shown to be essential in the iron-sensing pathway because HJV deficient mice show a complete lack of hepcidin expression and patients suffering from HJV-mediated hemochromatosis have very low concentrations of hepcidin in the urine. Lack of native HJV and the resulting lack of hepcidin, lead to severe iron overload in both hemochromatosis patients and HJV knock out mice (Niederkofler et al. 2005). Two forms of HJV protein can be found, one is GPI-linked to the plasma membrane and undergoes cleavage resulting in the release of the soluble HJV. The cleavage of membrane-bound HJV seems to be inhibited by iron according to *in vitro* studies in which, as transferrin saturation raised, the number of membrane-bound HJV increased (Nemeth & Ganz 2006, Lin et al. 2005). Cell-associated GPI-linked HJV induces expression of hepcidin through ligand binding, whereas soluble HJV competes with membrane-bound HJV for its ligand and decreases the stimulatory signal for expression of hepcidin. Thus, it can be speculated that soluble and cell-associated HJV reciprocally regulate hepcidin expression in response to changes in extracellular iron concentration (Figure 4). It has been also proposed that soluble HJV may signal the iron requirements for myoglobin synthesis, because skeletal muscle has a high concentration of HJV (Lin et al. 2005, Nemeth & Ganz 2006). HJV interacts with neogenin, and it has been proposed that this association is necessary for iron accumulation within cells and might therefore have an

important role in HJV signalling (Zhang et al. 2005). However, HJV was recently shown to be a BMP (bone morphogenetic protein) coreceptor that enhances BMP signaling via the classical BMP pathway which includes BMP ligands, BMP receptors and BMP receptor-activated SMADs. Both BMP receptors and BMP ligands are thus ligands for HJV. At least BMP-2 and BMP-4 are ligands for HJV and they positively regulate hepcidin expression through SMAD4. It is possible that soluble HJV represses hepcidin expression by binding and sequestering BMP ligands and thus inhibites HJV mediated BMP signaling. HJV deficiency leads to impaired BMP signaling, thus it is likely that HJV mediated BMP signaling is an important mechanism for regulating hepcidin expression (Babitt et al. 2006, Wang et al. 2005).

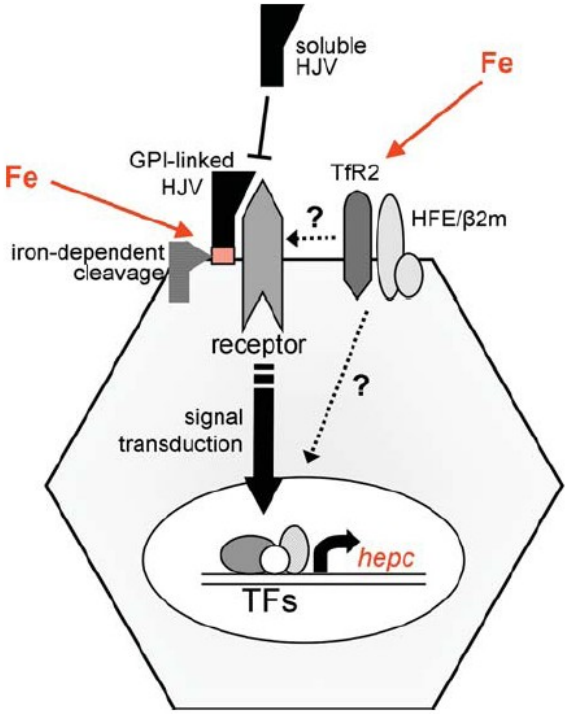

Figure 4. Regulation of the expression of hepcidin according to Nemeth & Ganz 2006. Roles of HFE, TfR2 and HJV (both soluble and membrane associated) in the regulation of hepcidin expression. Figure adopted from Nemeth & Ganz 2006.

Erythropoiesis is stimulated when tissue oxygen levels are low. At low oxygen levels erythropoietin (EPO) is produced and HIF proteins are stabilized. As it was previosly mentioned, IRPs can destabilize HIF-2α, thus when iron levels are high HIF-2α is active. Active HIF-2α can induce EPO production, which then leads to increased erythropoiesis (Muckenthaler et al. 2008). Both HIF-1 and HIF-2 are believed to directly suppress production of hepcidin and at the same time stimulate EPO production. This regulation is due to decreased von Hippel-Lindau (VHL) protein activity in HIF degradation in low oxygen levels. Thus HIFs are stabilized in low oxygen levels

through at least two different factors, and by decreasing hepcidin levels, they make more iron available for erythropoiesis (Peussonnaux et al. 2007). Direct effects of EPO *in* vivo have also been studied via EPO injections. In this study EPO lead to reduced iron storage in the liver and a significant decrease in serum iron and transferrin saturation, which can be due to decreased hepcidin levels. In the duodenum of rats, DMT1 and hephaestin expression were increased, allowing more iron to be absorbed from the diet and therefore increase the amount of iron available for erythropoiesis (Kong et al. 2008a). EPO injections also caused decreased iron retention in macrophages, which was a consequence of upregulation of Fpn and downregulation of DMT1. Also hepatic hepcidin levels decreased and it is likely that at least upregulation of Fpn was caused by this phenomenon (Kong et al. 2008b).

2.2 Iron metabolism in the Kidney

Although the body has no active mechanism to excrete iron, the kidney has been suggested to play a significant role in iron metabolism by filtration and reabsorption of iron. The possible role of IRPs in urinary excretion of iron has been also studied widely (Muckenthaler et al. 2008). A considerable amount of iron is filtered at the glomerulus, in free and transferrin-bound form. Only about 0.8 to 1.5% of this amount is actually excreted in the urine. Therefore, there must be an effective mechanism for reabsorption of iron (Wareing et al. 2000, Zhang et al. 2007). This reabsorption occurs in the thick ascending loop of Henle that is located between the proximal and distal tubules of the nephron (Wareing et al. 2000). Kidney cells can take up iron via TfR1 and megalin-dependent, cubilin-mediated endocytosis, thus it is likely that these mechanisms are responsible for the reabsorption of iron (Zhang et al. 2007, Muckenthaler et al. 2008).

It was long believed that DMT1, which is expressed highly in the kidney, was the main component of the reabsorption mechanism. Both its IRE-containing and IRE-lacking forms are expressed in the kidney cortex, outer medulla and inner medulla of rat kidney. However, it was shown that in the nephron DMT1 accumulates in the cytosol of proximal tubules and not on the apical brush-border membrane. Thus, DMT1 is not involved in translocation of iron across the apical membrane of the proximal tubule. In the distal tubule and the thick ascending limb of the loop of Henle expression of DMT1 was also observed in the apical membrane, therefore it is possible that DMT1 has a role in apical membrane transport of iron in these two locations (Ferguson et al. 2001). Experiments performed in mouse kidney indicate that there is indeed some expression of DMT1 in the apical membrane of proximal tubule. This suggests that the mechanisms of reabsorption of iron in mouse

differ from the mechanisms observed in rats and DMT1 may have a critical role in mouse renal iron regulation (Canonne-Hergaux & Gros 2002). More accurate location of DMT1 in the proximal tubule was later defined by Abouhamed and collagues. DMT1 was observed in the late endosomes and lysosomes, thus it could mediate the processing of transferrin and transport iron into intracellular pool (Abouhamed et al. 2006). The effects of an iron rich diet on DMT1 expression have also been studied. It was first observed that iron rich diet causes morphological changes in the kidney, especially in the cortex and at the corticomedullary junction. Furthermore, rats fed with iron rich diet had decreased renal DMT1 expression and rats fed with iron restricted diet had increased renal DMT1 expression. At the same time, renal iron excretion rate decreased in iron-restricted animals and increased in iron-overloaded animals. However, these facts may not be directly linked, but the observed increase in DMT1 in iron-restricted rats may be the cause of body's need of maintaining a supply of iron to the cells when serum iron is low (Wareing et al. 2003).

Nearly all important iron-related genes are expressed in the kidney; only expression of hepcidin remains controversial. Most studies indicate that hepcidin is not expressed in the kidney, while in some studies hepcidin mRNA has been detected in the kidney. However, hepcidin peptide has been localized to the kidney (Muckenthaler et al. 2008, Ludwiczek et al. 2005, Kulaksiz et al. 2005). For example, both IRPs, both ferritins, TfR1, transferrin, DMT1, Fpn, Dcytb and hephaestin are expressed in the kidney, although many of them in lower levels than in the liver (Muckenthaler et al. 2008, Ludwiczek et al. 2005). Expression of some of these genes has been studied in *Hfe*$^{-/-}$ mice; in knock out animals the expression of Dcytb, hephaestin, Fpn and L-ferritin was significantly lower than in wild type mice and the levels of DMT1 decreased in the iron-enriched knock outs. Also upregulation of L-ferritin and downregulation of TfR1 were observed in response to dietary iron supplementation (Ludwiczek et al. 2005). The bioactive hepcidin peptide is detected in the tubules of the renal cortex, medulla and papilla; especially in the epithelial cells of these compartments (Kulaksiz et al. 2005). Thus, hepcidin is likely to be involved in a sophisticated regulation of renal iron transport by modulating the levels of Fpn and DMT1 and lower levels circulating hepcidin may result in reduced renal DMT1 and Fpn expression and reduced renal iron excretion (Kulaksiz et al. 2005, Ludwiczek et al. 2005).

To date, the renal IRE/IRP system remains poorly characterized, even though both IRPs are expressed in the kidney, and this is the tissue where IRP1 is most highly expressed (Muckenthaler et al. 2008, Meyron-Holtz et al. 2004). Animals that lack IRP1 are unable to repress ferritin synthesis fully under conditions of iron deficiency. However, IRP1 binding activity is not

significantly altered by dietary iron challenge in the kidney, whereas IRP2 activity is not detectable in these conditions (Meyron-Holtz et al. 2004, Ludwiczek et al. 2005). In the kidney of *IRP1*$^{-/-}$ animals IRP2 can not compensate fully the activity of IRP1 and failure to repress ferritin synthesis leads to even more severe iron deficiency, because ferritin binds efficiently to free iron (Meyron-Holtz et al. 2004, Zhang et al. 2007). The high expression of IRP1 in the kidney may be partially explained by its aconitase activity. IRP1 is highly expressed in proximal tubules of the kidney and because proximal tubule reabsorbs 75 to 90% of the citrate that enters the glomerular filtrate, cytosolic aconitase activity may be needed at this location. Interstitial fibroblasts in the kidney secrete EPO as a respond to the hypoxia that results from decreased erythrocyte oxygen-carrying capacity. EPO production is significantly elevated in animals lacking IRP2 because of the anemia that results from incapability to repress ferritin synthesis and stabilize TfR1 mRNA. The activation of HIFs mediate the stimulation of EPO secretion and at the same time HIFs can independently increase the amount of both TfR1 and transferrin mRNA (Zhang et al. 2007).

2.3 Hereditary Hemochromatosis

2.3.1 General

HH is described as an iron overload disorder caused by a failure to prevent excessive absorption of dietary iron. It is characterized by progressive parenchymal iron overload with the potential for multiorgan damage and disease (Pietrangelo 2006). Patients with hemochromatosis absorb two to three times as much dietary iron as healthy persons, and their liver iron content can reach up to 25-30 g, whereas normal liver iron content is 0.3-1 g (Andrews 1999, Pietrangelo 2006). HH has four basic features; hereditary nature, increasing plasma transferrin saturation, progressive parenchymal iron deposits and non-impaired erythropoiesis and optimal response to therapeutic phlebotomy. Organs with progressive iron deposition include the liver, endocrine glands, heart, joints and skin (Pietrangelo 2006, Franchini & Veneri 2005). Early symptoms of HH are for example chronic fatigue, joint and muscle pain, decreased libido, lethargy and hepatomegaly. Untreated HH can lead to liver fibrosis and chirrhosis, hepatocellular carcinomas, heart failures and arrhytmias and insulin-dependet diabetes. Clinical expression of iron overload and its symptoms are more common in men than in women because women have greater blood losses due to menstrual cycles and pregnancies (Franchini & Veneri 2005).

Diagnosis of HH can be made using both biochemical and genetic tests, which make early diagnosis possible. The diagnosis can often be made before any clinical symptoms. Biochemical tests include evaluation of transferrin saturation and serum ferritin levels (Franchini & Veneri 2005). Transferrin saturation is the most sensitive and the earliest laboratory test for evaluation of body iron accumulation. The cuttoff value for diagnosing HH is usually 45%, whereas normal transferrin saturation is about 30%. HH patients may have transferrin saturation over 80%. The second biochemical marker for HH is serum ferritin. Levels over 200 μg/l in females and over 300 μg/l in males are considered pathologic. If serum ferritin levels exceed 1000 μg/l the state of HH is defined as severe and a liver biopsy must be performed to evaluate the state of liver damage. When these biochemical tests are used, it is important to rule out a wide range of inflammatory conditions, because they may also increase the levels of transferrin saturation and serum ferritin (Franchini & Veneri 2005, Brissot & de Bels 2006). Genetic tests include tests for mutations in *Hfe* and other genes known to be mutated in HH (Franchini & Veneri 2005). Usually the first gene to be tested is *Hfe*, but in some cases all existing tests must be performed and still the cause of the disease cannot be declared (Brissot & de Bels 2006).

The usual treatment of HH after 1950 has been therapeutic phlebotomy, which is the most effective, safest and most economical way to treat HH. In therapeutic phlebotomy one unit of blood (350-500 ml), containing 200 to 250 mg iron, is removed. At the beginning of the treatment one unit of blood is removed once or twice a week, depending on the patient's hematologic and subjective tolerance, until the patient has mild hypoferritinemia. In mild hypoferritinemia tranferrin saturation is below 50% and serum ferritin level below 50 μg/l. After this, phlebotomy is continued to keep the serum ferritin level below 50 μg/l; for women phlebotomy is needed one to two times a year and for men three to four times a year. Importantly, if phlebotomy is started before irreversible liver damage, patients have a normal life expectancy. The efficiency of the treatment could be improved by the use of EPO as a concomitant, using iron chelation drugs and finally by modifying the patient's diet. Patients with HH should avoid iron supplementation and restrict their intake of vitamin C because it facilitates the absorption of iron. Also alcohol and red meat should be avoided (Andrews 1999, Franchini & Veneri 2005).

2.3.2 HFE-mediated Hereditary Hemochromatosis

HH caused by mutations in *Hfe* is also called type 1 HH (Robson et al. 2004). The most common mutations in *Hfe* were found in 1996; the C282Y and the H63D mutations (Feder et al. 1996). Homozygosity for C282Y is found in more than 90% of North European patients with HH and over 80% of North American patients and its prevalence decreases from northern to southern Europe (Franchini & Veneri 2005). It is thought that the C282Y mutation was inherited from Celtic ancestor living 60 to 70 generations ago, thus the mutation is restricted to people of North West European origin (Andrews 1999, Robson et al. 2004). The mutation H63D is distributed worldwide, but the highest frequency of this mutation is among Basques and over 75% of individuals heterozygous for C282Y, are also heterozygous for H63D (Franchini & Veneri 2005, Robson et al. 2004). Another quite common mutation was defined in 1999, the S65C mutation. It is shown to account for 8% of hemochromatosis chromosomes that were neither C282Y nor H63D. At present at least 20 other mutations affecting *Hfe* are known and nearly all known mutations are inherited in recessive form (Figure 5) (Franchini & Verneri 2005, Robson et al. 2004). HFE-mediated HH usually comes clinically apparent during the 4^{th} or 5^{th} decade of life because of slow progressive accumulation of iron in various organs. However, penetrance of C282Y is quite low and the H63D and S65C mutations cause a milder form of HH (Franchini & Veneri 2005).

Effects of C282Y and H63D have been studied intensively. The C282Y mutation interrupts the formation of a disulfide bond essential for HFE's interaction with β_2-microglobulin (Figure 5) (Pietrangelo 2005, Feder et al. 1996). Interaction with β_2-microglobulin is necessary for transport of HFE to the cell surface, thus impaired interaction results in reduced amount of HFE delivered to the cell surface and blockage of the protein in the middle Golgi compartment (Waheed et al. 1997). Lack of HFE in the plasma membrane eliminates the interaction between TfR1 and HFE and thus affects signaling cascades (Feder et al. 1998, Pietrangelo 2006). The H63D mutant protein associates with β_2-microglobulin, and the complex is normally transported to the plasma membrane allowing normal HFE-TfR1 interaction. It has been suggested that the H63D mutation reduces affinity of HFE for an iron sensor protein or an iron binding protein present inside the cell or on the cell surface or it cannot reduce TfR1's affinity for transferrin (Waheed et al. 1997, Feder et al. 1998). Altogether, mutations in HFE cause aberrantly low hepcidin expression, which in turn leads to increased free iron in the circulation, thus HFE must be expressed in hepatocytes to prevent hemochromatosis (Bridle et al. 2003, Vujic Spasic et al. 2008).

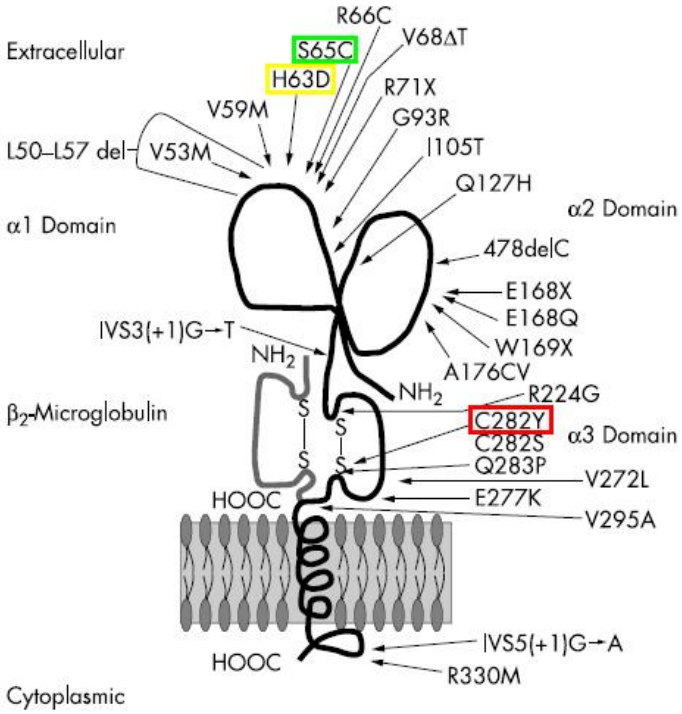

Figure 5. Mutations detected in HFE. The most common mutations; C282Y, H63D and S65C are marked with different colours. Figure from Robson et al. 2004.

2.3.3 Other Types of Hereditary Hemochromatosis

Type 2 HH is also called juvenile hemochromatosis (JH) because of its severity and early onset. It is, like HFE-mediated HH, autosomal recessive disorder and it consists of two types, 2A and 2B. Type 2A JH is caused by mutations in *HJV* gene and type 2B by mutations in *hepcidin* gene, of which type 2B is the more severe (Franchini & Veneri 2005, Pietrangelo 2006). JH is the most severe form of HH; it exhibits a faster progression than the other forms of HH. Equal numbers of females and males are affected and symptoms, including cardiomyopathy and endocrinopathy, appear earlier than in HFE-mediated HH, death before age of 30 is not unusual (Robson et al. 2004, Pietrangelo 2006). To date, 23 mutations have been identified in 43 JH families, the majority of which can be located in *HJV* gene. Only few mutations have been identified in *hepcidin* gene (Pietrangelo 2006). Most of the mutations in *HJV* are nonsense mutations which generate premature termination codons or missense substitutions affecting conserved amino acid residues but also frameshift mutations have been observed. Most of these mutations are private (Papanikolaou et al. 2004, Robson et al. 2004). Mutations in *hepcidin* include a frameshift mutation which leads to

elongated prohepcidin peptide and disordered cysteine motif, a nonsense mutation (R56X) which leads to truncated hepcidin molecule lacking all mature peptide sequences, and a missense mutation (C79R) which disrupts formation of disulfide bonds (Roetto et al. 2003, Robson et al. 2004). Digenic inheritance of both *hepcidin* and *Hfe* has been detected; these heterozygous mutations lead to increased risk of clinically expressed disease (Pietrangelo 2006).

Mutations in *TfR2* are the cause of type 3 HH, which is clinically equal to type 1 HH (Pietrangelo 2006). Mutations in *TfR2* are private and very rare; they include nonsense, missense and frameshift mutations (Robson et al. 2004). The first to be detected was a nonsense mutation (Y250X) leading to a truncated protein. To date for example mutations E60X, M172K, R455Q, Q690P and V221I have been described (Camaschella et al. 2000, Robson et al. 2004). Also mutations in *TfR2* can be inherited in combination with other mutant HH-related proteins, digenic inheritance often leads to more severe phenotypes (Pietrangelo 2006).

Ferroportin disease (FD) is sometimes called type 4 HH. It differs from other types of HH in many ways, for example it has autosomal-dominant inheritance and hepcidin levels are either normal or higher than normal (Pietrangelo 2006, De Domenico et al. 2006). Mutations in *Fpn* lead to two different clinical manifestations. One is indistinguishable from that of traditional HH with high transferrin saturation, hepatocyte iron loading and decreased iron in macrophages. The other differs from traditional HH in that Kupffer cells show early iron loading, serum ferritin is high and transferrin saturation is low (De Domenico et al. 2006). All known mutations in *Fpn* are missense mutations and the majority of them localize to the external face of the protein, in the extracellular loop between transmembrane domains 3 and 4 (De Domenico et al. 2006, Robson et al. 2004). The first mutations described were A77D and N144H. A77D mutation reduces the export activity of Fpn and N144H may disrupt folding of one transmembrane region of Fpn (Montosi et al. 2001, Njajou et al. 2001). Mutations in *Fpn* can be divided in two groups, one leading to traditional HH phenotype and the other leading to non-traditional HH phenotype. The first group consist of mutations that lead to inability to transport iron; these mutations are often linked to impaired plasma membrane localization of Fpn and the mutated protein does not respond to hepcidin. The second group of Fpn mutants are those that are appropriately targeted to the plasma membrane and are capable of exporting iron but which do not respond to hepcidin, thus they export iron in all circumstances. These mutants have been shown to bind hepcidin but the binding does not result in Fpn internalization and degradation. Patients with FD have both normal and mutant alleles of *Fpn*. The product of the normal allele may be sufficient to mediate intestinal iron export, but not to

mediate macrophage iron export. Therefore, the presence of only one mutant allele leads to clinical expression of HH and the disease is inherited in dominant form (De Domenico et al. 2006).

2.4 Mouse Models of Iron Metabolism

2.4.1 General

The first mouse models of iron metabolism were generated by breeding anemic mice that had spontaneous genetic defects. Phenotypes of these mice have been studied in detail and they provided information about defects in iron metabolism and genes involved in iron metabolism. The *hpx* mouse is a model for iron deficiency, these mice have severe microcytic, hypchromic anemia and all their non-hematopoietic tissues develop iron overload. The phenotype is caused by impaired transferrin cycle, which is based on inability to produce normal transferrin. The intestinal iron importer DMT1 is mutated in two animal models, the *mk* mouse and the *b* rat. The *mk* mice have severe microcytic anemia and their viability is low, also the *b* rat suffers from anemia although their state is not as severe as that of *mk* mice. DMT1 was discovered based on these animal models and its role in both intestinal absorption and the transferrin cycle was established. Altered iron export is detected in the *sla* mice which have sex-linked anemia; homozygous females and hemizygous males are born anemic because of a defect in placental iron transfer and dietary iron uptake. The *sla* gene was identified and named hephaestin. Because the *mk* mice develop much severe anemia than the *sla* mice, hephaestin was suggested to be important but not essential for iron metabolism (Andrews 2000).

Genetically engineered animal (especially mouse) models have been used widely to study functions of genes known to encode proteins important for iron homeostasis and in HH. To date many animal models for iron overload and hemochromatosis have been created (Andrews 2000). *Tfr1* was among the first engineered genes in mice. The $Trfr^{-/-}$ mice are homozygous for a *Tfr1* null allele, and all die before birth and embryonic day (E) 12.5. Before death, homozygotes for null allele have signs of fetal hydrops, growth retardation, pericardial effusions and anemia. All these symptoms are shown to be the result of the absence of a functional transferrin cycle, which is shown to be essential for normal growth and differentiation. The $Trfr^{+/-}$ heterozygotes mice develop normally, although they have abnormalities in erythropoiesis and iron homeostasis and their liver and spleen iron content is lower than that of wild-type littermates (Levy et al. 1999a). A mouse model was also created for the iron transporter Fpn. Like $Trfr^{-/-}$, also mice homozygous for null allele in *Fpn* gene ($Fpn^{null/null}$ mice)

die before birth, because they have a defect in iron transfer from the mother. Generated *Fpn*$^{null/+}$ mice are viable, although they are not a faithful model of HH, because their hepatic iron stores are not elevated. The *Fpn* gene has been also conditionally mutated; the *Meox2-Cre;Fpn*$^{flox/flox}$ mice express inactive Fpn in all tissues except placenta and extraembryonic visceral endoderm and the *Cre-ER*^{T2}*;Fpn*$^{flox/flox}$ mice express Fpn in all tissues except the intestine. Mice from both models suffered from iron deficiency, confirming the essential role of Fpn during pregnancy and in intestinal iron absorption (Donovan et al. 2005). The luminal transport system of iron is impaired in the *mk* mice, which have mutated DMT1. However, the mouse model for Dcytb null allele indicates that its function is not essential for dietary non-heme iron reduction and therefore for iron absorption (Gunshin et al. 2005).

The function of IRPs has also been studied using knock out mouse models. *Ireb2*$^{-/-}$ mice (IRP2 deficient mice) older than six months of age developed a progressive neurodegenerative disease and their serum ferritins were significantly elevated. They also had increased iron content in their liver and duodenal mucosa. All these symptoms were caused by absent IRP activity, which lead to increased levels of ferritin and apical and basolateral iron transport proteins. It was proposed that IRP2 contributes a high portion of IRP activity at least in neurons and intestinal mucosa (LaVaute et al. 2001). However, *Irp1*$^{-/-}$ mice did not have any pathological phenotype, all their major tissues and glands were histologically normal and also their serum chemistry was normal. Elevated ferritin levels were found only in the kidney and brown fat tissue and, therefore it was suggested that IRP2 is able to contribute fully the IRP activity in all tissues except kidney and brown fat tissue (Meyron-Holtz et al. 2004).

There are many mouse models for iron overload and HH. Most of them are generated by knocking out genes that encode proteins important in regulation of iron homeostasis, as *Hfe*, *β_2–microglubulin*, *Hjv* and *hepcidin*. β_2–microglubulin deficient mice, (*β2m−/−* mice) develop iron overload in the liver and their TfR1, L-ferritin and Fpn mRNA levels are decreased. They also present abnormally low hepcidin levels, which may be the cause of the iron accumulation in the liver. Lack of β_2–microglubulin affects also iron homeostasis in duodenum, where the expression of both DMT1 and Fpn is slightly increased (Muckenthaler et al. 2004). Mouse models of JH also exist; both HJV and hepcidin deficient mice have been engineered. HJV deficient mice were generated simultaneously by two research groups. Both *Hjv*$^{-/-}$ and *Hjv*-mutant mice showed massive iron overload in the liver, pancreas and heart and decreased iron accumulation in the spleen and duodenal enterocytes. At birth, HJV deficient mice do not differ from their wild type littermates,

but at four months of age they reach plateau levels of iron accumulation in tissues and their transferrin saturation is close to 100%. In these mice hepcidin mRNA levels are undetectable and as a result of this, Fpn protein expression is significantly increased. Total lack of hepcidin causes massive iron overload and, although mutant mice do not suffer from pathological conditions associated with JH, this animal model is a satisfactory model for JH (Niederkofler et al. 2005, Huang et al. 2005). The function of hepcidin has been studied widely using mouse models. The first hepcidin lacking mouse model was the *Usf2*$^{-/-}$ (upstream stimulatory factor 2) which also showed increased liver iron accumulation. The *Usf2* gene is located in close physical proximity to both *hepcidin* genes in the mouse genome, hence it was thought that the recombination event had also disrupted both *hepcidin* genes. However, the *hepcidin* genes are present in *Usf2*$^{-/-}$ mice and it was suggested that USF2 may regulate the expression of both *hepcidin* genes (Nicolas et al. 2001). The role of USF2 in the control of hepcidin expression was later disproved, and it was shown that lack of hepcidin caused the iron overload observed in the *Usf2*$^{-/-}$ mice (Nicolas et al. 2002a). The hepcidin 1 deficient and USF2 and hepcidin 2 expressing *Hepc1*$^{-/-}$ mouse model was later generated. Like *Hjv*$^{-/-}$ mice, also *Hepc1*$^{-/-}$ mice were born with no visible phenotype, but at four months of age they had massive iron accumulation in the liver, pancreas and heart and increased serum ferritin levels. Their phenotype is very similar to the *Usf2*$^{-/-}$ mice and the *Hjv*$^{-/-}$ mice and it mimics the phenotype in JH (Lesbordes-Brion et al. 2006). The role of hepcidin has also been studied using mouse models that overexpress hepcidin. The majority of these *Ttr-Hepc1* transgenic mice die after birth, likely from severe anemia; these mice have abnormal erythrocyte morphology and decreased iron levels. The early death may be caused by embryonal expression of hepcidin because in wild type animals hepcidin expression only reaches high levels in adult liver and, during embryonal development, endogenous hepcidin is not expressed at detectable levels. This model confirms the role of hepcidin as a negative regulator of iron absorption and transport (Nicolas et al. 2002a).

Animal models for classic HH phenotype can be obtained generating *Hfe* or *Tfr2* deficient mice. The *Tfr2*-KO mice develop significant iron overload by ten weeks of age and their transferrin saturation is significantly elevated; the gradient of iron accumulation in hepatocytes observed in these mice is typical for patients suffering from *Tfr2* associated HH. In these mice DMT1 and TfR1 levels are significantly induced and HFE and HJV levels are slightly reduced, causing a failure in the upregulation of hepcidin expression. Thus this mouse model is suitable for TfR2 associated HH (Wallace et al. 2005).

2.4.2 The *Hfe*$^{-/-}$ Mice

After the identification of HFE and its role in iron homeostasis, a HFE deficient mouse model was soon generated by deleting a specific area of *Hfe* gene (Zhou et al. 1998). All *Hfe*$^{-/-}$ mice developed normally and were born healthy, although expression of HFE was not detected. Both liver iron content and transferrin saturation were significantly increased in both *Hfe*$^{-/-}$ and *Hfe*$^{+/-}$ mice compared to wild type littermates. The effects of an iron rich diet were also studied; wild type mice fed with iron-enriched diet also showed increased liver iron contents, transferrin saturation and spleen iron content. Moreover, *Hfe*$^{-/-}$ mice showed even more elevated levels of these parameters, except for spleen iron accumulation, that was lower than in wild type mice fed with iron-enriched diet. This resistance of the spleen to iron loading, iron accumulation in the liver and increased transferrin saturation are similar to findings in human HH, hence the mouse model faithfully recapitulates the biochemical abnormalities and the histopatholgy of HH (Zhou et al. 1998, Levy et al. 1999). A mouse model for the most common mutation in *Hfe*, the C282Y, was also generated. The *Hfe Y/Y* mice have a phenotype intermediate between *Hfe*$^{-/-}$ mice and wild type. Accordingly it can be inferred that the C282Y mutation does not completely disrupt the function of HFE and the iron loading is not as severe as in mice having the null allele. These mice still have elevated iron accumulation in the liver, elevated transferrin saturation and decreased iron content of the spleen as do the *Hfe*$^{-/-}$ mice and patients suffering from HFE associated HH (Levy et al. 1999b).

Hfe$^{-/-}$ mice have been inbred with other mice to serve as mouse models for iron metabolism to evaluate potential genetic modifiers of mutations in the *Hfe* locus. The *Hfe*$^{-/-}$ mice inbred with *β2m*$^{-/-}$ mice have greater iron content in the liver than do the *Hfe*$^{-/-}$ mice. This is thought to be due to the fact that in the *β2m*$^{-/-}$ mice the expression of DMT1 is also increased and therefore iron absorption is elevated (Levy et al. 2000, Muckenthaler et al. 2004). Iron accumulation in the liver is decreased in mice carrying null alleles in both *Hfe* and *Dmt1*. These mice are generated by interbreeding the *mk* mice and the *Hfe*$^{-/-}$ mice. The iron accumulation is prevented by mutations in DMT1 and therefore it is presumed that iron accumulation develops mainly through an absorption pathway mediated by DMT1. Furthermore, *Hfe*$^{-/-}$ mice have been interbreeded with the *sla* mice and the *Trfr*$^{+/-}$ mice. Mice homozygous for mutations in both *hephaestin* and *Hfe* have less hepatic iron than the *Hfe*$^{-/-}$ mice, but more than the *sla* mice and wild type mice. However, the iron accumulates in intestinal mucosa because of diminished basolateral iron export. Hepatic iron loading greater than in the *Hfe*$^{-/-}$ mice was detected in mice lacking *Hfe* and having only one allele of *Tfr1* (Levy et al. 2000).

Mice with mutations in *Hfe* absorb normally more iron than do wild type mice. In iron-supplemented diet the amount of iron absorbed decreases, but also in this case HFE deficient mice absorb more iron than wild type mice. *Hfe*$^{-/-}$ mice present an augmented iron absorption also in response to reduced iron stores and accelerated erythropoiesis. Interestingly, when transferrin saturation reached the plateau level at five months of age, iron absorption was downregulated in these mice. Based on this study, HFE seems not to have the principal role in the regulation of iron homeostasis (Ajioka et al. 2002). It was also shown that transferrin-bound iron uptake is decreased in the duodenum of the *Hfe*$^{-/-}$ mice and when transferrin saturation increases, the uptake of transferrin-bound iron does not increase as much as in the wild type mice. This may lead to relatively iron deficient enterocytes and increased IRP activity, which in turn leads to increased DMT1 and Fpn activity and increased iron absorption. This kind of expression patterns are also observed in HH patients (Trinder et al. 2002).

2.5 Theory behind Methods

2.5.1 Principles of Microarray

Microarrays are microscope slides that contain an ordered series of samples; for example DNA, RNA, protein or tissue. The size of microarrays can vary widely; some arrays contain a few hundred of samples whereas others represent thousands of samples. The samples are in ordered fashion and therefore the data obtained from the microarray can be tracked back to any of the samples (Wong 2005). The most commonly used microarray type is the DNA microarray which can be used for expression profiling or genotyping. Usually mRNA expression is studied using cDNA microarrays which allow simultaneous determination of the mRNA levels of many genes; some arrays contain probes for an entire genome. There are three main applications for cDNA microarrays. One of them is an application which treats microarray data as a massively parallel expression assay; the data is used to determine genes that undergo changes in their expression profiles in response to particular treatments. The other application involves treating expression profiles as descriptions of collective behaviours; this application reveals for example the state of a cell with the help of detected expression levels of tens of thousands of genes. The last application is the mining of large expression profiling databases to characterize expression patterns of genes of interest over a wide range of tissue types, after various treatments or in different mutants. (Katagiri & Glazebrook 2004).

There are many sources of variation in a microarray experiment; biological variation, technical variation and measurement errors. Therefore the experiment should be carefully optimized and designed based on statistical considerations, such as randomization (Churchill 2002). Biological variation refers to real differences in the level of mRNA species between two samples that are replicates. This variation is influenced by genetic or environmental factors. For example, using two inbred mice as replicates leads to great biological variation and therefore lower statistical power of the results. Increasing numbers of replicates can sometimes lower the biological variation and at the same time increase the statistical significance. Technical variation results from variations in the mechanisms of the microarray experiment itself; it is introduced during the extraction, labeling and hybridization of the samples. Measurement error is associated with reading the fluorescent signals which may be affected by factors such as dust on the array (Churhill 2002, Katagiri & Glazebrook 2004).

Microarrays can be produced in many ways; spotted arrays are manufactured by printing probes to the surface, in *in situ* synthesis the probes are directly synthesized to a solid support material with the help of photolitography or arrays can be produced by binding the probe to a small bead that is present on the chip. Also the length of the probes varies between types of array; for example Affymetrix arrays that are synthesized directly to the membrane have quite short probes, typically 25 nucleotides, whereas bead-based Illumina probes are often 50 nucleotides long. Microarrays usually contain several probes for one gene to improve accurancy of the array (Wong 2005, Katagiri &Glazebrook 2004). To profile gene expression of certain samples, the first step is to isolate RNA and optionally reverse transcript it to cDNA. Then cDNA or RNA samples can be labelled using either fluorescent dyes or radioactive isotopes. After labelling cDNA or RNA is hybridized to the arrays and hybridization signals are detected using a laser scanner or a phosphorimager, resulting in the production of digital images. These images are the essential raw data for microarrays, which is further processed by using specialized imaging software (Hess et al. 2001, Wong 2005).

After scanning the signal value for each probe, the spot should be calculated. Because signal intensity is not uniform over the spot, careful consideration must be given to the best way to capture both the information relating to the amount of labelled cDNA on a given spot and also some measure of the quality of this information. There are many commercial programs that analyze the raw data and usually the average signal value is calculated using total spot intensity, background signal level, detected measured area of spot and variance of pixel intensity within detected spot. Background correction is crucial to estimate true expression levels because of nonspesific

background signal due to contaminations and nonspesific hybridization. After obtaining a signal value for each spot, values from each spot must be combined to yield a value for each gene (Katagiri & Glazebrook 2004, Hess et al. 2001). The next step in microarray analysis is to check the quality of the obtained data. This includes for example checking the quality of replicates, observing outliers and filtering bad data. The quality of replicates can be checked with simple methods, like scatter plots and pairwaise correlations, and hierarchical clustering techniques. Scatter plots are plots in which two to three replicates can be plotted against each other and if the replicates are completely similar, the data points fall onto a perfectly straight line. This analysis can be further improved by fitting a linear regression line to the data; Pearson's correlation coefficient should be in the range of 0.6 to 0.9 for the data. The quality of several replicates can be measured by hierarchical clustering, in which the distance between replicates in the dendogram tells whether replicates are good or not. Sometimes a replicate that differs significantly from the other replicates can be excluded from further analysis, although excluding replicate results in massive loss of information obtained from a microarray study. Outliers can occur in several different layers. For example, entire chips can deviate from other chips or a gene can deviate from other replicates of the same gene. Usually outliers can be excluded when the data is filtered. The idea of filtering is simple; to remove data that one has no confidence in and to proceed with remaining data. For example data that has intensity values smaller than certain cutoff value can not be trusted and it can be excluded by filtering. Another application is to filter out genes that show no change in their expression between two groups that are examined in the study, this filtering of uninteresting data is usually performed after the normalization (Tuimala 2005).

Normalization means to make the data more normally distributed and it is required because there are many sources of systemic variation in microarray experiments and because the expression levels are measured relative to the amount of labeled mRNA in the hybridization probes. Thus, normalization enables comparison of microarrays from one array to another. Data can be normalized in per-chip and per-gene fashion. Per-chip normalization is needed in multichip arrays because of the potential differences in experimental and processing conditions; per-chip normalization assumes that the median intensity stays relatively constant during the experiment, thus the median intensity of every chip is brought to the same level. Per-gene normalization accounts for the difference in the detection efficiency between different spots and it enables the comparison of relative gene expression levels and it can be used in tandem with per-chip normalization. There are different ways to perform the normalization; one is to normalize the data against a putative housekeeping gene or group of such genes. This application assumes that the

expression of the housekeeping genes stays relatively constant, which is not always the case; thus using large number of housekeeping genes is recommended. Another way to normalize data is to divide the observed expression values by the median value for the spots measured (Tuimala et al. 2005, Hess et al. 2001). After filtering and normalization further analysis of the data can be performed. Usually these analysis methods consist of different statistical tools, which should be selected carefully to fit the handled data (Katagiri & Glazebrook 2004).

2.5.2 Principles of Quantitative RT-PCR

Quantitative PCR (Q-PCR) or real-time PCR was developed to quantify the amount of DNA or RNA in a sample, because existing methods were only semi-quantitative or not quantitative at all. For example traditional PCR can only show whether a sample contains certain template or not, the initial amount of the template can not be determined. In Q-PCR the amount of product formed is monitored during the reaction by measuring the fluorescence of dyes or probes introduced into the reaction that is proportional to the product formed. This way the amount of the product can be determined anytime during the reaction (Kubista et al. 2006). Q-PCR is widely used to study gene expression patterns by quantifying steady-state mRNA levels, therefore the most common application of Q-PCR is called Q-RT-PCR (Bustin 2002).

The basic idea of Q-PCR is the same as in traditional PCR; a certain product is amplified using reagents such as specific primers, dNTPs, DNA polymerase and magnesium ions. The amplification is performed by temperature cycling; high temperature is applied to separate the strands of DNA, following lower temperature lets the primers anneal to the template and finally temperature is raised to a temperature optimal for the DNA polymerase, and the product is synthesized. The basic difference between Q-PCR and traditional PCR is that Q-PCR needs a fluorescent reporter that binds to the product formed and reports its presence by fluorencence. During the initial cycles the fluorescence signal is weak and can not be separated from the unspecific background signal. As the amount of product increases, the signal begins to increase exponentially and finally the signal is saturated when some of the reagents has run out. The amount of product formed can be verified at any time point during the exponential increase of the signal (Figure 6). The difference between two samples is quantified by comparing the number of amplification cycles required for the samples' response curves to reach a particular threshold fluorescence signal level; the number of cycles required to reach threshold is called the CT value (Figure 6). The absolute or relative amount of

product can be determined using a standard curve that is formed by serial dilution of a standard and plotting obtained CT values against the logarithm of the concentration of the standard. The amount of the product in a sample can then be determined based on its CT value. Also the efficiency of a PCR assay can be estimated from the slope of a standard curve; efficiency = $10^{-1/slope}$-1. Efficiency is usually around 90%. Even though the efficiency of the standard dilution series is good, it may decrease when using real biological samples because they may contain common PCR inhibitors, such as heme and lipids (Kubista et al. 2006). The sensitivity of the experiment can also be affected by competing side reactions like mispriming and primer dimerisation. These reactions can be avoided by careful design of the primers and probes and by using heat-activatable enzymes that provide more specific hot start PCR conditions (Bustin 2002).

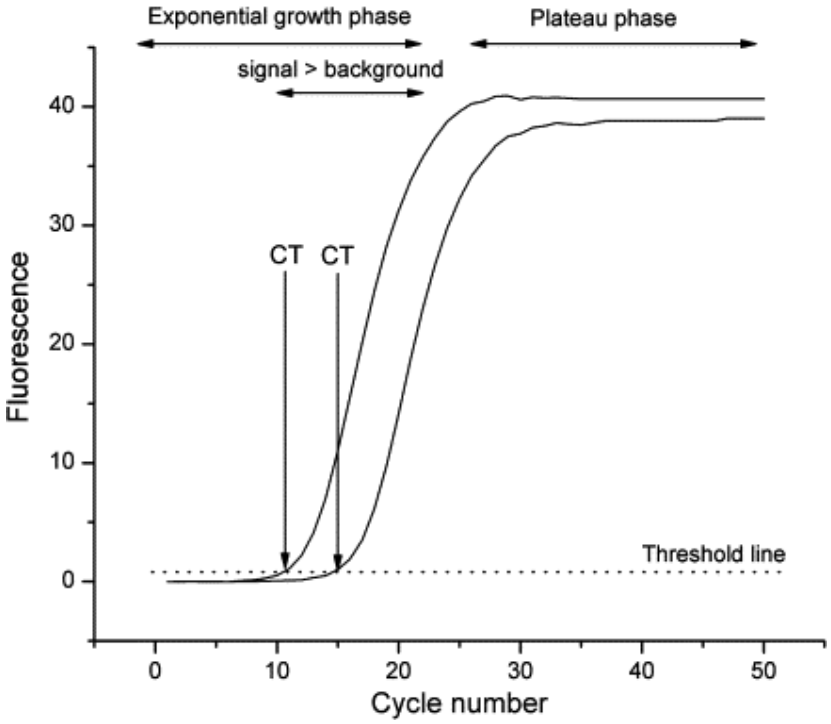

Figure 6. Q-RT-PCR response curves. The threshold line can be located at any level in the exponential growth phase. CT values are obtained from the crossing points of the threshold line and the sample curves. Figure adopted from Kubista et al. 2006.

Nowadays fluorescence is exclusively used as the detection method in Q-PCR, sequence specific probes and non-specific labels are available as reporters. Most popular detection mechanisms are asymmetric cyanine dyes such as SYBR Green I and BEBO which can be used with both non-labeled probes and primers (Kubista et al. 2006, Bustin 2002). Both dyes have virtually no fluorescence when they are free in solution but they become brightly fluorescent when they bind to any double stranded DNA. The fluorescence increases with the amount of double stranded product

formed, thus these dyes are excellent for quantifying the PCR product when the only double stranded DNA in the solution is the product. When using non-specific dyes also the specifity of the product can be determined by doing a melting curve. In this kind of analysis temperature is slowly raised and when the melting temperature of the product is reached, the strands are separated and the fluorescence disappears (Kubista et al. 2006). Another detection application is the use of labeled primers and probes which are usually based on nucleic acids or their synthetic analogues like peptide nucleic acid (PNA) or locked nucleic acids (LNA). In PNAs the phosphate backbone is replaced with repeating N-(2.aminoethyl)-glycine units linked by peptide bonds and they are useful probes for Q-PCR assays because of the high stability of the complex that they form with DNA (Kubista et al. 2006, Bustin et al. 2002). The detection mechanism of the labeled primers and probes is based on changes on the fluorescence of the markers when the primer or probe is bound to DNA. Usually they contain two different dyes; for example Taqman probes, Molecular Beacons, Hybridization probes and the Lion probes have two dyes that form a donor-acceptor pair that transfers energy and forms a fluorescence signal when the probe is bound to DNA. Nowadays, the other dye is usually a quencher. An example of a probe based on a single dye is represented by the LightUp probes. The advantage of using probes is that several products can be amplified in the same tube and detected in parallel, whereas the signal from non-specific dyes can not be separated to different products. However, dyes are much cheaper than labeled probes and primers (Kubista et al. 2006).

To date, many instruments for Q-PCR have been established, most of them are true real-time systems in which progress can be monitored at any time during thermal cycling, rather than having to wait until the end of the run. The main differences between them are the excitation and emission wavelengths that are available, the speed, and the number of reactions that can be run at the same time. Also reaction containers and lamps used for excitation of the dyes differ; the most popular lamps used are lasers and tungsten-halogen lamps (Kubista et al. 2006, Bustin 2002). Examples of Q-PCR instruments are the Applied Biosystems 7300 and 7500 instruments, the Exicycler from Bioneer, the iCycler from Biorad and the LightCycler 480 system from Roche (Kubista et al. 2006).

A critical step for accurate and sensitive gene expression measurements is the RT step; the amount of cDNA produced must accurately represent the mRNA input amounts. Another important step for sensitive quantification of mRNA is elimination of genomic DNA from the sample. This is usually performed by DNase treatment when RNA is isolated. Also the use of intron spanning primers lowers the risk of genomic DNA contamination (Bustin 2002, Kubista et al. 2006). The three basic

priming strategies in RT reactions are based on oligo(dT) primers, random sequence primers and gene specific primers. Oligo(dT) primers should perform the reverse transcription for all mRNA molecules, random primers (usually hexamer or nonamers) for all RNA, and the gene specific primers for mRNA of a certain gene. There are two widely used reverse transcriptases; the Moloney Murine Leukemia Virus (MMLV) and the Avian Myeloblatosis Virus (AMV) (Kubista et al. 2006).

The comparison of two samples is not reliable without normalization; it is required to compensate the differences in the amount of biological material in the tested samples. Reliable methods for normalization are normalization of the samples to total RNA content of the sample, to ribosomal RNA of the sample, to externally added RNA sample or to internal reference genes (housekeeping genes). The use of housekeeping genes is the most popular way to normalize although there is no universal housekeeping gene with a constant expression in all tissues and conditions; therefore, the housekeeping genes used must be carefully chosen (Kubista et al. 2006, Bustin 2002).

It is shown that correlations between microarray and Q-RT-PCR data are strong and that Q-RT-PCR is a powerful mechanism to confirm and further study the results obtained from microarray (Dallas et al. 2005, Kubista et al. 2006). Therefore, to first study a small number of representative samples using microarray technology to identify the genes that are most sensitive to the studied conditions and then study these genes in greater detail and in many more samples by the more sensitive and cost efficient Q-RT-PCR, is a powerful experimental strategy for expression profiling. Expression profiling by Q-RT-PCR has many important advantages to expression profiling by microarrays; for example data quality is much better, sensitivity is higher, dynamic range is wider and non-interesting genes do not interrupt the measurement. Q-RT-PCR generates a CT value for each gene selected for further studies in each sample, and because Q-RT-PCR is usually a cheaper method than microarray, the number of samples can be multiplied and hence the statistical significance of the results is commonly improved (Kubista et al. 2006).

3 AIMS OF THE STUDY

The aims of this research were:

- To study the expression of certain iron related genes in the kidney of iron overloaded mice and further understand the role of the kidney in iron homeostasis.
- To identify genes of which expression patterns are affected by primary (iron-rich diet) or secondary (*HFE* deficiency) iron overload in mice using a genome-wide mRNA expression analysis.

4 METHODS

4.1 Animals and Tissue Samples

Dietary iron overload mice were generated in the University of Oulu and the experiments were approved by the Animal Care and Use Committee of the University of Oulu. Five mice from each of three strains (Balb/c, C57BL/6, and DBA/2) were placed on a diet consisting on standard chow (Lactamin, Stockholm, Sweden) supplemented with 2% carbonyl iron (Sigma-Aldrich Sweden AB, Stockholm, Sweden) at the age of 10-12 weeks. The control groups consisted of an equivalent amount of littermates fed the standard chow diet without iron supplementation (0.02% iron). After 6 weeks of treatment, kidney samples were collected and immediately immersed in RNAlater (Ambion, Huntington, UK). The procedure carried out to obtain an *Hfe*$^{-/-}$ mouse model has been described elsewhere (Zhou et al. 1998). 5 *Hfe* knock out mice with a C57BL/6J genetic background were provided Dr. Sly and colleagues from Saint Louis University. The control group consisted of 5 male wild type littermates. Kidney samples from these mice were also stored in RNAlater (Ambion).

4.2 RNA Isolation

Total RNA was isolated using RNAeasy RNA isolation kit (Qiagen, Hilden, Germany), according to the procedure recommended by the manufacturer. Possible remaining genomic DNA was removed from the samples using RNase-free DNase (Qiagen). The concentration and purity of the samples was determined using optical density (OD) measurements at 260 and 280 nm; the ratio OD260/OD280 in all of the samples was above 2.00, indicating purity of the RNA.

4.3 Microarray

4.3.1 Microarray Analysis, Hybridization, and Scanning

Microarray studies were performed with Illumina software in the Finnish DNA Microarray Centre at Turku Centre for Biotechnology. 4 RNA samples derived from dietary iron overload C57BL/6 mice and 2 samples derived from their control group, as well as 4 RNA samples derived from *Hfe*

knock out mice and 2 from their control group were used in the microarray study. 2800 ng of total RNA was sent to Turku of which 400 ng was amplified using Illumina TotalPrep RNA Amplification kit (Ambion). During the following *in vitro* transcription reaction, which was conducted for 14 hours, the cRNA was biotinylated. The quality and the concentration of RNA/cRNA were estimated before and after amplifications using OD measurements and electrophoresis. 1.50 μg of each amplified and labeled sample was then hybridized to Illumina's Sentrix Mouse 6v1.1 Expression BeadChips (Illumina Inc., San Diego, CA) at 58°C for 17 hours according to Illumina BeadStation 500X protocol. Arrays were stained with 1μg/ml cyanine3-streptavidine (GE Healthcare Biosciences, Buckinghamshire, UK), in order to detect hybridization. The next step was to scan the arrays with Illumina BeadArray Reader as instructed by the manufacturer and finally the numerical results were extrcated with BeadStudio v3.0.19.0 without normalization or background correction.

4.3.2 Microarray Data Analysis

The data obtained from BeadStudio was analyzed using Chipster software version 1.1.1. (CSC, Helsinki, Finland). Both mouse models were regarded as independent experiments; groups consisted of 4 "treated" and 2 control samples. The quantile normalization method was used and fold change values were calculated for each probe using the same software. Quality control of the data included non-metric multidimensional scaling, dendograms, hierarchical clustering, and 2-way clustering (heatmaps). These analyses showed that in both mouse models one treated sample diverged considerably from the other three. Therefore, these outlying samples were excluded from further analyses, leaving three samples in the treated group and two in the control. The normalized data was filtered based on the probe's standard deviation (SD). The percentage of data that was filtered out was adjusted to 99.4%; implicating nearly 3SD. The remaining probes in both experiments were further filtered by fold change with +/-1.4 as the cutoff value. The KEGG pathway analysis was performed using a hypergeometric test.

4.4 Quantitative RT-PCR

4.4.1 Reverse Transcription Reactions

RNA extracts of each sample were converted to cDNA using First Strand cDNA Synthesis kit (Fermentas, Burlington, UK). A total of 3 μg of RNA was reverse transcribed using random hexamer primers according to the protocol recommended by the manufacturer. After cDNA synthesis, the obtained samples were diluted to half concentration using RNase-free water (Qiagen). These samples were used in the Q-RT-PCR reactions.

4.4.2 Obtention of Standards and Primer Design

The quantitative PCR method of choice in this study was relative quantification with external standards. This means that a standard curve must be built for each of the genes to be tested. For this purpose, dilutions of a standard solution are needed. The standard solution was obtained by amplifying the specific product of each primer set from Mouse Multiple Tissue cDNA Panel I (BD Biosciences, Palo Alto, CA) cDNA samples. Standard dilutions were made separately for each gene. Sequences of primers used in this study are shown in Appensix E. Most of the primer pairs are designed using Primer3, based on the complete cDNA sequences deposited in GenBank. The specifity of the primers was checked using NCBI Basic Local Alignment and Search Tool. If possible, in order to avoid amplification of remaining genomic DNA, the sequences of the primers from one pair were located in different exons.

In the PCR reactions performed to obtain the standards ReddyMix PCR Master Mix (ABgene, Epsom, UK) was used, containing all the reagents required in the PCR reaction, except for the primers and the DNA sample. Reactions were as follows:

ReddyMix PCR Master Mix	45 μl
forward primer (10 μM)	1 μl
reverse primer (10 μM)	1 μl
cDNA	1 μl
water	2 μl

These reactions were amplified in XP Thermal Cycler (Bioer, Hangzhou, China) or in DNA Engine Gradient Cycler (MJ Research Inc.,Watertown, MA). The follwing PCR program was used:

Denaturation	94 °C, 1 min
35 cycles of:	
Denaturatioon	94 °C, 30 sec
Annealing	specific temperature, 30 sec
Elongation	72 °C, 30 sec
Extension	72 °C, 3 min

The purity of the PCR products was confirmed using agarose gel electrophoresis. The analysis was performed in 1.5% agarose gel containing 1 µl of ethidium bromide in 100 ml of agarose gel with DNA standard GeneRuler 100 bp ladder (Fermentas). The product was purified from the gel using illustra GFX PCR DNA and Gel Band Purification kit (GE Healthcare) and the concentration of the extract was measured using OD. The amount of product in the obtained solution was calculated using the formula:

$$\text{copy number}/\mu\text{l} = \left[\frac{\text{concentration}\left[{}^{\text{ng}}/_{\mu\text{l}}\right]}{\text{product lenght} \times 660} \right] \times 6.022 \times 10^{23}$$

Serial ten-fold dilutions were done based on the copy number value ranging from 10×10^{11} to 10×10^{3} copies per µl. Six of these dilutions were used in a standard run, in the LightCycler detection system (Roche, Rotkreuz, Switzerland), from which and a standard curve was created. Standards were always run in duplicate. One of the standard dilutions was later included in each sample run, also in duplicate, to serve as a reference to calculate the relative amount of mRNA in the samples.

4.4.3 Performing Q-RT-PCR

Relative expression levels of each gene studied were assessed by quantitative real-time RT-PCR using the LightCycler detection system. The fold change values obtained from the Q-RT-PCR were

generated using 4 samples and 4 controls of dietary iron overload C57BL/6 mice and 4 samples and 3 controls of *Hfe* knock out mice. The dietary iron overload Balb/c and DBA/2 mice were used only in the expression studies of hepcidin genes; groups studied consisted of 4 samples and 4 controls. QuantiTect SYBR Green PCR kit (Qiagen, Hilden, Germany) was used as areaction mix. PCR reactions of 20 µl were done as follows:

SYBR Green Master Mix	10 µl
forward primer (10 µM)	1 µl
reverse primer (10 µM)	1 µl
RNase-free water	7 µl
template cDNA	1 µl

The amplification and detection program was (temperature, time, ramp):

Initial activation step	95 °C, 15 min, 20 °C/sec
45 cycles of	
Denaturation	94 °C, 15 sec, 20 °C/sec
Annealing	specific temperature, 20 sec, 20 °C/sec
Extension	72 °C, 15 sec, 2 °C/sec
Melting curve	95 °C, 20 °C/s
	65 °C, 20 °C/s
	95 °C, 0.1 °C/s
Cooling	40 °C, 1 min

Melting curve analysis was used to check the specificity of the obtained PCR products. Each unknown sample was tested in triplicates. Mean and SD of the three CT values for each sample were calculated and a SD cutoff value of 0.200 was considered. Accordingly, if the SD of the triplicates of a sample was greater than 0.200 the most outlying replicate was excluded and the analysis was continued with the two resting replicates. The CT values were transformed by the Lightcycler software into copy number values. The final relative expression value for each sample was the mean of copy numbers of the sample's replicates.

4.4.4 Normalization and Data Analysis

Obtained relative expression values were normalized using 4 housekeeping genes as internal controls. The normalization factor was the geometric mean of the relative expression values of *GAPDH* (glyceraldehyde-3-phosphate dehydrogenase), *SDHA* (succinate dehydrogenase complex subunit A), *HPRT1* (hypoxanthine phosphoribosyl-transferase 1), and *actB* (β-actin). Using the geometric mean of four housekeeping genes is considered to be an accurate approach to normalize for possible differences in quantity and quality of sample material (Vandesomple et al. 2002). The normalization factor can be used to obtain accurate relative gene expression levels. The normalization factor was considered as a value of 100 so that the final relative expression values were obtained by dividing the obtained relative expression level by the normalization factor and multiplying this by 100.

A relative expression value was obtained individually for every sample and mean and SD were calculated for each group. Values from treated and control groups were compared and statistical significance was tested by the Mann-Whitney epaparametric test. Statistical analyses were performed by Tiina Luukkala, from the department of biometry in the faculty of health sciences of the University of Tampere. Due to the low number of samples within each group, the statistical significance is considered as orientative.

5 RESULTS

5.1 Microarray

Table 1. Genes of which expression was regulated in both *Hfe* knock out mice and dietary iron overload mice. FC indicates fold change. The cutoff value for FC was 1.4.

Gene name	Symbol	GenBank	FC during dietary iron overload	FC in HFE knock out
cytokine inducible SH2-containing protein	Cish	NM_009895	-1.92	3.14
haptoglobin	Hp	NM_017370	-1.70	2.05
serine (or cysteine) peptidase inhibitor, clade A, member 1b	Serpina1b	NM_009244	2.66	1.90
suppressor of cytokine signaling 2	Socs2	NM_007706	-1.95	1.72
serine (or cysteine) peptidase inhibitor, clade A, member 1a	Serpina1a	NM_009243	2.51	1.69
ring finger protein 24	Rnf24	NM_178607	-1.98	1.67
nuclear factor, interleukin 3, regulated	Nfil3	NM_017373	-2.06	1.64
acyl-Coenzyme A dehydrogenase, medium chain	Acadm	NM_007382	-1.74	1.58
transthyretin	Ttr	NM_013697	-5.74	1.55
DnaJ (Hsp40) homolog, subfamily B, member 1	Dnajb1	NM_018808	-2.69	1.54
serum/glucocorticoid regulated kinase	Sgk	NM_011361	-1.64	1.54
SNRPN upstream reading frame	Snurf	NM_033174	-1.84	1.53
C1q and tumor necrosis factor related protein 3	C1qtnf3	NM_030888	-2.64	1.49
RIKEN cDNA 9030619P08 gene	9030619P08Rik	NM_001039720	-2.29	1.48
caveolin 2	Cav2	NM_016900	-2.05	1.48
ATPase, H+ transporting, lysosomal accessory protein 2	Atp6ap2	NM_027439	-2.27	1.46
RIKEN cDNA C730048C13	C730048C13Rik	NM_177002	-3.05	1.42
annexin A13	Anxa13	NM_027211	-2.02	-1.44
methyl-CpG binding domain protein 1	Mbd1	AK007371	-1.60	-1.50
cytochrome P450, family 4, subfamily a, polypeptide 12a	Cyp4a12a	NM_177406	-2.58	-1.51
steroid 5 alpha-reductase 2	Srd5a2	NM_053188	-1.91	-1.54
cysteine and histidine-rich domain (CHORD)-containing, zinc-binding protein 1	Chordc1	NM_025844	-2.02	-1.54
cytochrome P450, family 4, subfamily a, polypeptide 12b	Cyp4a12b	NM_172306	2.03	-1.56
heat shock protein 1	Hspb1	NM_013560	-2.60	1.77
heat shock protein 105	Hsp105	NM_013559	-2.56	-1.95
cytochrome P450, family 26, subfamily b, polypeptide 1	Cyp26b1	NM_175475	1.78	-5.26
F-box and WD-40 domain protein 5	Fbxw5	NM_013908	-7.98	-7.35

When fold change values of 1.5 and -1.5 were considered as cutoff values a list of forty up-regulated genes and 157 down-regulated genes was obtained from microarray analysis of animals fed an iron-rich diet (Appendix A, Appendix B). In *Hfe* knock out mice iron overload caused up-regulation of 37 genes and down-regulation of 57 genes when 1.5 and -1.5 were used as cutoff values (Appendix C, Appendix D). There are only two genes that are up-regulated by both types of

iron overload and eight down-regulated, when cutoff values of 1.4 and -1.4 are used. 17 genes show opposite regulation in the two iron overload models (Table 1).

Table 2. Over-represented pathways and genes involved in them among up-regulated genes in dietary iron overload mice. FC indicated fold change.

Pathway	Symbol	Gene name	FC
PPAR signaling pathway	Cyp4a14	cytochrome P450, family 4, subfamily a, polypeptide 14	33.21
	Hmgcs2	3-hydroxy-3-methylglutaryl-Coenzyme A synthase 2	6.90
	Cyp4a10	cytochrome P450, family 4, subfamily a, polypeptide 10	3.25
	Angptl4	angiopoietin-like 4	2.46
	Cyp4a12b	cytochrome P450, family 4, subfamily a, polypeptide 12B	2.03
	Apoc3	apolipoprotein C-III	1.95
Fatty acid metabolism	Cyp4a14	cytochrome P450, family 4, subfamily a, polypeptide 14	33.21
	Cyp4a10	cytochrome P450, family 4, subfamily a, polypeptide 10	3.25
	Cyp4a12b	cytochrome P450, family 4, subfamily a, polypeptide 12B	2.03
	Acaa1b	acetyl-Coenzyme A acyltransferase 1B	1.89
Arachidonic acid metabolism	Cyp4a14	cytochrome P450, family 4, subfamily a, polypeptide 14	33.21
	Cyp4a10	cytochrome P450, family 4, subfamily a, polypeptide 10	3.25
	Cyp4a12b	cytochrome P450, family 4, subfamily a, polypeptide 12B	2.03
Complement and coagulation cascades	Serpina1b	serine (or cysteine) peptidase inhibitor, clade A, member 1b	2.66
	Serpina1a	serine (or cysteine) peptidase inhibitor, clade A, member 1a	2.51
	Serpina1d	serine (or cysteine) peptidase inhibitor, clade A, member 1d	1.69
Valine, leucine and isoleucine degradation	Hmgcs2	3-hydroxy-3-methylglutaryl-Coenzyme A synthase 2	6.90
	Acaa1b	acetyl-Coenzyme A acyltransferase 1B	1.89
Styrene degradation	Hgd	homogentisate 1, 2-dioxygenase	1.89
Benzoate degradation via hydroxylation	Acaa1b	acetyl-Coenzyme A acyltransferase 1B	1.89
Synthesis and degradation of ketone bodies	Hmgcs2	3-hydroxy-3-methylglutaryl-Coenzyme A synthase 2	6.90

Table 3. Over-represented pathways and genes involved in them among up-regulated genes in *Hfe* knock out mice. FC indicates fold change.

Pathway	Symbol	Gene name	FC
Complement and coagulation cascades	Cfd	complement factor D (adipsin)	2.77
	Serpina1e	serine (or cysteine) peptidase inhibitor, clade A, member 1e	2.12
	Serpina1b	serine (or cysteine) peptidase inhibitor, clade A, member 1b	1.90
	Serpina1a	serine (or cysteine) peptidase inhibitor, clade A, member 1a	1.69
PPAR signaling pathway	Ucp1	uncoupling protein 1 (mitochondrial, proton carrier)	1.74
	Acadm	acyl-Coenzyme A dehydrogenase, medium chain	1.58
	Apoa2**	apolipoprotein A-II	1.47

The KEGG (Kyoto Encyclopedia of Genes and Genomes) pathway analysis was performed for each list obtained, the analysis reveals pathways that are over-represented in the lists, and thus lists include the pathways that have more linked genes than it would be predicted by chance. Pathway

analysis of both up- and down-regulated genes in high iron fed mice revealed over-representation of genes involved in PPAR (peroxisome proliferator-activated receptor) signaling pathway and fatty acid metabolism. The list of pathways over-represented from up-regulated genes also included arachidonic acid metabolism pathway and complement and coagulation cascades (Table 2, Table 4). PPAR signaling pathway and fatty acid metabolism linked genes encode for example cytochrome P450 proteins and acyl-Coenzyme A linked proteins, whereas complement and coagulation cascade involved genes encode complement factors and serine peptidase inhibitors. Complement and coagulation cascades and PPAR signaling pathway were also over-represented in the analysis of up-regulated genes in *Hfe* knock out mice, while cytokine-cytokine receptor interactions and toll-like receptor signaling pathway were over-represented in the analysis of down-regulated genes of these mice (Table 3, Table 5). The genes associated to cytokine-cytokine receptor interaction and toll-like receptor signaling pathway encode mainly chemokine ligands.

Table 4. Over-represented pathways and genes involved in them among down-regulated genes in dietary iron overload mice. FC indicates fold change.

Pathway	Symbol	Gene name	FC
PPAR signaling pathway	Acox1	acyl-Coenzyme A oxidase 1, palmitoyl	-2.38
	Lpl	lipoprotein lipase	-1.96
	Acadm	acyl-Coenzyme A dehydrogenase, medium chain	-1.74
Fatty acid metabolism	Hadhb	hydroxyacyl-Coenzyme A dehydrogenase/3-ketoacyl-Coenzyme A thiolase/enoyl-Coenzyme A hydratase (trifunctional protein), beta subunit	-1.82
	Acadm	acyl-Coenzyme A dehydrogenase, medium chain	-1.74
Circadian rhythm	Bhlhb2	basic helix-loop-helix domain containing, class B2	-2.14
	Per2	period homolog 2 (Drosophila)	-1.67
Alzheimer's disease	Lpl	lipoprotein lipase	-1.96
	App	amyloid beta (A4) precursor protein	-1.71
Bile acid biosynthesis	Srd5a2	steroid 5 alpha-reductase 2	-1.91
	Hadhb	hydroxyacyl-Coenzyme A dehydrogenase/3-ketoacyl-Coenzyme A thiolase/enoyl-Coenzyme A hydratase (trifunctional protein), beta subunit	-1.82

Table 5. Over-represented pathways and genes involved in them among down-regulated genes in *Hfe* knock out mice. FC indicates fold change.

Pathway	Symbol	Gene name	FC
Cytokine-cytokine receptor interaction	Tnfrsf12a	tumor necrosis factor receptor superfamily, member 12a	-1.87
	Cxcl9	chemokine (C-X-C motif) ligand 9	-1.66
	Cxcl14	chemokine (C-X-C motif) ligand 14	-1.61
	Ccl5	chemokine (C-C motif) ligand 5	-1.61
	Ccl4	chemokine (C-C motif) ligand 4	-1.60
	Ccl12	chemokine (C-C motif) ligand 12	-1.53
	Osmr	oncostatin M receptor	-1.51
	Xcl1	chemokine (C motif) ligand 1	-1.48
Arachodonic acid metabolism	Gpx6	glutathione peroxidase 6	-10.83
	Cyp4a12b	cytochrome P450, family 4, subfamily a, polypeptide 12B	-1.56
	Cbr1	carbonyl reductase	-1.49
Toll-like receptor signaling pathway	Cxcl9	chemokine (C-X-C motif) ligand 9	-1.66
	Ccl5	chemokine (C-C motif) ligand 5	-1.61
	Ccl4	chemokine (C-C motif) ligand 4	-1.60

5.2 Q-RT-PCR

From the lists of microarray results 10 genes from dietary iron overload mice and 15 from *Hfe* knock out mice were selected for further analysis, because they were interesting and had notable fold change values (Table 6, Table 7). The expression levels of these genes were analyzed by Q-RT-PCR. The results from Q-RT-PCR correlated well with the results from microarray; only 2 genes from dietary iron overload mice (*Xbp1* and *Fbxw5*) and 4 genes from *Hfe* knock out mice (*Gdf15*, *Slc25a37*, *Tnfrsf12a* and *Fbxw5*) turned out to be false positives (Table 6, Table 7). The regulated genes showed the same direction of change in their fold change values. Representations of these Q-RT-PCR results are shown in figures 7 and 8; the calculated fold change values differ slightly from those obtained from microarray data analysis, but altogether the changes of their fold change values are still significant.

Table 6. Genes that were selected to Q-RT-PCR analysis from dietary iron overload mice and their fold change values obtained from both methods used.

Gene name	Symbol	Accession.	Fold change microarray	Fold change Q-RT-PCR
cytochrome P450, family 4, subfamily a, polypeptide 14	Cyp4a14	NM_007822	33.21	45.3
angiopoietin-like 4	Angptl4	NM_020581	2.46	2.1
acyl-CoA thioesterase 3	Acot3	NM_134246	2.18	2.7
acetyl-Coenzyme A acyltransferase 1B	Acaa1b	NM_146230	1.89	2.4
F-box and WD-40 domain protein 5	Fbxw5	NM_013908	-7.98	NS
transthyrethin	Ttr	NM_013697	-5.74	-5.9
heat shock protein 1A	Hspa1a	NM_010479	-2.70	-7.3
DnaJ (Hsp40) homolog, subfamily B, member 1	Dnajb1	NM_018808	-2.69	-2.7
heat shock protein 105	Hsp105	NM_013559	-2.56	-2.7
X-box binding protein	Xbp1	NM_013842	-1.83	NS

Table 7. Genes that were selected to Q-RT-PCR analysis from *Hfe* knock out mice and their fold change values obtained from both methods used.

Gene name	Symbol	Accession.	Fold change microarray	Fold change Q-RT-PCR
cytokine inducible SH2-containing protein	Cish	NM_009895	3.14	1.9
complement factor D (adipsin)	Cfd	NM_013459	2.77	13.6
haptoglobin	Hp	NM_017370	2.05	3.9
uncoupling protein 1 (mitochondrial, proton carrier)	Ucp1	NM_009463	1.74	4.5
transthyrethin	Ttr	NM_013697	1.55	1.9
DnaJ (Hsp40) homolog, subfamily B, member 1	Dnajb1	NM_018808	1.54	1.5
glutathione peroxidase 6	Gpx6	NM_145451	-10.83	-13.0
F-box and WD-40 domain protein 5	Fbxw5	NM_013908	-7.35	NS
cytochrome P450, family 26, subfamily b, polypeptide 1	Cyp26b1	NM_175475	-5.29	-3.7
cysteine-rich with EGF-like domains 2	Creld2	NM_029720	-2.5	-2.3
heme oxygenase (decycling) 1	Hmox1	NM_010442	-2.06	-1.5
heat shock protein 105	Hsp105	NM_013559	-1.95	-1.7
tumor necrosis factor receptor superfamily, member 12a	Tnfrsf12a	NM_013749	-1.87	NS
solute carrier family 25, member 37	Slc25a37	AK034948	-1.59	NS
growth differentiation factor 15	Gdf15	NM_011819	-1.54	NS

Expression patterns of selected iron-related genes were also studied; these genes include *hepcidin1*, *hepcidin2*, *Hfe*, *Hjv*, *neogenin*, *Tfr2*, *Tfr1* and *Irp1*. None of these genes were differentially expressed according to microarray studies, but because one aim of this study was to explore the expression patterns of iron-related genes in the kidney, they were included in the Q-RT-PCR analysis. *Hepcidin1* and *hepcidin2* were studied in *Hfe* knock out mice and all three strains of dietary iron overload mice; DBA2, Balb/C, and C57BL6, whereas all other genes were studied in *Hfe* knock out mice and C57BL6 dietary iron overload mice. The expression of both *hepcidin1* and *hepcidin2* was not detectable in any of the mice studied (data not shown), thus it seems that hepcidin is not expressed in the kidney and therefore its expression in the kidney is not influenced

by iron overload. Also *Hjv* showed no expression in the kidney of both dietary iron overload and *Hfe* knock out mice (data not shown). The proposed receptor of HJV, neogenin, was expressed in the kidney of both studied mice strains, but its expression was not influenced by iron overload (data not shown). In *Hfe* knock out mice the only gene of which expression was regulated was *Tfr2*. Its fold change was calculated to be 1.5, thus its expression was slightly up-regulated. In dietary iron overload mice differential expression patterns of *Tfr2*, *Hfe*, *Tfr1* and *Irp1* were detected. *Tfr2*, *Hfe* and *Irp1* showed a slight increase in their expression, while *Tfr1* showed a slight decrease in its expression (Figure 9).

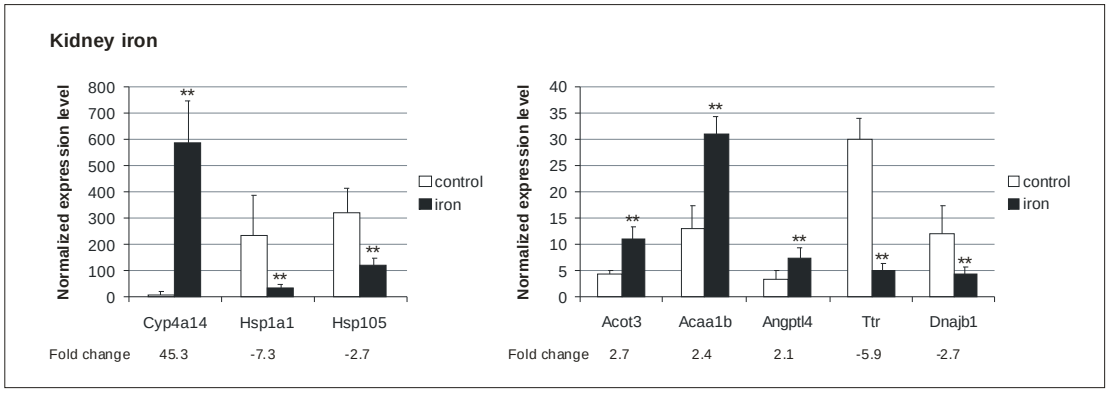

Figure 7. Regulated genes in dietary iron overload mice: normalized expression values and fold changes values obtained from Q-RT-PCR. * indicates p-value below 0.065, ** indicates p-value below 0.05 and *** indicates p-value below 0.02.

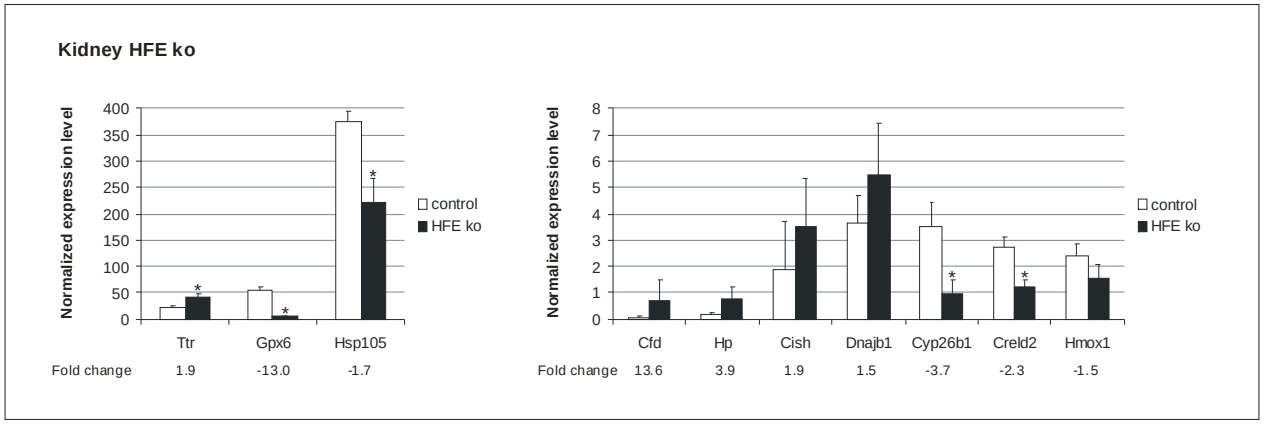

Figure 8. Regulated genes in *Hfe* knock out mice: normalized expression values and fold changes values obtained from Q-RT-PCR. * indicates p-value below 0.065, ** indicates p-value below 0.05 and *** indicates p-value below 0.02.

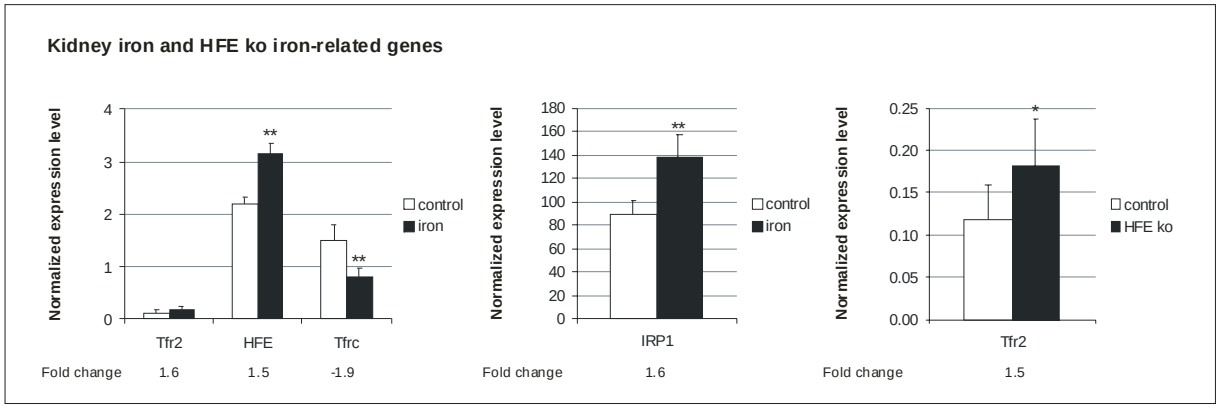

Figure 9. Normalized expression levels and fold change values of iron-related genes in both dietary iron overload mice and *Hfe* knock out mice. * indicates p-value below 0.065, ** indicates p-value below 0.05 and *** indicates p-value below 0.02.

6 DISCUSSION

Although kidney is the main excreting organ, its role in iron homeostasis has not been studied widely. Its ability to adjust the concentration of various ions by affecting the amount of ions and the amount of water reabsorbed could provide a mechanism to overcome the changes in the body caused by iron overload. Like the liver, also the kidney has an important role in degrading various exogenous ligands such as pharmaceuticals and thus it has for example high cytochrome P450 activity. It is assumed that the oxidative stress caused by iron overload induces the expression of various acute phase proteins that protect cells from oxidative damage; also the expression of various iron-related proteins is assumed to be altered. The current microarray study revealed previously unknown expression patterns of certain genes during iron overload and it also indicated that certain pathways have high precendence in the lists obtained from microarray data analysis. The role of these genes and pathways during iron overload has to be inspected in detail to confirm their role and function during these circumstances.

6.1 Cyp4 protein family, peroxisome β-oxidation, and PPAR pathway

Cyp4a14 is a member of Cyp4 family of cytochrome P450 proteins that catalyze the ω-hydroxylation of saturated, branched chain, and unsaturated fatty acids, including eicosanoids, prostaglandins, leukotrienes and arachidonic acid. Hydroxylation occurs in the terminal ω-carbon and, to a lesser extent, the ω-1 position, yielding to dicarboxylic acids. These hydroxylated products can be further metabolized by the peroxisome β-oxidation system. The ω-hydroxylation pathway is a minor pathway in the metabolism of fatty acids, but its importance is increased during starvation, by ethanol, hypolipidemic drugs, peroxisome proliferators, and in different metabolic diseases; like diabetes mellitus (Hardwick 2008, Merryman Simpson 1997). The Cyp4a family is specialized in hydroxylating medium chain fatty acids (C10-C16) and their expression is induced by peroxisome proliferators and regulated by fasting, high fat diet, ethanol consumption, and in diabetes mellitus. After hydroxylation the medium chain acyl-CoAs undergo two to three rounds of peroxisome β-oxidation producing succinyl-CoA and acetyl-CoA. The Cyp4a family also mediates the formation of 20-HETE (20-hydroxyeicosatetraenoic acid) by ω-hydroxylating arachidonic acid. In kidney 20-HETE regulates salt and water reabsorption and vascular tone by inhibiting various ion channels; increased 20-HETE levels increase vascular constriction and reduce blood pressure by decreasing sodium reabsorption (Hardwick 2008). A recent study revealed that Cyp4a14 is almost inactive as

an arachidonic acid hydroxylase in mouse kidney, but it was capable of producing small amounts of 11,12-epoxyeicosatrienoic acid. The Cyp4a14 upregulation we observed in the kidney of mice fed an iron-rich diet might be related to other functions than 20-HETE production; for example 11,12-epoxyeicosatrienoic acid formation or medium chain fatty acid oxidation enhanced in peroxisomes. Cyp4a14 seems to be a female specific isoform, which explains its low expression levels at normal conditions (Muller et al. 2007). The present microarray study revealed also other members of Cyp4a family of which expression was induced (*Cyp4a10*, *Cyp4a12b*, Cyp4a31) or repressed (*Cyp4a12a*) under dietary iron overload. The product of *Cyp4a10* is capable of also only weak 20-HETE formation, whereas Cyp4a12a and Cyp4a12b are the predominant 20-HETE synthases in mice. In kidney the amount of Cyp4a12b is very low, hence Cyp4a12a is the main 20-HETE synthase in this tissue (Muller et al. 2007). The down-regulation of *Cyp4a12a* that we observed in our experiments agrees with the fact that 20-HETE production is actually decreased during dietary iron overload. The upregulation of several Cyp4a members shown in this study might be explained by their induction in diabetes mellitus, which is a common metabolic disease associated with HH, or due to their role in preventing lipotoxicity (Pietrangelo 2006, Hardwick 2008).

The ω-hydroxylated fatty acids that are produced by Cyp4a enzymes are preferentially metabolized by the peroxisome β-oxidation which results in shorter acyl-CoAs (Hardwick 2008). The peroxisomal system consists of unique enzymes differing from the mitochondrial enzymes; it oxidizes not only long chain fatty acids but also very long chain fatty acids, eicosanoids, pristanic acid, bile acid intermediates, and side-chains of xenobiotics. These compounds are not metabolized by mitochondria or their oxidation is very slow (Hashimoto 1999, Poirier et al. 2006). The current Q-RT-PCR data revealed up-regulation of two genes involved in peroxisomal β-oxidation; *Acot3* (acyl-CoA thioesterase 3) and *Acaa1b* (acetyl-CoA acyltransferase 1B, also known as 3-ketoacyl-CoA thiolase B). Acaa-enzymes catalyze the third and final step in the peroxisomal β-oxidation; the thiolytic cleavage of 3-ketoacyl-CoA to acetyl-CoA and acyl-CoA shortened by two carbons (Poirier et al. 2006). There are two transcripts of Acaa-enzymes of which B transcript is mainly expressed in the kidney and its expression is shown to be induced after peroxisome proliferator treatment, while transcript A shows no response to this treatment (Chevillard et al. 2004, Poirier et al. 2006, Hashimoto 1999). Acyl-CoA thioesterases are a group of enzymes that catalyze the hydrolysis of acyl-CoAs to the free fatty acid and CoA, providing potential to regulate intracellular levels of acyl-CoAs, free fatty acids and CoASH. Acots act in many locations; in mouse at least three of them are located in peroxisomes (including Acot3), while humans only have one

peroxisomal Acot (Poirier et al. 2006, Hunt et al. 2006). Acots can mediate the hydrolysis of CoA esters of different chain lengths; Acot3 is specialized in processing of medium to long chain acyl-CoAs and unsaturated acyl-CoAs (Hardwick 2008, Hunt et al. 2006, Poirier et al. 2006). It is suggested that Acots may serve essential functions in peroxisomes to regulate β-oxidation and CoASH levels, in addition to their role in the termination of β-oxidation at various chain lengths for their export out of the organelle (Hunt et al. 2006). The up-regulation of these two genes and ω-hydroxylation mediating cytochromes could indicate an increased peroxisomal β-oxidation. However, according to the microarray data, the expression of the enzyme catalyzing the first reaction in the peroxisomal β-oxidation is repressed. This enzyme, Acox1 (acyl-CoA oxidase 1), is specific for long and medium straight chain substrates and it is thought to be the main enzymatic step controlling the flux through the pathway; thus it is regarded as the rate limiting step of the β-oxidation reactions (Poirier et al. 2006, Hashimoto 1999). The down-regulation of Acox1 may suggest a negative feed-back mechanism involved in the pathway; thus dietary iron overload may induce the peroxisomal β-oxidation and when enough products are formed, down-regulation of Acox1 occurs. This short-term regulation of the activity of Acox1 has previously been suggested, although it has not been well characterized (Hashimoto 1999).

Both peroxisomal β-oxidation and the activity of Cyp4a family are induced by peroxisome proliferators, which include a wide variety of compounds. Different composition of fatty acids in diet, different content of fat in diet, starvation, and diabetes mellitus induce the formation of peroxisome proliferators (Hashimoto 1999, Hardwick 2008). Interestingly, the peroxisome proliferator-activated receptor (PPAR) pathway is the most over-represented in our microarray data. PPARs are members of nuclear receptor superfamily, and they function as biological sensors of altered lipid metabolism, particularly sensing the intracellular fatty acid levels. The PPAR subfamily has three members of which PPARα is highly expressed in cells that have active fatty acid oxidation capacity including the proximal tubule cells of kidney. PPARs are activated by peroxisome proliferators and certain fatty acids and their metabolites, and they act through binding to specific response elements in their target genes (Burns & Vanden Heuvel 2007). The activity of important fatty acid oxidation enzymes, such as Acox1 and Acaa1b, is induced by PPAR pathway (Burns & Vanden Heuvel 2007, Hashimoto 1999, Poirier et al. 2006). All three enzymes of peroxisomal fatty acid β-oxidation are shown to be induced in parallel by PPARs. However, this induction is only observed in the liver, and therefore, it is possible that in other organs, including kidney, the induction of peroxisomal β-oxidation is not so straightforward (Hashimoto 1999). Other

possible explanation for induction of Acaa1b and repression of Acox1 is indeed the previously mentioned short-term regulation and the negative feed-back loop. The induction of peroxisomal β-oxidation linked genes further suggests that peroxisome proliferators are present during dietary iron overload. Interestingly, diabetes mellitus, a condition associated with increased formation of peroxisome proliferators is commonly present in HH patients. The fact that peroxisome proliferators raise upon dietary iron overload could be a mechanism that could explain the association between these two diseases. It is interesting that none of these peroxisomal β-oxidation linked enzymes is regulated in *Hfe* knock out mice; only down-regulation of both *Cyp4a12a* and *Cyp4a12b* was observed in the microarray data.

6.2 Angptl4

Angptl4 (angiopoietin-like 4) belongs to the angiopoietin-like family of secreted proteins which potently regulate angiogenesis and of which some are also regulators of lipid, glucose, and energy metabolism (Hato et al. 2008). Like other proteins in this family, Angptl4 is present in two forms, the full length and truncated forms, which are present in a tissue-dependent fashion (Kersten 2005). The highest expression of Angptl4 is observed in white adipose tissue, lower levels are detected in the liver, heart, skeletal muscle, intestine, placenta, and pituitary gland. Angptl4 is known to up-regulate serum triglyceride levels by inhibiting lipoprotein lipase (LPL) activity causing a hyperglyceridemia. The effect of Angptl4 in glucose metabolism remains controversial, however, some reports indicate that *Angptl4* expression is linked to decreased insulin sensitivity and thus directly to diabetes mellitus (Hato et al. 2008, Kersten 2005). Therefore, the up-regulation of *Angptl4* might be linked to the development of diabetes mellitus, common in HH patients. Microarray data also show transcriptional down-regulation of *Lpl*, which agrees with increased plasma triglyceride levels. In addition *Angptl4* is up-regulated by PPARs which indicates the presence of peroxisome proliferators and shows a possible relation between plasma triglyceride levels and peroxisome β-oxidation (Kersten 2005, Hato et al. 2008).

6.3 Heat shock proteins

Heat shock proteins (Hsp) are proteins that are expressed in cells during heat shock and other stress stimuli, including oxidative stress caused by ROIs. There are several different Hsp families; the best known Hsps are 70 kDa heat shock proteins (Hsp70). Hsp70s are chaperones that assist folding

processes; they prevent aggregation, promote folding to the native state, and solubilize and refold aggregated proteins (Mayer & Bukau 2005). Hsp40s (40 kDa heat shock proteins) interact with Hsp70s to specify the cellular action of Hsp70 proteins; interactions create a wide variety of Hsp70-Hsp40 pairs that have specific functions at distinct locations within the cell. The main function of Hsp40s is to regulate ATP-dependent polypeptide binding by Hsp70 proteins; they stimulate the hydrolysis of the bound ATP which stabilizes the Hsp70-polypeptide complexes. Some Hsp40 proteins can independently act as chaperones and prevent aggregation of misfolded proteins (Fan et al. 2003). A recently identified function of Hsp70 subfamily Hsp110/105 (110/105 kDa heat shock proteins) is their role in binding Hsp70 and inducing the exchange of nucleotides. Like Hsp40 proteins, also Hsp110/105 proteins can independently prevent aggregate formation (Shaner & Morano 2007). In the present study, the down-regulation of several heat shock proteins was confirmed using Q-RT-PCR. In dietary iron overload mice the expression of *Hsp105* (member of Hsp110/105 family), *Dnajb1* (member Hsp40 family) and *Hspa1a* (member of Hsp70 family) was decreased, whereas in *Hfe* knock out mice decreased expression of *Hsp105* and increased expression of *Dnajb1* were observed. According to microarray results there are even more down-regulated heatshock protein genes; in dietary iron overload mice (*Hspd1*, *Hspb1*, *Hsp90aa1* and *Dnaja4*) and in *Hfe* knock out mice (*Hspb8*, *Hspb1*, *Hspa8* and *Hsp90b1*). Similar expression patterns are also detected in the skeletal muscle, heart and liver of iron overload mice. These results may indicate the presence unknown regulatory mechanism under these experimental conditions as proposed earlier (Rodriguez et al. 2007b).

6.4 Oppositely regulated genes

Q-RT-PCR analysis confirmed the opposite regulation of two genes; *Dnajb1* and *Ttr* (transthyretin) between dietary iron overload and *Hfe* knock out mice. Transthyretin was slightly up-regulated in *Hfe* knock out mice and significantly down-regulated in dietary iron overload mice. Ttr is a carrier of thyroid hormones, such as thyroxine, and it is expressed at least in the liver and choroid plexus. It is also known to form a complex with retinol and prevent its filtration through the renal glomeruli; however, most of the Ttr in the circulation is not bound to retinol. Ttr is one of the proteins of which mutated forms can mediate amyloidosis, a disease caused by extracellular deposition of insoluble amyloid fibrils. These derive from misfolded proteins, which are soluble under normal conditions (Hou et al. 2007). A likely explanation for the differential expression of these two genes in our mouse models could be differences in hormone status between these two mice.

6.5 Other regulated genes in Hfe knock out mice

Excess free iron catalyzes the formation of ROIs, capable of oxidizing lipids, proteins, and nucleic acids (Papanikolaou & Pantopoulos 2005, Aisen et al. 2001). Glutathione peroxidases (Gpx) are antioxidant enzymes that reduce hydroperoxides to corresponding alcohols by means of glutathione (Brigelius-Flohé 2006). It would be assumed that expression of at least one Gpx would be enhanced as a response to ROI formation but the only observed change in expression of any of these genes was the remarkable down-regulation of *Gpx6* in *Hfe* knock out mice. Not much is known about Gpx6; in humans its expression has been detected only in the olfactory epithelium and it is known to be a cysteine homologue while other Gpxs have selenocysteines. However, apparently all six known Gpxs seem to carry out very different biological roles, differing in substrate specifity and localization (Brigelius-Flohé 2006). The observed ten fold downregulation of *Gpx6* may indicate some novel sophisticated regulatory mechanisms in *Hfe* knock out animals and not the direct stimulation of expression by ROIs.

Other genes regulated in *Hfe* knock out mice and validated by Q-RT-PCR were *Cfd* (complement factor D), *Cish* (cytokine inducible SH2-containing protein), *Ucp1* (uncoupling protein 1), *Cyp26b1* (cytochrome P450, family 26, subfamily b, polypeptide 1), and *Creld2* (cysteine-rich with EGF-like domains 2). In three of these genes (*Cfd*, *Cish*, and *Ucp1*) variation within groups was large, and thus statistical significance is low, even though calculated fold change values for these genes were high. The function of Creld2 is poorly known but this secreted protein may compete with its homologue Creld1 for the same ligands and thus be associated with common heart defects linked to Creld1 function. One of its transcripts is also shown to bind to nicotinic acetylcholine receptor (Maslen et al. 2006). Also the role of Cyp26b1 has not been studied well; it is known to be associated with retinoic acid metabolism which is important in growth and differentiation (Nelson 1999). According to the data obtained in this study the expression of *Cyp26b1* is down-regulated in the kidney of *Hfe* knock out mice. However, according to the microarray data from this study and a previous study by Rodriguez and colleagues, in dietary iron overload mice *Cyp26b1* expression seems to be up-regulated in the kidney, heart, and skeletal muscle (Rodriguez et al. 2007b). Consequently, Cyp26b1 is regulated in an opposite manner in mice with primary and secondary iron overload. The mechanism behind is most likely related, directly or undirectly, with the presence or absence of HFE.

6.6 Over-represented pathways

The microarray data indicated that, in addition to PPAR signaling pathway and fatty acid metabolism, the over-represented pathways also included complement and coagulation cascades, cytokine-cytokine receptor interactions, and toll-like receptor signaling pathway. Complement and coagulation cascades appeared to be over-represented among upregulated genes in both dietary iron overload mice and *Hfe* knock out mice, whereas cytokine-cytokine receptor interactions and toll-like receptor signaling pathway were over-represented among downregulated genes in *Hfe* knock out mice. The genes upregulated and involved in complement and coagulation cascades included mainly serpins (serine protease inhibitors) and especially serpina1 genes. Serpins are the largest superfamily of protease inhibitors; most serpins inhibit serine proteases, some inhibit caspases and papain-like cysteine proteases. Serpins may also serve as hormone transporters, molecular chaperones and tumor suppressors. Inhibitory serpins are single use inhibitors that accomplish a unique, irreversible, and extensive conformation change to inhibit proteases, thus they must be regulated tightly (Law et al. 2006). Serpina1 is also known as α_1-antitrypsin of which targets are neutrophil elastase and APC (activated protein C). APC is an important component in coagulation pathway; it is able to inactivate factors Va and VIIIa and therefore limit further thrombin generation. Consequently, inhibition of APC by serpina1 leads to uncontrolled thrombin formation and clotting (Rau et al. 2007). Up-regulation of serpina1 mRNA shown by the microarray data may indicate a requirement for thrombin formation and clotting or it may be caused also by some disorder in the organism. For example serpina1 levels are increased after pediatric ischemic stroke independent of other prothrombotic factors (Rau et al. 2007). However, as an anti-inflammatory protein, serpina1 is also shown to inhibit ertyhropoiesis by impairing transferrin binding to TfR1 and subsequent internalization of the complex formed (Means 2004). Thus it may have a greater role in iron metabolism; it may directly regulate transferrin-TfR1 interactions also under non-inflammatory conditions. Cytokine-cytokine receptor interactions and toll-like receptor signaling pathway are usually linked to inflammation and infections; in the microarray data chemokine ligands were the most abundant among genes linked to either of these pathways. Inflammation is a process involving changes in hemodynamics, vascular reaction of endothelial cells, leukocyte adhesion, activation, and migration. These functions are mediated by cytokines and cytokine receptors (Segerer et al. 2000). The family of toll-like receptors are among the first mediators of immune reactions; they sense conserved structures found in pathogens and cause innate immunity responses, including cytokine and chemokine secretion (Kawai & Akira 2005). Chemokines have

roles during the movement of leukocytes; they bind to the specific chemokine receptors expressed in the cell membrane of leukocytes. In addition to this, the over-production of chemokines is associated to many diseases; such as arthritis, multiple sclerosis, and pneumonia, and they may serve as mediators of allergic diseases (Murdoch & Finn 2000). However, the microarray data indicated that, in fact, cytokine-cytokine receptor interaction and toll-like receptor signaling pathway linked genes are downregulated in the kidney of HFE deficient mice. The expression of chemokines can be repressed by glucocorticoids, other cytokines (like TGF-β), and prostaglandins. Because prostaglandins and TGF-β are also expressed during inflammation, the expression of chemokines may depend on the balance between proinflammatory and anti-inflammatory agents (Segerer et al. 2000). Therefore, inflammation in kidney in *Hfe* knock out mice is not overruled, even though up-regulated genes do not include cytokines. The expression of chemokines can also be suppressed by PPAR ligands; PPAR ligands seem to be important mediators of reduction of inflammatory cell recruitment (Straus & Glass 2007). Interestingly, in *Hfe* knock out mice the PPAR signaling pathway was slightly over-represented among the up-regulated genes, thus it is possible that the peroxisome proliferators cause the reduction of chemokines. However, the amount of up-regulated genes linked to PPAR signaling was significantly smaller than in dietary iron overload mice. The most likely explanations for reduced cytokine signaling are the balance between proinflammatory and anti-inflammatory agents during inflammation or some complicated signaling mechanism specific for the Hfe null genotype.

6.7 Expression of iron-related genes

In *Hfe* knock out mice Q-RT-PCR analysis confirmed the regulation of two iron-related genes also present in the microarray results. The observed genes were *Hp* (haptoglobin), which was upregulated, and *Hmox1*, which was down-regulated. Haptoglobin is a circulating protein that binds free iron in the circulation, and haptoglobin-iron complexes are then transported into the macrophages of the RES (Muckenthaler et al. 2008). Thus, it could be assumed that an increasing amount of free circulating iron during iron overload stimulates the formation of haptoglobin to prevent damage mediated by free iron. On the other hand, the decreased amount of Hmox1 indicates decreased heme oxygenation rate. This suggests that the breaking down of old and damaged erythrocytes is decelerated, maybe because of excess iron in the body.

Other studied iron-related genes did not show dramatic increases or decreases in their expression. The only gene of which expression was altered in the *Hfe* knock out mice was *Tfr2* whose increased

expression was also observed in dietary iron overload mice. The behaviour of TfR2 during iron overload in kidney is likely to be the same as in the liver; its amount increases when the saturation of transferrin increases (Graham et al. 2007). Thus, the purpose of its up-regulation is to stimulate the expression of *hepcidin*. Also changes in the expression of *Tfr1* were analoguos to the changes in the liver in dietary iron overload mice. The expression patterns of IRP1 were particularly interesting because of its special status in the kidney. The observed up-regulation further confirmed its role in regulating iron metabolism in the kidney, thus it also seems to have IRE binding activity in addition to its aconitase activity. Also the expression of *Hfe* was increased in kidney of dietary iron overload mice; this may be a mechanism of response to the need to increase the amount of hepcidin in the body. The expression of HJV and its possible receptor neogenin in the kidney were also studied. The expression of *neogenin* remained constant in both mouse types, whereas HJV mRNA amounts were not detectable at all. This same observation has been made earlier (Rodriguez et al. 2007a). It is impossible to conclude anything about HJV-neogenin interactions in kidney based on this data; the only conclusion is that *Hjv* is not expressed in kidney. Three different mouse strains with dietary iron overload and one strain with *Hfe* null allele were used in the *hepcidin* expression study. There is controversial information about hepcidin expression in the kidney; this study indicates that none of the hepcidin genes are expressed in kidney of any of the mouse strains studied. Previous studies show alternation in expression of *hepcidin1* and *hepcidin2* expression between different strains and in the amount of hepcidin produced (Rodriguez et al. 2007b). However, both *hepcidin1* and *hepcidin2* were not expressed in detectable amounts in any of the mice studied, even DBA2 mice showed no expression although they expressed small amounts of hepcidin2 in skeletal muscle and in the heart. Based on this study and the previous results, it may be concluded that the liver is the main organ to produce both hepcidins in mice.

6.8 Combining microarray and Q-RT-PCR

Combination of microarray and Q-RT-PCR in expression analysis is a widely used method. Usually a microarray analysis is performed first with fewer samples and Q-RT-PCR experiments are done based on the results of microarray. Q-RT-PCR analysis can be done using more samples and its accurancy is considered better than that of microarray analysis; as the amount of samples increases, also the statistical significance increases. It is also a cheaper way to analyze multiple samples used in the study. When the microarray data analysis is done carefully, the Q-RT-PCR should be able to confirm the differential expression of genes selected from the microarray results. In this study, the Q-RT-PCR analysis quite faithfully confirmed regulation of most of the genes identified by the

microarray analysis. Among the selected genes, only four out of 15 genes were false positives in *Hfe* knock out mice and two were false positive in dietary iron overload mice. However, half of them had suggestive p-values above 0.05, obtained from the microarray data analysis, which is considered to be the cutoff limit between statistically significant and non-significant values. It may result from one sample that behaves differentially from others during the microarray study. Other genes that have acceptable p-values do not have great fold change values, and therefore, their false positivity may be caused by errors in measurements or not suitable normalization methods during the microarray data analysis. Based on this information, microarray analysis should not be regarded as entirely reliable, even though most of the information derived from it was accurate.

Q-RT-PCR data was normalized using four different housekeeping genes of which expression was shown to stay nearly constant under all circumstances. The normalization factor used was calculated for each sample by calculating the geometric mean of the expression levels of all four genes. This method should eliminate the significance of possible outliers among the housekeeping genes and thus improve accurancy of the analysis. However, one housekeeping gene used, *actin β,* showed induced expression in dietary iron overload mice according to the microarray data. The fold change value observed was quite low, 1.69, and the suggestive p-value obtained, 0.0482, was near the cutoff value. Genes in microarray data of dietary iron overload mice have in general very low p-values, the value of *actin β* is among the greatest, and thus its significance is not clear. The suitability of *actin β* as a housekeeping gene was confirmed by evaluating and comparing the fold change value obtained using all four housekeeping genes and the one calculated using only three remaining housekeeping genes. The fold change of *actin β* when normalizing to all four housekeeping genes was 1.16, and when normalized to other three housekeeping genes the value was 1.22. Based on these values it can be concluded that the expression of *actin β* does not change significantly and it can therefore be used as a housekeeping gene. The fold change values obtained from the Q-RT-PCR correlated well with the ones obtained from the microarray analysis; most of them were nearly the same. Some changes still occurred. Most of them could be caused by different normalization methods between these two methods or because of the higher sensitivity of Q-RT-PCR. It is often seen that fold change values obtained from the Q-RT-PCR are greater than those of microarray data, but this was not the case in this study (DeNardo et al. 2005). Based on the present data, it can be concluded that microarray is a powerful tool for searching genes potentially regulated, but Q-RT-PCR should be used to confirm the differential expression.

7 CONCLUSIONS

The aim of this study was to investigate the effects of iron overload on the gene expression profile of kidney. Based on the results of this study, it can be concluded that there is a remarkable response to iron overload in this organ. The microarray study revealed up- and down-regulation of many genes and interesting pathways could be linked to these changes in expression patterns. Further studies are needed to confirm and specify the roles of the regulated genes. The PPAR signalling pathway that was linked to many genes in both mouse models is especially interesting and thus its role in kidney and other organs should be further explored. Through this study, we could also compare the effects of primary iron overload, caused by disruption of *Hfe* gene and characterized by absence or very low hepcidin, and secondary iron overload, caused by an iron-rich diet and characterized by high hepcidin, on renal transcriptional profile. The data revealed that there is a common response to iron overload, independently of its origin. However, kidney has as well specific responses depending on the cause of iron burden.

Several classical iron-related genes are expressed in the kidney, and they are regulated in response to iron overload. This indicates that, in addition to the liver, also kidney is able to regulate the expression of these genes and mediate changes needed to avoid the harmful effects of excess iron. However, the absence of *Hjv*, *hepcidin1*, and *hepcidin2* mRNA in kidney incates, that this organ has not a role in the regulation of iron homeostasis as liver does.

REFERENCES

Abouhamed M, Gburek J, Liu W, Torchalski B, Wilhelm A, Wolff NA, Christensen EI, Thévenod F, Smith GP. Divalent metal transporter 1 in the kidney proximal tubule is expressed in late endosomes/lysosomal membranes: implications for renal handling of protein metal complexes. Am J Physiol Renal Physiol 2006;290:F1525-33.

Aisen P, Enns C, Wessling-Resnick M. Chemistry of eukaryotic iron metabolism. Review. The International Journal of Biochemistry & Cell Biology 2001;33:940-59.

Ajioka RS, Levy JE, Andrews NC, Kushner JP. Regulation of iron absorption in *Hfe* mutant mice. Blood 2002;100(4):1465-9.

Anderson GJ, Frazer DM, McKie AT, Vulpe CD, Smith A. Mechanisms of haem and non-haem iron absorption: Lessons from inherited disorders of iron metabolism. BioMetals 2005;18:339-48.

Andrews NC. Disorders of iron metabolism. N Engl J Med 1999;341:1986-95.

Andrews NC. IRON HOMEOSTASIS: INSIGHTS FROM GENETICS AND ANIMAL MODELS. Nature Reviews Genetics 2000;1:208-17.

Andrews NC, Schmidt PJ. Iron homeostasis. Annu Rev Physiol 2007;69:16.1-16.17.

Babitt JL, Huang FW, Wrighting DM, Xia Y, Sidis Y, Samad TA, Campagna JA, Chung RT, Schneyer AL, Woolf CJ, Andrews NC, Lin HY. Bone morphogenetic protein signaling by hemojuvelin regulates hepcidin expression. Nature Genetics 2006;38(5):531-9.

Bauminger ER, Harrison PM, Hechel D, Hodson NW, Nowik I, Treffry A, Yewdall SJ. Iron (II) oxidation and early intermediates of iron-core formation in recombinant human H-chain Ferritin. Biochem J 1993;296:709-19.

Bridle KR, Frazer DM, Wilkins SJ, Dixon JL, Purdie DM, Crawford DHG, Subramaniam VN, Powell LW, Anderson GJ, Ramm GA. Disrupted hepcidin regulation in HFE-associated haemochromatosis and the liver as a regulator of body iron homoeostasis. Lancet 2003;361:669-73.

Brigelius-Flohé R. Review. Glutathione peroxidases and redox-regulated transcription factors. Biol Chem 2006;387:1329-35.

Brissot P, de Bels F. Current Approaches to the Management of Hemochromatosis. Hematology Am Soc Hematol Educ Program 2006:36-41.

Burns KA, Vanden Heuvel JP. Review. Modulation of PPAR activity via phosphorylation. Biochimica et Biophysica Acta 2007;1771:952-60.

Bustin SA. Quantification of mRNA using real-time reverse transcription PCR (RT-PCR): trends and problems. Journal of Molecular Endocrinology 2002;29:23-39.

Canonne-Hergaux F, Gros P. Expression of the iron transporter DMT1 in kidney from normal and anemic *mk* mice. Kidney International 2002;62:147-56.

Chamaschella C, Roetto A, Cali A, De Gobbi M, Garozzo G, Carella M, Majorano N, Totaro A, Gasparini P. The gene *TfR2* is mutated in a new type of haemochromatosis mapping to 7q22. Nature Genetics 2000;25:14-5.

Chen J, Chloupkova M, Gao J, Chapman-Arvedson TL, Enns CA. HFE Modulates Transferrin Receptor 2 Levels in Hepatoma Cells via Interactions That Differ from Transferrin Receptor 1-HFE Interactions. Journal of Biological Chemistry 2007;282(51):36862-70.

Chevillard G, Clémencet M-C, Etienne P, Martin P, Pineau T, Latruffe N, Nicolas-Francès V. Molecular cloning, gene structure and expression profile of two mouse peroxisomal 3-ketoacyl-CoA thiolase genes. BMC Biochemistry 2004;5:3.

Churchill GA. Fundamentals of experimental design for cDNA microarrays. Nature Genetics Supplement 2002;32:490-5.

Conrad ME, Umbreit JN. Pathways of Iron Absorption. Blood Cells, Molecules, and Diseases 2002;29(3):336-55.

Dailey HA, Finnegan MG, Johnson MK. Human ferrochelatase is an iron-sulfur protein. Biochemistry 1994;33:403-7.

Dallas PB, Gottardo NG, Furth MJ, Beesley AH, Hoffman K, Terry PA, Freitas JR, Boag JM, Cummings AJ, Kees UR. Gene expression levels assessed by oligonucleotide microarray analysis and quantitative real-time RT-PCR – how well do they correlate? BMC Genomics 2005;6:59.

Davies PS, Zhang AS, Anderson EL, Roy CN, Lampson MA, McGraw TE, Enns CA. Evidence for the interaction of the hereditary haemochromatosis protein, HFE, with the transferrin receptor in endocytic compartments. Biochem J 2003;373:145-53.

De Domenico I, McVey Ward D, Langelier C, Vaughn MB, Nemeth E, Sundquist WI, Ganz T, Musci G, Kaplan J. The Molecular Mechanism of Hepcidin-mediated Ferroportin Down-Regulation. Molecular Biology of the Cell 2007;18:2569-78.

De Domenico I, McVey Ward D, Musci G, Kaplan J. Iron overload due to mutations in ferroportin. Haematologica 2006;91:92-5.

DeNardo DG, Kim HT, Hilsenbeck S, Cuba V, TsimelzonA, Brown PH. Global gene expression analysis of estrogen receptor transcription factor cross talk in breast cancer: indentification of estrogen-induced/activator protein-1-dependent genes. Mol Endocrinol 2005;19(2):362-78.

Donovan A, Brownlie A, Zhou Y, Shepard J, Pratt SJ, Moynihan J, Paw BH, Drejer A, Barut B, Zapata A, Law TC, Brugnara C, Lux SE, Pinkus GS, Pinkus JL, Kingsley PD, Palis J, Fleming MD, Andrews NC, Zon LI. Positional cloning of zebrafish *ferroportin1* identifies a conserved vertebrate iron exporter. Nature 2000;191:776-81.

Donovan A, Lima CA, Pinkus JL, Pinkus GS, Zon LI, Robine S, Andrews NC. The iron exporter ferroportin/Slc40a1 is essential for iron homeostasis. Cell Metabolism 2005;1:191-200.

Fan C-Y, Lee S, Cyr DM. Mechanisms for regulation of Hsp70 function by Hsp40. Cell Stress & Chaperones 2003;8(4):309-16.

Feder JN, Gnirke A, Thomas W, Tsuchihashi Z, Ruddy DA, Basava A, Dormishian F, Domingo R, Ellis MC Jr., Fullan A, Hinton LM, Jones NL, Kimmel BE, Kronmal GS, Lauer P, Lee VK, Loeb DB, Mapa FA, McClelland E, Meyer NC, Mintier GA, Moeller N, Moore T, Morikang E, Prass CE, Quintana L, Starnes SM, Schatzman RC, Brunke KJ, Drayna DT, Risch NJ, Bacon BR, Wolff RK. A novel MHC class I-like gene is mutated in patients with hereditary haemochromatosis. Nature Genetics 1996;13:399-408.

Feder JN, Penny DM, Irrinki A, Lee VK, Lebrón JA, Watson N, Tsuchihashi Z, Sigal E, Bjorkman PJ, Schwatzman RC. The hemochromatosis gene product complexes with the transferrin receptor and lowers its affinity for ligand binding. Proc Natl Acad Sci USA 1998;95:1472-7.

Ferguson CJ, Wareing M, Ward DT, Green R, Smith CP, Riccardi D. Cellular localization of divalent metal transporter DMT-1 in rat kidney. Am J Physiol Renal Physiol 2001;280:F803-14.

Fleming MD, Trenor III CC, Su MA, Foernzler D, Beier DR, Dietrich WF, Andrews NC. Microcytic anemis mice have a mutation in *Nramp2*, a candidate iron transporter gene. Nat Genet 1997;16:383-6.

Fleming MD, Romano MA, Su MA, Garrick LM, Garrick MD, Andrews NC. *Nramp2* is mutated in the anemic Belgrade (b) rat: Evidence of a role of Nramp in endosomal iron transport. Proc Natl Acad Sci USA 1998;95:1148-53.

Franchini M, Veneri D. Recent advances in hereditary hemochromatosis. Ann Hematol 2005;84:347-52.

Frazer DM, Wilkins SJ, Becker EM, Murphy TL, Vulpe CD, McKie AT, Anderson GJ. A rapid decrease in the expression of DMT1 and Dcytb but not Ireg1 or hephaestin explains the mucosal block phenomenon of iron absorption. Gut 2003;52:340-6.

Galy B, Ferring-Appel D, Kaden S, Gröne HJ, Hentze MW. Iron regulatory proteins are essential for intestinal function and control key iron absorption molecules in the duodenum. Cell Metab 2008;7(1):79-85.

Ganz T, Nemeth E. Regulation of iron acquisition and iron distribution in mammals. Biochimica et Biophysica Acta 2006;1763:690-9.

Goswami T, Andrews NC. Hereditary Hemochromatosis Protein, HFE, Interaction with Transferrin Receptor 2 Suggests a Molecular Mechanism for Mammalian Iron Sensing. Journal of Biological Chemistry 2006;281(39):28494-8.

Graham RM, Chua ACG, Herbison CE, Olynyk JK, Trinder D. Liver iron transport. World J Gastroenterol 2007;13(35):4725-36.

Gunshin H, Mackenzie B, Berger UV, Gunshin Y, Romero MF, Boron WF, Nussberger S, Gollan JL, Hediger MA. Cloning and characterization of a mammalian proton-coupled metal-ion transporter. Nature 1997;388:482-8.

Gunshin H, Starr CN, DiRenzo C, Fleming MD, Jin J, Greer EL, Sellers VM, Galica SM, Andrews NC. Cybrd1 (duodenal cytochrome b) is not necessary for dietary iron absorption in mice. Blood 2005;106(5):2879-82.

Halliwell B, Gutteridge JMC. The role of free radicals and catalytic metal ions in human disease: an overview. Methods Enzymol. 1990;186:1-85.

Hardwick JP. Commentary. Cytochrome P450 omega hydroxylase (CYP4) function in fatty acid metabolism and metabolic diseases. Bioccchemical Pharmacology 2008;75:2263-75.

Hashimoto T. Peroxisomal β-Oxidation Enzymes. Neurochemical Research 1999;24(4);551-63.

Hato T, Tabata M, Oike Y. The Role of Angiopoietin-Like Proteins in Angiogenesis and Metabolism. Trends Cardiovasc Med 2008;18:6-14.

Hess KR, Zhang W, Baggerly KA, Stivers DN, Coombes KR. Microarrays: handling the deluge of data and extracting reliable information. TRENDS in Biotechnology 2001;19(11):463-8.

Hou X, Aguilar M-I, Small DH. Transthyretin and familial amyloidotic polyneuropathy. Recent progress in understanding the molecular mechanism of neurodegeneration. FEBS Journal 2007;274:1637-50.

Huang FW, Pinkus JL, Pinkus GS, Fleming MD, Andrews NC. A mouse model of juvenile hemochromatosis. J Clin Invest 2005;115(8):2187-91.

Hunt JR. Bioavailability of iron, zinc, and other trace minerals from vegetarian diets. Am J Clin Nutr 2003;78:633S-9S.

Hunt MC, Rautanen A, Westin MAK, Svensson LT, Alexson SHE. Analysis of the mouse and human acyl-CoA thioesterase (ACOT) gene clusters shows that convergent, functional evolution results in a reduced number of human peroxisomal ACOTs. The FASEB Journal 2006;20:1855-64.

Hvidberg V, Maniecki MB, Jacobsen C, Hojrup P, Moller HJ, Moestrup SK. Identification of the receptor scavenging hemopexin-heme complexes. Blood 2005;106(7):2572-9.

Ilyin G, Courselaud B, Troadec MB, Pigeon C, Alizadeh M, Leroyer P, Brissot P, Loreal O. Comparative analysis of mouse hepcidin 1 and 2 genes: evidence for different patterns of expression and co-inducibility during iron overload. FEBS Lett 2003;542(1-3):22-6.

Katagiri F, Glazebrook J. Overview of mRNA Expression Profiling Using Microarrays. Current Protocols in Molecular Biology 2004:22.4.1-8.

Kawai T, Akira S. Toll-like receptor downstream signaling. Arthritis Res Ther 2005;7(1):12-9.

Kersten S. Regulation of lipid metabolism via angiopoietin-like proteins. Biochemical Society transactions 2005;33:1059-62.

Kong W-N, Chang Y-Z, Wang S-M, Zhai X-L, Shang J-X, Li L, Duan X-L. Effect of erythropoietin on hepcidin, DMT1 with IRE, and hephaestin gene expression in duodenum of rats. J Gastroenterol 2008;43:136-43.

Kong W-N, Zhao S-E, Duan X-L, Yang Z, Qian Z-M, Chang Y-Z. Decreased DMT1 and Increased Ferroportin 1 Expression Is the Mechanisms of Reduced Iron Retention in Macrophages by Erythropoietin in Rats. Journal of Cellular Biochemistry 2008;104:629-641.

Krause A, Neitz S, Mägert H-J, Schulz A, Forssman W-G, Schulz-Knappe P, Adermann K. LEAP-1, a novel highly disulfide-bonded human peptide, exhibits antimicrobial activity. FEBS Letters 2000;480:147-50.

Kristiansen M, Graversen JH, Jacobsen C, Sonne O, Hoffman H-J, Law SKA, Moestrup SK. Identification of the haemoglobin scavenger receptor. Nature 2001;409:198-201.

Kubista M, Andrade JM, Bengtsson M, Forootan A, Jonák J, Lind K, Sindelka R, Sjöback R, Sjögreen B, Strömbom L, Ståhlberg A, Zoric N. The real-time polymerase chain reaction. Review. Molecular Aspects of Medicine 2006;27:95-125.

Kulaksiz H, Theilig F, Bachmann S, Gehrke SG, Rost D, Janetzko A, Cetin Y, Stremmel W. The iron-regulatory peptide hormone hepcidin: expression and cellular localization in the mammalian kidney. Journal of Endocrinology 2005;184:361-70.

LaVaute T, Smith S, Cooperman S, Iwai K, Land W, Meyron-Holtz E, Drake SK, Miller G, Abu-Asab M, Tsokos M, Switzer R III, Grinberg A, Love P, Tresser N, Rouault TA. Targeted deletion of the gene encoding iron regulatory protein-2 causes misregulation of iron metabolism and neurodegenerative disease in mice. Nature Genetics 2001;27:209-14.

Law RHP, Zhang Q, McGowan S, Buckle AM, Silverman GA, Wong W, Rosado CJ, Langendorf CG, Pike RN, Bird PI, Whisstock JC. Review. An overview of the serpin superfamily. Genome Biology 2006;7:216.

Lesbordes-Brion J-C, Viatte L, Bennoun M, Lou D-Q, Ramey G, Houbron C, Hamard G, Kahn A, Vaulont S. Targeted disruption of the hepcidin 1 gene results in severe hemochromatosis. Blood 2006;108(4):1402-5.

Levy JE, Jin O, Fujiwara Y, Kuo F, Andrews NC. Transferrin receptor is necessary for development of erythrocytes and the nervous system. Nature genetics 1999;21:396-9.

Levy JE, Montross LK, Andrews NC. Genes that modify the hemochromatosis phenotype in mice. J Clin Invest 2000;105:1209-16.

Levy JE, Montross LK, Cohen DE, Fleming MD, Andrews NC. The C282Y Mutation Causing Hereditary Hemochromatosis Does Not Produce a Null Allele. Blood 1999;94(1):9-11.

Lin L, Goldberg YP, Ganz T. Competitive regulation of hepcidin mRNA by soluble and cell-associated hemojuvelin. Blood 2005;106(8):2884-9.

Ludwiczek S, Theurl I, Bahram S, Schümann K, Weiss G. Regulatory Networks for the Control of Body Iron Homeostasis and Their Dysregulation in HFE Mediated Hemochromatosis. Journal of Cellular Physiology 2005;204:489-99.

Maslen CL, Babcokc D, Redig JK, Kapeli K, Akkari YM, Olson SB. CRELD2: Gene mapping, alternate splicing, and comparative genomic identification of the promoter region. Gene 2006;382:111-20.

Mayer MP, Bukau B. Review. Hsp70 chaperones: Cellular functions and molecular mechanism. CMLS Cell Mol Life Sci 2005;62:670-84.

McKie AT, Barrow D, Latunde-Dada GO, Rolfs A., Sager G, Mudaly E, Mudaly M, Richardson C, Barlow D, Bomford A, Peters TJ, Raja KB, Shirali S, Hediger MA, Farzaneh F, Simpson RJ. An Iron-Regulated Ferric Reductase Associated with the Absorption of Dietary Iron. Science 2001;291:1755-9.

McKie AT, Marciani P, Rolfs A, Brennan K, Wehr K, Barrow D, Miret S, Bomford A, Peters TJ, Farzaneh F, Hediger MA, Hentze MW, Simpson RJ. A Novel Duodenal Iron-Regulated Transporter, IREG1, Implicated in the Basolateral Transfer of Iron to the Circulation. Molecular Cell 2000;5:299-309.

Means RT Jr. Hepcidin and Anaemia. Blood Reviews 2004;18:219-225.

Mena NP, Esparza A, Tapia V, Valdés P, Núñez MT. Hepcidin inhibits apical iron uptake in intestinal cells. Am J Physiol Gastrointest Liver Physiol 2008;294:G192-8.

Merryman Simpson AEC. Review. The Cytochrome P450 4 (CYP4) Family. Gen Pharmac 1997;28(3):351-9.

Meyron-Holtz EG, Ghosh MC, Iwai K, LaVaute T, Brazzolotto X, Berger UV, Land W, Ollivierre-Wilson H, Grinberg A, Love P, Rouault TA. Genetic ablations of iron regulatory proteins 1 and 2 reveal why iron regulatory protein 2 dominates iron homeostasis. The EMBO Journal 2004;23(2):386-95.

Montosi G, Donovan A, Totaro A, Garuti C, Pignatti E, Cassanelli S, Trenor CC, Gasparini P, Andrews NC, Pietrangelo A. Autosomal-dominant hemochromatosis is associated with a mutation in the ferroportin (*SLC11A3*) gene. J Clin Invest 2001;108:619-23.

Muckenthaler MU, Galy B, Hentze MW. Systemic Iron Homeostasis and the Iron-Responsive Element/Iron-Regulatory Protein (IRE/IRP) Regulatory Network. Annu Rev Nutr 2008;28:3.1-3.17.

Muckenthaler MU, Rodrigues P, Macedo MG, Minana B, Brennan K, Cardoso EM, Hentze MW, de Sousa M. Molecular analysis of iron overload in β2-microglobulin-deficient mice. Blood Cells, Molecules, and Diseases 2004;33:125-31.

Muller DN, Schmidt C, Barbosa-Sicard E, Wellner M, Gross V, Hercule H, Markovic M, Honeck H, Luft FC, Schunck W-H. Mouse Cyp4a isoforms: enzymatic properties, gender- and strain-specific expression, and role in renal 20-hydroxyeicosatetraenoic acid formation. Biochem J 2007;403:109-18.

Murdoch C, Finn A. Chemokine receptors and their role in inflammation and infectious diseases. Blood 2000;95(10):3032-43.

Nelson DR. A Second CYP26 P450 in Humans and Zebrafish: CYP26B1. Archives of Biochemistry and Biophysics 1999;371(2):345-7.

Nemeth E, Ganz T. Regulation of Iron Metabolism by Hepcidin. Annu Rev Nutr 2006;26:323-42.

Nemeth E, Tuttle MS, Powelson J, Vaughn MB, Donovan A, McVey Ward D, Ganz T, Kaplan J. Hepcidin Regulates Cellular Iron Efflux by Binding to Ferroportin and Inducing Its Internalization. Science 2004;306:2090-3.

Nicolas G, Bennoun M, Devaux I, Beaumont C, Grandchamp B, Kahn A, Vaulont S. Lack of hepcidin gene expression and severe tissue iron overload in upstream stimulatory factor 2 (*USF2*) knockout mice. PNAS 2001;98(15):8780-5.

Nicolas G, Bennoun M, Porteu A, Mativet S, Beaumont C, Grandchamp B, Sirito M, Sawadogo M, Kahn A, Vaulont S. Severe iron deficiency anemia in transgenic mice expressing liver hepcidin. PNAS 2002;99(7):4596-601.

Nicolas G, Chauvet C, Viatte L, Danan JL, Bigard X, Devaux I, Beaumont C, Kahn A, Vaulont S. The gene encoding the iron regulatory peptide hepcidin is regulated by anemia, hypoxia, and inflammation. J Clin Invest 2002;110(7):1037-44.

Niederkofler V, Salie R, Arber S. Hemojuvelin is essential for dietary iron sensing, and ist mutation leads to severe iron overload. J Clin Invest 2005;115(8):2180-6.

Njajou OT, Vaessen N, Joosse M, Berghuis B, van Dongen JWF, Breuning MH, Snijders PJLM, Rutten WPF, Sandkuijl LA, Oostra BA, van Duijn CM, Heutink P. A mutation in *SLC11A3* is associated with autosomal dominant hemochromatosis. Nature Genetics 2001;28:213-4.

Ohgami RS, Campagna DR, Greer EL, Antiochos P, McDonald A, Chen J, Sharp JJ, Fujiwara Y, Barker JE, Fleming MD. Identification of a ferrireductase required for efficient transferrin-dependent uptake in erythroid cells. Nature genetics 2005;37(11):1264-9.

Papanikolaou G, Samuels ME, Ludwig EH, MacDonald MLE, Franchini PL, Dubé M-P, Andres L, MacFarlane J, Sakellaropoulos N, Politou M, Nemeth E, Thompson J, Risler JK, Zaborowska C, Babakaiff R, Radomski CC, Pape TD, Davidas O, Christakis J, Brissot P, Lockitch G, Ganz T, Hayden MR, Goldberg YP. Mutations in *HFE2* cause iron overload in chromosome 1q-linked juvenile hemochromatosis. Nature Genetics 2004;36(1):77-82.

Papanikolaou G, Pantopoulos K. Iron metabolism and toxicity. Review. Toxicology and Applied Pharmacology 2005;202:199-211.

Park CH, Valore EV, Waring AJ, Ganz T. Hepcidin, a Urinary Antimicrobial Peptide Synthesized in the Liver. The Journal of Biological Chemistry 2001;276(11):7806-10.

Parkkila S, Waheed A, Britton RS, Bacon BR, Zhou XY, Tomatsu S, Fleming RE, Sly WS. Association of the transferrin receptor in human placenta with HFE, the protein defective in hereditary hemochromatosis. Proc Natl Acad Sci USA 1997;94:13198-202.

Peussonnaux C, Zinkernagel AS, Schuepbach RA, Rankin E, Vaulont S, Haase VH, Nizet V, Johnson RS. Regulation of iron homeostasis by the hypoxia-inducible transcription factors (HIFs). J Clin Invest 2007;117(7):1926-32.

Pietrangelo A. Hereditary Hemochromatosis. Annu Rev Nutr 2006;26:251-70.

Pigeon C, Ilyin G, Courselaud B, Leroyer P, Turlin B, Brissot P, Loréal O. A New Mouse Liver-spesific Gene, Encoding a Protein Homologous to Human Antimicrobial Peptide Hepcidin, Is Overexpressed during Iron Overload. The Journal of Biological Chemistry 2001;276(11):7811-19.

Poirier Y, Antonenkov VD, Glumoff T, Hiltunen JK. Review. Peroxisomal β-oxidation – A metabolic pathway with multiple functions. Biochimica et Biophysica Acta 2006;1763:1413-26.

Ponka P, Beaumont C, Richardson DR. Function and regulation of transferrin and ferritin. Semin Hematol 1998;35:35-54.

Poss KD, Tonegawa S. Heme oxygenase 1 is required for mammalian iron reutilization. Proc Natl Acad Sci USA 1997;94:10919-24.

Primer3 [http://fokker.wi.mit.edu/primer3/input.htm]

Qiu A, Jansen M, Sakaris A, Min SH, Chattopadhay S, Tsai E, Sandoval C, Zhao R, Akabas MH, Goldman ID. Identification of an intestinal folate transporter and the molecular basis for hereditary folate malabsorption. Cell 2006;127(5):917-28.

Rau JC, Beaulieu LM, Huntington JA, Church FC. Serpins in thrombosis, hemostasis and fibrinolysis. J Thromb Haemost 2007;5(Suppl. 1):102-15.

Robson KJH, Merryweather-Clarke AT, Cadet E, Viprakasit V, Zaahl MG, Pointon JJ, Weatherall DJ, Rochette J. Recent advances in understanding haemochromatosis: a transition state. J Med Genet 2004;41:721-30.

Rodriguez A, Pan P, Parkkila S. Expression Studies of Neogenin and Its Ligand Hemojuvelin in Mouse Tissues. Journal of Histochemistry and Cytochemistry 2007;55(1):85-96.

Rodriguez A, Hilvo M, Kytömäki L, Fleming RE, Britton RS, Bacon BR, Parkkila S. Effects of iron loading on muscle: genome-wide mRNA expression profiling in the mouse. BMC Genomics 2007; 8:379.

Roetto A, Papanikolaou G, Politou M, Alberti F, Girelli D, Christakis J, Loukopoulos D, Camaschella C. Mutant antimicrobial peptide hepcidin is associated with severe juvenile hemochromatosis. Nature Genetics 2003;33:21-2.

Sanchez M, Galy B, Muckenthaler MU, Hentze MW. Iron-regulatory proteins limit hypoxia-inducible factor-2α expression in iron deficiency. Nature Structural & Molecular Biology 2007;14(5):420-6.

Schmidt PJ, Toran PT, Giannetti AM, Bjorkman PJ, Andrews NC. The Transferrin Receptor Modulates Hfe-Dependent Regulation of Hepcidin Expression. Cell Metabolism 2008;7:205-14.

Segerer S, Nelson PJ, Schlöndorff D. Chemokines, Chemokine Receptors, and Renal Disease: From Basic Science To Pathophysiologic and Therapeutic Studies. J Am Soc Nephrol 2000;11:152-76.

Shaner L, Morano KA. All in the family: atypical Hsp70 chaperones are conserved modulators of Hsp70 activity. Cell Stress & Chaperones 2007;12(1):1-8.

Sharp P, Srai SK. Molecular mechanisms involved in intestinal iron absorption. World J Gastroenterol 2007;13(35):4716-24.

Shayeghi M, Latunde-Dada GO, Oakhill JS, Laftah AH, Takeuchi K, Halliday N, Khan Y, Warley A, McCann FE, Hider RC, Frazer DM, Anderson GJ, Vulpe CD, Simpson RJ, McKie AT. Identification of an Intestinal Heme Transporter. Cell 2005;122:789-801.

Straus DS, Glass CK. Anti-inflammatory actions of PPAR ligands: new insights on cellular and molecular mechanisms. TRENDS in Immunology 2007;28(12):551-8.

Tandy S, Williams M, Leggett A, Lopez-Jimenez M, Dedes M, Ramesh B, Srai SK, Sharp P. Nramp2 Expression Is Associated with pH-dependent Iron Uptake across the Apical Membrane of Human Intestinal Caco-2 Cells. The Journal of Biological Chemistry 2000;275(2):1023-9.

Theurl M, Theurl I, Hochegger K, Obrist P, Subramaniam N, van Rooijen N, Schuemann K, Weiss G. Kupffer cell modulate iron homeostasis in mice via regulation of hepcidin expression. J Mol Med 2008;DOI 10.1007/s00109-008-0346-y.

Trinder D, Olynyk JK, Sly WS, Morgan EH. Iron uptake from plasma transferrin by the duodenum is impaired in the *Hfe* knockout mouse. PNAS 2002;99(8):5622-6.

Tuimala J. Processing of data. In: Hovatta I, Kimppa K, Lehmussola A, Pasanen T, Saarela J, Saarikko I, Saharinen J, Tiikkainen P, Toivanen T, Tolvanen M, Vihinen M, Wong G, Tuimala J (eds), Laine MM (eds), DNA Microarray Data Analysis, Picaset Oy, Helsinki, 2005, pp. 89-93.

Tuimala J, Saarikko I, Laine MM. Normalization. In: Hovatta I, Kimppa K, Lehmussola A, Pasanen T, Saarela J, Saarikko I, Saharinen J, Tiikkainen P, Toivanen T, Tolvanen M, Vihinen M, Wong G, Tuimala J (eds), Laine MM (eds), DNA Microarray Data Analysis, Picaset Oy, Helsinki, 2005, pp. 99-106.

Vandesompele J, De Preter K, Pattyn F, Poppe B, VanRoy N, De Paepe A, Speleman F. Accurate normalization of real-time quantitative RT-PCR data by geometric averaging ofmultiple internal control genes. Genome Biol 2002;3(7):1-11.

Vujic Spasic M, Kiss J, Herrmann T, Galy B, Martinache S, Stolte J, Gröne H-J, Stremmel W, Hentze MW, Muckenthaler MU. Hfe Acts in Hepatocytes to Prevent Hemochromatosis. Cell Metabolism 2008;7:173-8.

Waheed A, Britton RS, Grubb JH, Sly WS, Fleming RE. HFE association with transferrin receptor 2 increases cellular uptake of transferrin-bound iron. Arch Biochem Biophys 2008;474(1):193-7.

Waheed A, Parkkila S, Zhou XY, Tomatsu S, Tsuchihashi Z, Feder JN, Schatzman RC, Britton RS, Bacon BR, Sly WS. Hereditary hemochromatosis: Effects of C282Y and H63D mutations on

association with β_2-microglobulin, intracellular processing, and cell surface expression of the HFE protein in COS-7 cells. Proc Natl Acad Sci USA 1997;94:12384-9.

Wallace DF, Summerville L, Lusby PE, Subramaniam VN. First phenotypic description of transferrin receptor 2 knockout mouse, and the role of hepcidin. Gut 2005;54:980-6.

Wang R-H, Li C, Xu X, Zheng Y, Xiao C, Zerfas P, Cooperman S, Eckhaus M, Rouault T, Mishra L, Deng C-X. A role of SMAD4 in iron metabolism through positive regulation of hepcidin expression. Cell Metabolism 2005;2:399-409.

Wareing M, Ferguson CJ, Delannoy M, Cox AG, MacMahon RFT, Green R, Riccardi D, Smith GP. Altered dietary iron intake is a strong modulator of renal DMT1 expression. Am J Physiol Renal Physiol 2003;285:F1050-9.

Wareing M, Ferguson CJ, Green R, Riccardi D, Smith GP. *In vivo* characterization of renal iron transport in the anaesthetized rat. Journal of Physiology 2000;524.2:581-6.

Wong G. Introduction. In: Hovatta I, Kimppa K, Lehmussola A, Pasanen T, Saarela J, Saarikko I, Saharinen J, Tiikkainen P, Toivanen T, Tolvanen M, Vihinen M, Wong G, Tuimala J (eds), Laine MM (eds), DNA Microarray Data Analysis, Picaset Oy, Helsinki, 2005, pp. 15-23.

Yersin A, Osada T, Ikai A. Exploring Transferrin-Receptor Interactions at the Single-Molecule Level. Biophysical Journal 2008;94:230-40.

Zhang A-S, West AP Jr., Wyman AE, Bjorkman PJ, Enns CA. Interaction of Hemojuvelin with Neogenin Results in Iron Accumulation in Human Embryonic Kidney 293 Cells. Journal of Biological Chemistry 2005;280(40):33885-94.

Zhang D, Meyron-Holtz E, Rouault TA. Renal Iron Metabolism: Transferrin Iron Delivery and the Role of Iron Regulatory Proteins. J Am Soc Nephrol 2007;18:401-6.

Zhou XY, Tomatsu S, Fleming RE, Parkkila S, Waheed A, Jiang J, Fei Y, Brunt EM, Ruddy DA, Prass CE, Schatzman RC, O'Neill R, Britton RS, Bacon BR, Sly WS. HFE gene knockout produces mouse model of hereditary hemochromatosis. Proc Natl Acad Sci USA 1998;95:2492-7.

Appendix A

Genes of which expression was enhanced in the microarray study of dietary iron overload mice. The list was created using probe profile, thus certain genes can have more than one fold change value. P-values obtained from the microarray data analysis are suggestive, FC indicates fold change.

Gene name	Symbol	Accession.	p-value	FC
cytochrome P450, family 4, subfamily a, polypeptide 14	Cyp4a14	NM_007822	0	33.21
3-hydroxy-3-methylglutaryl-Coenzyme A synthase 2	Hmgcs2	NM_008256	0.0003	6.90
cytochrome P450, family 4, subfamily a, polypeptide 10	Cyp4a10	NM_010011	0.0003	3.25
cytochrome P450, family 27, subfamily b, polypeptide 1, nuclear gene encoding mitochondrial protein	Cyp27b1	NM_010009	0.0002	3.01
prolactin receptor	Prlr	NM_011169	0.0068	2.74
serine (or cysteine) preptidase inhibitor, clade A, member 1b	Serpina1b	NM_009244	0.0016	2.66
cytochrome P450, family 24, subfamily a, polypeptide 1	Cyp24a1	NM_009996	0.0084	2.55
serine (or cysteine) peptidase inhibitor, clade A, member 1a	Serpina1a	NM_009243	0.0013	2.51
angiopoietin-like 4	Angptl4	NM_020581	0.0091	2.46
serine (or cysteine) preptidase inhibitor, clade A, member 1b	Serpina1b	NM_009244	0.0023	2.31
acyl-CoA thioesterase 3	Acot3	NM_134246	0.0019	2.18
S100 calcium binding protein A8 (calgranulin A)	S100a8	NM_013650	0.0117	2.15
serine (or cysteine) peptidase inhibitor, clade A, member 1a	Serpina1a	NM_009243	0.0017	2.10
cytochrome P450, family 4, subfamily a, polypeptide 10	Cyp4a10	NM_010011	0.0008	2.04
cytochrome P450, family 4, subfamily a, polypeptide 12B	Cyp4a12b	NM_172306	0.0026	2.03
cytochrome P450, family 4, subfamily a, polypeptide 31	Cyp4a31	NM_201640	0.0028	1.98
glutathione S-transferase, theta 2	Gstt2	AK079739	0.006	1.97
SLIT and NTRK-like family, member 1	Slitrk1	NM_199065	0.0011	1.97
stimulated by retinoic acid gene 6	Stra6	NM_009291	0.0035	1.96
apolipoprotein C-III	Apoc3	NM_023114	0.0024	1.95
monoglyceride lipase	Mgll	NM_011844	0.0106	1.95
NUAK family, SNF1-like kinase, 1	Nuak1	NM_001004363	0.0027	1.94
acetyl-Coenzyme A acyltransferase 1B	Acaa1b	NM_146230	0.0011	1.89
homogentisate 1, 2-dioxygenase	Hgd	AK050193	0.0031	1.89
alkaline phosphatase 2, liver	Akp2	NM_007431	0.0019	1.83
solute carrier family 38, member 3	Slc38a3	NM_023805	0.0015	1.83
carbonic anhydrase 5a, mitochondrial	Car5a	NM_007608	0.0024	1.82
receptor accessory protein 6	Reep6	NM_139292	0.002	1.81
centaurin, gamma 2	Centg2	AK083235	0.0032	1.79
cytochrome P450, family 26, subfamily b, polypeptide 1	Cyp26b1	NM_175475	0.1991	1.78
cytoplasmic polyadenylation element binding protein 3	Cpeb3	NM_198300	0.0095	1.76
cyclin D1	Ccnd1	NM_007631	0.0207	1.76
serine (or cysteine) peptidase inhibitor, clade A, member 1d	Serpina1d	NM_009246	0.0193	1.69
actin, beta, cytoplasmic	Actb	NM_007393	0.0482	1.69
glycerol kinase	Gyk	AK086200	0.0411	1.67
hypothetical gene LOC100034734	LOC100034734	AK011989	0.1609	1.66
kynureninase (L-kynurenine hydrolase)	Kynu	NM_027552	0.0287	1.66
monoglyceride lipase	Mgll	NM_011844	0.0408	1.64
myeloid ecotropic viral integration site-related gene 1	Mrg1	AK045126	0.0584	1.60
G0/G1 switch gene 2	G0s2	NM_008059	0.1695	1.55
chymotrypsinogen B1	Ctrb1	NM_025583	0.4445	1.44

Appendix B

Genes of which expression was repressed in the microarray study of dietary iron overload mice. The list was created using probe profile, thus certain genes can have more than one fold change value. P-values obtained from the microarray data analysis are suggestive, FC indicates fold change.

Gene name	Symbol	Accession.	**p-value**	FC
F-box and WD-40 domain protein 5	Fbxw5	NM_013908	0.0991	-7.98
transthyretin	Ttr	NM_013697	0.0001	-5.74
cytochrome P450, family 4, subfamily b, polypeptide 1	Cyp4b1	NM_007823	0.0001	-3.39
RIKEN cDNA C730048C13 gene	C730048C13Rik	NM_177002	0.0003	-3.05
RIKEN cDNA E030010A14 gene	E030010A14Rik	NM_183160	0.001	-3.05
Mpv17 transgene, kidney disease mutant-like	Mpv17l	NM_033564	0.0015	-2.94
heat shock protein 1 (chaperonin)	Hspd1	NM_010477	0.0002	-2.92
lysophospholipase 1	Lypla1	NM_008866	0.0009	-2.80
heat shock protein 1A	Hspa1a	NM_010479	0.0341	-2.70
hydroxysteroid 11-beta dehydrogenase 1	Hsd11b1	NM_008288	0.0005	-2.70
DnaJ (Hsp40) homolog, subfamily B, member 1	Dnajb1	NM_018808	0.0132	-2.69
C1q and tumor necrosis factor related protein 3	C1qtnf3	NM_030888	0.0003	-2.64
heat shock protein 1	Hspb1	NM_013560	0.0137	-2.60
carboxypeptidase E	Cpe	NM_013494	0.0004	-2.58
cytochrome P450, family 4, subfamily a, polypeptide 12a	Cyp4a12a	NM_177406	0.0004	-2.58
expressed sequence AI747699	AI747699	NM_001013770	0.0004	-2.57
heat shock protein 105	Hsp105	NM_013559	0.0061	-2.56
meprin 1 beta	Mep1b	NM_008586	0.0009	-2.54
splicing factor, arginine/serine-rich 10 (transformer 2 homolog, Drosophila)	Sfrs10	NM_009186	0.0007	-2.52
heterogeneous nuclear ribonucleoprotein K	Hnrpk	NM_025279	0.0015	-2.51
RIKEN cDNA C730048C13 gene	C730048C13Rik	NM_177002	0.001	-2.51
cytochrome P450, family 2, subfamily j, polypeptide 13	Cyp2j13	NM_145548	0.0003	-2.51
solute carrier family 17 (sodium phosphate), member 3	Slc17a3	NM_134069	0.0005	-2.50
syndecan binding protein	Sdcbp	NM_016807	0.0004	-2.46
myosin Va	Myo5a	NM_010864	0.0021	-2.45
nudix (nucleoside diphosphate linked moiety X)-type motif 12	Nudt12	NM_026497	0.0007	-2.45
kynurenine 3-monooxygenase (kynurenine 3-hydroxylase)	Kmo	NM_133809	0.0007	-2.39
acyl-Coenzyme A oxidase 1, palmitoyl	Acox1	NM_015729	0.0017	-2.38
procollagen, type IV, alpha 3	Col4a3	NM_007734	0.0007	-2.36
organic solute transporter alpha	Osta	NM_145932	0.0024	-2.35
ets variant gene 1	Etv1	NM_007960	0.0008	-2.33
N-acylsphingosine amidohydrolase 1	Asah1	NM_019734	0.001	-2.32
flavin containing monooxygenase 5	Fmo5	NM_010232	0.0006	-2.31
RIKEN cDNA 9030619P08 gene	9030619P08Rik	NM_001039720	0.0007	-2.29
transmembrane emp24 protein transport domain containing 7	Tmed7	AK076210	0.0013	-2.29
ATPase, H+ transporting, lysosomal accessory protein 2	Atp6ap2	NM_027439	0.0016	-2.27
solute carrier organic anion transporter family, member 1a1	Slco1a1	NM_013797	0.0037	-2.26
acyl-CoA synthetase medium-chain family member 3	Acsm3	NM_016870	0.0022	-2.26
ATPase, H+ transporting, lysosomal accessory protein 2	Atp6ap2	NM_027439	0.0023	-2.21
solute carrier family 6 (neurotransmitter transporter), member 15	Slc6a15	NM_175328	0.0007	-2.19
transmembrane protein 33	Tmem33	NM_028975	0.0032	-2.19

acyl-CoA synthetase medium-chain family member 3	Acsm3	NM_016870	0.0055	-2.19
retinoblastoma binding protein 7	Rbbp7	NM_009031	0.0047	-2.18
aspartyl-tRNA synthetase	Dars	NM_145507	0.0005	-2.17
ATPase, H+ transporting, lysosomal accessory protein 2	Atp6ap2	NM_027439	0.0017	-2.16
major facilitator superfamily domain containing 2	Mfsd2	NM_029662	0.0393	-2.16
basic helix-loop-helix domain containing, class B2	Bhlhb2	NM_011498	0.0057	-2.14
ubiquitin-conjugating enzyme E2G 1 (UBC7 homolog, C. elegans)	Ube2g1	NM_025985	0.0023	-2.14
TSC22 domain family, member 1	Tsc22d1	NM_009366	0.0043	-2.12
translocating chain-associating membrane protein 1	Tram1	NM_028173	0.0015	-2.09
heat shock protein 90kDa alpha (cytosolic), class A member 1	Hsp90aa1	NM_010480	0.0138	-2.09
cDNA sequence BC013481	BC013481	NM_178446	0.0013	-2.09
eukaryotic translation initiation factor 4, gamma 2	Eif4g2	NM_013507	0.001	-2.09
polo-like kinase 3 (Drosophila)	Plk3	NM_013807	0.0573	-2.07
glucosamine-6-phosphate deaminase 1	Gnpda1	NM_011937	0.0072	-2.07
nuclear factor, interleukin 3, regulated	Nfil3	NM_017373	0.0725	-2.06
alcohol dehydrogenase, iron containing, 1	Adhfe1	NM_175236	0.0043	-2.06
caveolin 2	Cav2	NM_016900	0.0013	-2.05
hydroxysteroid 11-beta dehydrogenase 1	Hsd11b1	NM_008288	0.0017	-2.04
protein phosphatase 1, catalytic subunit, beta isoform	Ppp1cb	NM_172707	0.0007	-2.04
membrane-associated ring finger (C3HC4) 6	March6	NM_172606	0.0055	-2.03
annexin A13	Anxa13	NM_027211	0.0011	-2.02
cysteine and histidine-rich domain (CHORD)-containing, zinc-binding protein 1	Chordc1	NM_025844	0.0023	-2.02
met proto-oncogene	Met	NM_008591	0.0029	-2.02
DnaJ (Hsp40) homolog, subfamily A, member 4	Dnaja4	NM_021422	0.0055	-2.02
3-hydroxybutyrate dehydrogenase, type 1	Bdh1	NM_175177	0.0022	-2.02
chromobox homolog 3 (Drosophila HP1 gamma)	Cbx3	NM_007624	0.0015	-2.01
splicing factor, arginine/serine-rich 10 (transformer 2 homolog, Drosophila)	Sfrs10	NM_009186	0.0032	-1.99
Cobl-like 1	Cobll1	NM_177025	0.0027	-1.98
epidermal growth factor receptor pathway substrate 8	Eps8	NM_007945	0.0008	-1.98
ring finger protein 24	Rnf24	NM_178607	0.0113	-1.98
coenzyme Q10 homolog B (S. cerevisiae)	Coq10b	NM_026424	0.005	-1.98
CDC like kinase 4	Clk4	NM_007714	0.0035	-1.97
transmembrane protein 49	Tmem49	NM_029478	0.0016	-1.97
CCR4 carbon catabolite repression 4-like (S. cerevisiae)	Ccrn4l	NM_009834	0.0099	-1.97
thioredoxin domain containing 14	Txndc14	NM_025868	0.0079	-1.96
lipoprotein lipase	Lpl	NM_008509	0.0072	-1.96
lactate dehydrogenase D	Ldhd	NM_027570	0.0011	-1.96
nudix (nucleoside diphosphate linked moiety X)-type motif 19	Nudt19	NM_033080	0.002	-1.96
Bcl2-associated athanogene 3	Bag3	NM_013863	0.0071	-1.96
heterogeneous nuclear ribonucleoprotein A2/B1	Hnrpa2b1	NM_182650	0.0025	-1.95
suppressor of cytokine signaling 2	Socs2	NM_007706	0.1693	-1.95
RIKEN cDNA D630023F18 gene	D630023F18Rik	NM_175293	0.0028	-1.94
abhydrolase domain containing 3	Abhd3	NM_134130	0.0086	-1.94
C1q and tumor necrosis factor related protein 3	C1qtnf3	NM_030888	0.0038	-1.94
retinoblastoma binding protein 7	Rbbp7	NM_009031	0.0059	-1.93
secreted and transmembrane 1B	Sectm1b	NM_026907	0.0092	-1.92
cortexin 3	Ctxn3	AK042789	0.0038	-1.92
spectrin beta 2	Spnb2	NM_175836	0.0026	-1.92

cytokine inducible SH2-containing protein	Cish	NM_009895	0.354	-1.92
steroid 5 alpha-reductase 2	Srd5a2	NM_053188	0.0023	-1.91
CKLF-like MARVEL transmembrane domain containing 6	Cmtm6	NM_026036	0.0035	-1.91
solute carrier family 47, member 1	Slc47a1	NM_026183	0.0011	-1.91
tumor necrosis factor receptor superfamily, member 21	Tnfrsf21	NM_178589	0.0036	-1.90
transmembrane emp24 domain trafficking protein 2	Tmed2	NM_019770	0.0023	-1.90
succinate-Coenzyme A ligase, ADP-forming, beta subunit	Sucla2	NM_011506	0.0036	-1.90
RING1 and YY1 binding protein	Rybp	NM_019743	0.0018	-1.90
F-box protein 3	Fbxo3	NM_212433	0.0031	-1.88
ring finger protein 181	Rnf181	NM_025607	0.0029	-1.88
hook homolog 1 (Drosophila)	Hook1	NM_030014	0.0021	-1.88
Bmi1 polycomb ring finger oncogene	Bmi1	NM_007552	0.0056	-1.87
homocysteine-inducible, endoplasmic reticulum stress-inducible, ubiquitin-like domain member 1	Herpud1	NM_022331	0.0032	-1.87
moesin	Msn	NM_010833	0.0039	-1.87
glucosamine-6-phosphate deaminase 1	Gnpda1	NM_011937	0.0121	-1.86
eukaryotic translation initiation factor 5	Eif5	NM_173363	0.0019	-1.86
glycerol kinase	Gyk	NM_008194	0.0111	-1.86
kelch-like 9 (Drosophila)	Klhl9	NM_172871	0.0013	-1.86
RAB7, member RAS oncogene family	Rab7	NM_009005	0.0055	-1.85
RAB6, member RAS oncogene family	Rab6	BC019118	0.0033	-1.85
zinc metallopeptidase, STE24 homolog (S. cerevisiae)	Zmpste24	NM_172700	0.0017	-1.85
heterogeneous nuclear ribonucleoprotein K	Hnrpk	NM_025279	0.0064	-1.85
NADH dehydrogenase chain 5 (Fragment)		AK018737	0.005	-1.85
regulator of calcineurin 1	Rcan1	NM_019466	0.0066	-1.84
hairy and enhancer of split 1 (Drosophila)	Hes1	NM_008235	0.0083	-1.84
SNRPN upstream reading frame	Snurf	NM_033174	0.0038	-1.84
transmembrane protein 49	Tmem49	NM_029478	0.0037	-1.84
alpha-2-glycoprotein 1, zinc	Azgp1	NM_013478	0.0031	-1.84
ERBB receptor feedback inhibitor 1	Errfi1	NM_133753	0.0156	-1.83
solute carrier family 22 (organic anion transporter), member 9	Slc22a9	NM_144785	0.0108	-1.83
ubiquitin specific peptidase 8	Usp8	NM_019729	0.0049	-1.83
X-box binding protein 1	Xbp1	NM_013842	0.0051	-1.83
amyotrophic lateral sclerosis 2 (juvenile) chromosome region, candidate 2 (human)	Als2cr2	NM_172656	0.0029	-1.82
ATPase, Ca++ transporting, cardiac muscle, slow twitch 2	Atp2a2	AK081191	0.0034	-1.82
B-cell translocation gene 1, anti-proliferative	Btg1	NM_007569	0.0017	-1.82
dual specificity phosphatase 6	Dusp6	NM_026268	0.0367	-1.82
hydroxyacyl-Coenzyme A dehydrogenase/3-ketoacyl-Coenzyme A thiolase/enoyl-Coenzyme A hydratase (trifunctional protein), beta subunit	Hadhb	NM_145558	0.0338	-1.82
zinc metallopeptidase, STE24 homolog (S. cerevisiae)	Zmpste24	NM_172700	0.0041	-1.81
mitochondrial carrier homolog 2 (C. elegans)	Mtch2	NM_019758	0.0035	-1.81
crystallin, zeta	Cryz	NM_009968	0.0364	-1.80
eukaryotic translation initiation factor 4A2	Eif4a2	NM_013506	0.007	-1.80
proteasome (prosome, macropain) subunit, alpha type 1	Psma1	NM_011965	0.0068	-1.80
sorting nexin 2	Snx2	NM_026386	0.0025	-1.80
kinesin family member 20B	Kif20b	NM_183046	0.0138	-1.79
B-cell translocation gene 1, anti-proliferative	Btg1	NM_007569	0.003	-1.79
bisphosphate 3'-nucleotidase 1	Bpnt1	NM_011794	0.0047	-1.78
selenoprotein	Sep15	NM_053102	0.0108	-1.78

MOB1, Mps One Binder kinase activator-like 3 (yeast)	Mobkl3	NM_025283	0.0043	-1.77
adenosine kinase	Adk	NM_134079	0.013	-1.77
GATA zinc finger domain containing 1	Gatad1	NM_026033	0.0085	-1.77
acyl-Coenzyme A dehydrogenase, medium chain	Acadm	NM_007382	0.0247	-1.74
SEC23A (S. cerevisiae)	Sec23a	NM_009147	0.0088	-1.74
RIKEN cDNA 1110057K04 gene	1110057K04Rik	NM_172401	0.0168	-1.74
transmembrane protein 45b	Tmem45b	NM_144936	0.0186	-1.73
ATPase, class VI, type 11A	Atp11a	AK028779	0.0154	-1.71
selenoprotein	Sep15	NM_053102	0.0144	-1.71
amyloid beta (A4) precursor protein	App	AY267348	0.0202	-1.71
haptoglobin	Hp	NM_017370	0.2577	-1.70
period homolog 2 (Drosophila)	Per2	NM_011066	0.1068	-1.67
low density lipoprotein-related protein 12	Lrp12	NM_172814	0.0551	-1.67
serum/glucocorticoid regulated kinase	Sgk	NM_011361	0.0428	-1.64
histone cluster 1, H4h	Hist1h4h	NM_153173	0.0601	-1.63
RIKEN cDNA 9630055N22 gene	9630055N22Rik	AK036315	0.0441	-1.63
aminolevulinic acid synthase 1	Alas1	NM_020559	0.041	-1.63
histone cluster 1, H4h	Hist1h4h	NM_153173	0.0794	-1.62
methyl-CpG binding domain protein 1	Mbd1	AK007371	0.3316	-1.60
haptoglobin	Hp	NM_017370	0.4048	-1.55
Jun oncogene	Jun	NM_010591	0.2404	-1.54

Appendix C

Genes of which expression was enhanced in the microarray study of *Hfe* knock out mice. The list was created using probe profile, thus certain genes can have more than one fold change value. P-values obtained from the microarray data analysis are suggestive, FC indicates fold change.

Gene name	Symbol	Accession.	p-value	FC
major urinary protein 1	Mup1	NM_031188	0.2456	4.39
cytokine inducible SH2-containing protein	Cish	NM_009895	0.0266	3.14
complement factor D (adipsin)	Cfd	NM_013459	0.2387	2.77
WD repeat and FYVE domain containing 1	Wdfy1	NM_027057	0.1287	2.42
serine (or cysteine) peptidase inhibitor, clade A, member 1e	Serpina1e	NM_009247	0.2357	2.12
haptoglobin	Hp	NM_017370	0.0608	2.05
SEC14-like 4 (S. cerevisiae)	Sec14l4	NM_146013	0.0143	1.96
serine (or cysteine) peptidase inhibitor, clade A, member 1b	Serpina1b	NM_009244	0.017	1.90
histone cluster 1, H4f	Hist1h4f	NM_175655	0.0053	1.89
serine (or cysteine) peptidase inhibitor, clade A, member 1b	Serpina1b	NM_009244	0.0165	1.87
RIKEN cDNA A930034L06 gene	A930034L06Rik	NM_175692	0.0101	1.76
uncoupling protein 1 (mitochondrial, proton carrier)	Ucp1	NM_009463	0.3357	1.74
suppressor of cytokine signaling 2	Socs2	NM_007706	0.0214	1.72
serine (or cysteine) peptidase inhibitor, clade A, member 1a	Serpina1a	NM_009243	0.0209	1.69
uridine phosphorylase 2	Upp2	NM_029692	0.0265	1.67
ring finger protein 24	Rnf24	NM_178607	0.0133	1.67
RIKEN cDNA 2200001I15 gene	2200001I15Rik	NM_183278	0.0226	1.65
nuclear factor, interleukin 3, regulated	Nfil3	NM_017373	0.0266	1.64
solute carrier family 7, (cationic amino acid transporter, y+ system) member 13	Slc7a13	AK002431	0.0234	1.60
prostate stem cell antigen	Psca	NM_028216	0.1048	1.60
acyl-Coenzyme A dehydrogenase, medium chain	Acadm	NM_007382	0.0292	1.58
small glutamine-rich tetratricopeptide repeat (TPR)-containing, beta	Sgtb	NM_144838	0.0249	1.58
uridine phosphorylase 2	Upp2	NM_029692	0.0261	1.56
cold inducible RNA binding protein	Cirbp	NM_007705	0.0239	1.56
solute carrier family 35, member F3	Slc35f3	NM_175434	0.0475	1.55
prostaglandin D2 synthase (brain)	Ptgds	NM_008963	0.0302	1.55
transthyretin	Ttr	NM_013697	0.0333	1.55
DnaJ (Hsp40) homolog, subfamily B, member 1	Dnajb1	NM_018808	0.0315	1.54
serum/glucocorticoid regulated kinase	Sgk	NM_011361	0.0445	1.54
SNRPN upstream reading frame	Snurf	NM_033174	0.0349	1.53
elongation factor RNA polymerase II-like 3	Ell3	NM_145973	0.0665	1.52
chemokine (C-C motif) ligand 28	Ccl28	NM_020279	0.1212	1.52
AXIN1 up-regulated 1	Axud1	NM_153287	0.0759	1.51
disabled homolog 2 (Drosophila)	Dab2	NM_198643	0.069	1.51
glypican 1	Gpc1	NM_016696	0.0301	1.51
solute carrier family 5 (sodium-dependent vitamin transporter), member 6	Slc5a6	NM_177870	0.0322	1.51
uridine phosphorylase 2	Upp2	NM_029692	0.0563	1.51
coiled-coil domain containing 3	Ccdc3	NM_028804	0.0381	1.49
RIKEN cDNA 9930109F21 gene	9930109F21Rik	NM_183194	0.0357	1.49
C1q and tumor necrosis factor related protein 3	C1qtnf3	NM_030888	0.0508	1.49
T-cell lymphoma invasion and metastasis 1	Tiam1	NM_009384	0.0381	1.49

gene model 106, (NCBI)	Gm106	NM_001033288	0.0531	1.49
RIKEN cDNA 9030619P08 gene	9030619P08Rik	NM_001039720	0.0682	1.48
caveolin 2	Cav2	NM_016900	0.0767	1.48
aquaporin 4	Aqp4	NM_009700	0.2049	1.47
activin receptor IIB	Acvr2b	NM_007397	0.1227	1.47
apolipoprotein A-II	Apoa2	NM_013474	0.2199	1.47
hemopexin	Hpx	NM_017371	0.2653	1.46
apolipoprotein C-I	Apoc1	NM_007469	0.2799	1.46
ATPase, H+ transporting, lysosomal accessory protein 2	Atp6ap2	NM_027439	0.0588	1.46
cytochrome c oxidase, subunit VIIIb	Cox8b	NM_007751	0.3287	1.45
SEC14-like 3 (S. cerevisiae)	Sec14l3	NM_001029937	0.0907	1.43
aldo-keto reductase family 1, member C14	Akr1c14	NM_134072	0.0961	1.42
RIKEN cDNA C730048C13 gene	C730048C13Rik	NM_177002	0.0956	1.42

Appendix D

Genes of which expression was repressed in the microarray study of *Hfe* knock out mice. The list was created using probe profile, thus certain genes can have more than one fold change value. P-values obtained from the microarray data analysis are suggestive, FC indicates fold change.

Gene name	Symbol	Accession.	p-value	FC
glutathione peroxidase 6	Gpx6	NM_145451	0	-10.83
F-box and WD-40 domain protein 5	Fbxw5	NM_013908	0.082	-7.35
cytochrome P450, family 26, subfamily b, polypeptide 1	Cyp26b1	NM_175475	0.0001	-5.29
B-cell leukemia/lymphoma 6	Bcl6	NM_009744	0.0714	-2.69
general transcription factor II H, polypeptide 2	Gtf2h2	NM_022011	0.0004	-2.61
erythroid differentiation regulator 1	Erdr1	NM_133362	0.0008	-2.59
cysteine-rich with EGF-like domains 2	Creld2	NM_029720	0.0017	-2.50
predicted gene, EG633640	EG633640	AK050607	0.0172	-2.19
spinster homolog 3 (Drosophila)	Spns3	NM_029932	0.0454	-2.09
heme oxygenase (decycling) 1	Hmox1	NM_010442	0.0019	-2.06
solute carrier family 18 (vesicular monoamine), member 1	Slc18a1	AK049514	0.0085	-1.98
heat shock protein 105	Hsp105	NM_013559	0.0049	-1.95
tumor necrosis factor receptor superfamily, member 12a	Tnfrsf12a	NM_013749	0.0115	-1.87
heat shock protein 8	Hspb8	NM_030704	0.0493	-1.83
ectonucleoside triphosphate diphosphohydrolase 4	Entpd4	NM_026174	0.0052	-1.83
histone cluster 1, H4f	Hist1h4f	NM_175655	0.007	-1.79
mitochondrial ribosomal protein S27	Mrps27	NM_173757	0.0059	-1.78
heat shock protein 1	Hspb1	NM_013560	0.0095	-1.77
erythroid differentiation regulator 1	Erdr1	NM_133362	0.0085	-1.76
growth arrest and DNA-damage-inducible 45 alpha	Gadd45a	NM_007836	0.0581	-1.76
Fc receptor, IgG, low affinity IV	Fcgr4	NM_144559	0.0104	-1.75
MITOCHONDRIAL CARRIER-LIKE PROTEIN homolog [Mus musculus]		AK031288	0.009	-1.73
stress-induced phosphoprotein 1	Stip1	NM_016737	0.011	-1.72
protease (prosome, macropain) 26S subunit, ATPase 1	Psmc1	NM_008947	0.2416	-1.70
serine (or cysteine) peptidase inhibitor, clade H, member 1	Serpinh1	NM_009825	0.0101	-1.70
tubulin, beta 2b	Tubb2b	NM_023716	0.0174	-1.69
matrix Gla protein	Mgp	NM_008597	0.0302	-1.69
weakly similar to 2010003O02RIK PROTEIN [Mus musculus]		AK044077	0.0118	-1.69
ladinin	Lad1	NM_133664	0.083	-1.67
chemokine (C-X-C motif) ligand 9	Cxcl9	NM_008599	0.0156	-1.66
histone cluster 1, H4a	Hist1h4a	NM_178192	0.0151	-1.65
chemokine (C-X-C motif) ligand 14	Cxcl14	NM_019568	0.0376	-1.61
chemokine (C-C motif) ligand 5	Ccl5	NM_013653	0.0321	-1.61
histone cluster 1, H1c	Hist1h1c	NM_015786	0.0256	-1.60
four jointed box 1 (Drosophila)	Fjx1	NM_010218	0.022	-1.60
chemokine (C-C motif) ligand 4	Ccl4	NM_013652	0.0184	-1.60
solute carrier family 25, member 37, Mitoferrin	Slc25a37	AK034948	0.0185	-1.59
B-cell leukemia/lymphoma 2 related protein A1b	Bcl2a1b	NM_007534	0.025	-1.58
protein disulfide isomerase associated 4	Pdia4	NM_009787	0.023	-1.57
cytochrome P450, family 4, subfamily a, polypeptide 12B	Cyp4a12b	NM_172306	0.1371	-1.56
B-cell leukemia/lymphoma 2 related protein A1d	Bcl2a1d	NM_007536	0.0411	-1.55
AHA1, activator of heat shock protein ATPase homolog 1 (yeast)	Ahsa1	NM_146036	0.0267	-1.55

cysteine and histidine-rich domain (CHORD)-containing, zinc-binding protein 1	Chordc1	NM_025844	0.0273	-1.54
steroid 5 alpha-reductase 2	Srd5a2	NM_053188	0.0671	-1.54
CDC42 effector protein (Rho GTPase binding) 3	Cdc42ep3	NM_026514	0.0354	-1.54
lysyl oxidase-like 1	Loxl1	NM_010729	0.036	-1.54
transmembrane protein 119	Tmem119	NM_146162	0.03	-1.54
growth differentiation factor 15	Gdf15	NM_011819	0.0647	-1.54
tubulin, beta 6	Tubb6	NM_026473	0.0277	-1.54
predicted gene, EG226654	EG226654	XM_129558	0.0484	-1.53
chemokine (C-C motif) ligand 12	Ccl12	NM_011331	0.0332	-1.53
cytochrome P450, family 4, subfamily a, polypeptide 12a	Cyp4a12a	NM_177406	0.0575	-1.51
oncostatin M receptor	Osmr	NM_011019	0.0308	-1.51
four and a half LIM domains 2	Fhl2	NM_010212	0.0354	-1.51
histocompatibility 2, class II antigen A, beta 1	H2-Ab1	NM_207105	0.0264	-1.51
methyl-CpG binding domain protein 1	Mbd1	AK007371	0.0616	-1.50
ecto-NOX disulfide-thiol exchanger 1	Enox1	NM_172813	0.0317	-1.50
mannose receptor, C type 2	Mrc2	NM_008626	0.0505	-1.49
ectonucleoside triphosphate diphosphohydrolase 4	Entpd4	NM_026174	0.0376	-1.49
carbonyl reductase 1	Cbr1	NM_007620	0.0592	-1.49
HEAT repeat containing 1	Heatr1	NM_144835	0.0425	-1.49
tubulin, beta 2b	Tubb2b	NM_023716	0.0407	-1.49
heat shock protein 8	Hspa8	NM_031165	0.0345	-1.49
matrix metallopeptidase 13	Mmp13	NM_008607	0.0933	-1.48
transcription factor 2	Tcf2	NM_009330	0.0558	-1.48
chemokine (C motif) ligand 1	Xcl1	NM_008510	0.037	-1.48
transcription factor 2	Tcf2	NM_009330	0.0503	-1.48
heat shock protein 90kDa beta (Grp94), member 1	Hsp90b1	NM_011631	0.0467	-1.48
5' nucleotidase, ecto	Nt5e	NM_011851	0.1679	-1.47
brain abundant, membrane attached signal protein 1	Basp1	NM_027395	0.0484	-1.46
potassium channel, subfamily K, member 5	Kcnk5	NM_021542	0.0889	-1.46
coronin, actin binding protein 1A	Coro1a	NM_009898	0.0513	-1.46
annexin A13	Anxa13	NM_027211	0.0676	-1.44
lymphocyte specific 1	Lsp1	NM_019391	0.0585	-1.44
apolipoprotein M	Apom	NM_018816	0.0751	-1.44
RIKEN cDNA 4933437K13 gene	4933437K13Rik	AK086865	0.0702	-1.43
RIKEN cDNA 4933403G14 gene	4933403G14Rik	NM_028908	0.0722	-1.43

Appendix E

Sequences of the primers used in this study. (* designed using Primer3 (http://fokker.wi.mit.edu/primer3/input.htm))

Primers of iron-related genes and housekeeping genes.

Symbol	Gene name	GenBank Accession No.	Forward primer (5'-3')	Reverse primer (5'-3')	Source
hepcidin1	hepcidin 1	NM_032541	CCTATCTCCATCAACAGATG	AACAGATACCACACTGGGAA	Ilyin et al. 2003
hepcidin2	hepcidin 2	NM_183257	CCTATCTCCATCAACAGATG	AACAGATACCACAGGAGGGT	Ilyin et al. 2003
HFE	hemochromatosis protein	NM_010424	TGGAATGGGACGAGCACAAG	GAGCCTGACACCTTAGAGAG	*
HJV	hemojuvelin	NM_027126	TCTGACCTGAGTGAGACTGC	GATGATGAGCCTCCTACCTA	Rodriguez et al. 2007a
IRP1	iron regulatory protein 1	NM_007386	TTGATGTGGTGGGCTACGG	TTGGCTCGTGTGTTAGGATG	*
Neo	neogenin	NM_008684	CCCTGGTCTCTACTCGCTTC	CCTGGCTGGCTGGTATTCTC	Rodriguez et al. 2007a
TfR1	transferrin receptor 1	NM_011638	TCATGAGGGAAATCAATGATCGTA	GCCCCAGAAGATATGTCGGAA	Rodriguez et al. 2007b
TfR2	transferrin receptor 2	NM_015799	CTTCAATCAAACCCAGTTCC	TCCCAGCCGATAAGGAGAG	*
Actb	actin beta	NM_007393	AGAGGGAAATCGTGCGTGAC	CAATAGTGATGACCTGGCCGT	Rodriguez et al. 2007a
Gapdh	glyceraldehyde-3-phosphate dehydrogenase	NM_008084	ATGGTGAAGGTCGGTGTG	CATTCTCGGCCTTGACTG	Rodriguez et al. 2007a
Hprt1	hypoxanthine phosphoribosyl-transferase 1	NM_013556	AGCTACTGTAATGATCAGTCAACG	AGAGGTCCTTTTCACCAGCA	Rodriguez et al. 2007a
Sdha	succinate dehydrogenase complex subunit A	NM_023281	GCTTGCGAGCTGCATTTGG	CATCTCCAGTTGTCCTCTTCCA	Rodriguez et al. 2007a

Primers of genes selected from the microarray data.

Symbol	Gene name	GenBank Accession No.	Forward primer (5'-3')	Reverse primer (5'-3')	Source
Acaa1b	acetyl-Coenzyme A acyltransferase 1B	NM_146230	TGTCCCAGAGAGGGAACCA	CCTGCTTCTGCCGTGAAAC	*
Acot3	acyl-CoA thioesterase 3	NM_134246	ACTTTGAGGAAGCTGTGACC	CGCCGATGTTGGATATAGAG	*
Angptl4	angiopoietin-like 4	NM_020581	CACGCACCTAGACAATGGA	AGAGGCTGGATCTGGAAA	Rodriguez et al. 2007b
Cfd	complement factor D (adipsin)	NM_013459	AACCGGACAACCRGCAATC	CCCACGTAACCACACACCTTC	Rodriguez et al. 2007b
Creld2	cysteine-rich with EGF-like domains 2	NM_029720	GAACGAGACCCACAGCATC	CCACATCCACACAGGCATC	*
Cish	cytokine inducible SH2-containing protein	NM_009895	AACAAGGCAGGTGGAGGAG	AGACACAGTTCAGGTGGCAAG	*
Cyp26b1	cytochrome P450, family 26, subfamily b, polypeptide 1	NM_175475	CAAGCTCGGCAGATCCTTCA	ACTCCAGGGTTCCATCCTTC	*
Cyp4a14	cytochrome P450, family 4, subfamily a, polypeptide 14	NM_007822	CAAGACCCTCCAGCATTTCC	CCCAGAACCACCTTCACATAG	*
Dnajb1	DnaJ (Hsp40) homolog, subfamily B, member 1	NM_018808	CGACCGCTATGGAGAGGAA	GCCACCGAAGAACTCAGCA	Rodriguez et al. 2007b
Fbxw5	F-box and WD-40 domain protein 5	NM_013908	TCACGTACTCACCGCATCAG	GTCCAGGGCATCAAAGAAGG	*
Gdf15	growth differentiation factor 15	NM_011819	TGCTGTTCCTGCTGCTGTTG	AGTCCTCTCGGCTCTGGTTG	*
Gpx6	glutathione peroxidase 6	NM_145451	GAAGGCTGAGAGCAGAAACC	GGGTGAGAGCAAACCACATC	*
Hmox1	heme oxygenase (decycling) 1	NM_010442	CAGAGGAACACAAAGACCAGA	CCAACAGGAAGCTGAGAGTG	*
Hp	haptoglobin	NM_017370	GCTGGTGGAGATTGAGAAGG	TTGGAAGGCAGGCAGATAGG	*
Hsp105	heat shock protein 105	NM_013559	TCACCATCTCCACGGCTTC	GCTTCACTGTTGTCTTGCTG	*
Hspa1a	heat shock protein 1A	NM_010479	TTCGTGGAGGAGTTCAAGAG	GCGTGATGGATGTGTAGAAG	*
Slc25a37	solute carrier family 25, member 37	AK034948	GAGGACTACGAGAACCTACC	TCAAACTCTGCATCCGTGTC	*
Tnfrsf12a	tumor necrosis factor receptor superfamily, member 12a	NM_013749	CGTCGTCCATTCATTCATTC	GAACTCTAAGCCCAGTCC	*
Ttr	transthyretin	NM_013697	TCGCTGGACTGGTATTTGTG	GTCTTCCCAGAGGCAAAGG	*
Ucp1	uncoupling protein 1(mitochondrial, proton carrier)	NM_009463	CAGAAGGATTGCCGAAACTG	AATGAACACTGCCACACCTC	*
Xbp1	X-box binding protein 1	NM_013842	AAGAAGAGAACCACAAACTCC	CAGCGTGTCCATTCCCAAG	*